New synthetic hosts for sulfate and nucleoside triphosphates: understanding non-covalent interactions

von der Fakultät für Naturwissenschaften der Technischen Universität Chemnitz
genehmigte Dissertation zur Erlangung des akademischen Grades

doktor rerum naturalium

(Dr. rer. nat.)

vorgelegt von Dipl.-Chem. Tatiana A. Shumilova

geboren am 05. Februar 1993 in Nowosibirsk, Russland

eingereicht am 17. Oktober 2017

Gutachter: apl. Prof. Dr. Evgeny Kataev
Prof. Dr. Klaus Banert

Tag der Verteidigung: 16. Februar 2018

Bibliographic description and abstract

Shumilova, Tatiana Aleksandrovna

New synthetic hosts for sulfate and nucleoside triphosphates: understanding non-covalent interactions

Technische Universität Chemnitz, Fakultät für Naturwissenshaften, Institut für Chemie, doctoral dissertation (English language), 2017

The dissertation contains 121 pages, 56 figures, 9 schemes, 8 tables.

The present work describes new aspects of organic and supramolecular chemistry. The scientific contribution consists of two parts, which focus on the development of receptors for the sulfate anion and quantitative assessment of stacking interactions between an anthracene dye and nucleobases in an aqueous solution.

In Chapter 1, basic concepts concerning supramolecular chemistry and recognition of cations and anions are discussed, as well as modern methods for the determination of binding constants. Particular attention is paid to fluorescence sensing of ions and underlying mechanisms of binding-induced fluorescence responses. Chapter 2 is dedicated to the design and synthesis of new fluorescent sulfate receptors functioning in aqueous solution. After a short review of the most effective sulfate receptors/probes created so far, a new design of PET probes for sulfate sensing is presented. The syntheses and anion binding properties of new compounds are described. The experimental data obtained for the receptors are discussed in detail to reveal the origin of high selectivity towards sulfate. Chapter 3 explores the importance of nucleobase–arene stacking interactions in recognition of nucleotides by synthetic receptors. Various experimental and theoretical approaches are presented to assess dispersion interactions between aromatic rings and nucleobases in the receptor–nucleotide complexes.

Keywords: supramolecular chemistry, anion, sulfate recognition, fluorescent probe, naphthalimide, pK_a shift, nucleobase, stacking and dispersion interactions.

Table of contents

Epigraph

Они были магами потому, что очень много знали, так много, что количество у них, наконец, перешло в качество, и они стали с миром в других отношения, нежели обычные люди. Они работали в институте, который занимался прежде всего проблемами человеческого счастья и смысла человеческой жизни, но даже среди них никто точно не знал, что такое счастье и в чем именно смысл жизни. И они приняли рабочую гипотезу, что счастье в непрерывном познании неизвестного и смысл жизни в том же. Каждый человек – маг в душе, но он становится магом только тогда, когда начинает меньше думать о себе и больше о других, когда работать ему становится интереснее, чем развлекаться в старинном смысле этого слова.

А. и Б. Стругацкие

"Понедельник начинается в субботу"

They were magi because they had a tremendous knowledge, so much indeed that quantity had finally been transmuted into quality, and they had come into a different relationship with the world than ordinary people. They worked in an Institute that was dedicated above all to the problems of human happiness and the meaning of human life, and even among them, not one knew exactly what was happiness and what precisely was the meaning of life. So they took it as a working hypothesis that happiness lay in gaining perpetually new insights into the unknown and the meaning of life was to be found in the same process. Every man is a magus in his inner soul, but he becomes one only when he begins to think less about himself and more about others, when it becomes more interesting for him to work than to recreate himself in the ancient meaning of the word.

A. and B. Strugatsky

"**Monday begins on Saturday**"

List of abbreviations

ΔG	change of Gibbs free energy
δ	chemical shift
NMR	nuclear magnetic resonance
UV-vis	ultraviolet-visible spectrophotometry
PET	photoinduced electron transfer
DMSO	dimethyl sulfoxide
M	mol/l
CD	circular dichroism
HEPES	4-(2-hydroxyethyl)-1-piperazineethanesulfonic acid
THF	tetrahydrofuran
ACN	acetonitril
EtOAc	ethylacetate
ROESY	rotating frame nuclear Overhauser effect spectroscopy
DMF	dimethylformamide
Boc	*tert*-butyloxycarbonyl
DCM	dichloromethane
TFA	trifluoroacetic acid or trifluoroacetyl
EDC	1-ethyl-3-(3-dimethylaminopropyl)carbodiimid
HOBt	1-hydroxybenzotriazol
TBA	tetrabutylammonium
I, I_0	intensity, initial intensity
ESI-TOF	electrospray ionization with time-of-flight detection
MS	mass spectrometry
h	hour (hours)
min	minute (minutes)
r.t.	room temperature
equiv	equivalent (equivalents)
ppm	parts per million
DFT	density functional theory
DCC	N, N'-dicyclohexylcarbodiimid

DIPEA	diisopropylethylamine
a.u.	arbitrary units
DNA	deoxyribonucleic acid
ATP	adenosine triphosphate
EDTA	ethylenediaminetetraacetic acid
K_a	acid dissociation constant
Ts	4-toluenesulfonyl
Ms	methanesulfonyl
DIAD	diisopropyl azodicarboxylate
M.p.	melting point
calcd	calculated
2D	two-dimensional
NMP	nucleoside monophosphate
NDP	nucleoside diphosphate
NTP	nucleoside triphosphate
A	adenine or adenosine (depending on context)
G	guanine or guanosine (depending on context)
C	cytosine or cytidine (depending on context)
T	thymine or thymidine (depending on context)
U	uracil or uridine (depending on context)
cAMP	cyclic adenosine monophosphate
TRIS	tris(hydroxymethyl)aminomethane
conf.	configuration
COSMO model	conductor-like screening model

1. Introduction and motivation

1.1. Supramolecular chemistry: the past and the present

Supramolecular chemistry is one of the youngest research fields of modern chemistry; nevertheless, it is already considered as a "classic" one. The very first stone in the history of supramolecular chemistry was arguably made by a discovery of chlorine hydrate by Sir Humphry Davy in 1810. After 84 years Emil Fischer proposed famous "lock and key" principle suggesting that enzyme and substrate must fit geometrically to provide an effective interaction. This idea has become a foundation of molecular recognition and it has been exploited since then with correction to up-to-date knowledge.

However, modern supramolecular chemistry is considered to be born and matured in the late 1960s and early 1970s . The fast progress in this period is tightly connected with the names of D. J. Cram, J.-M. Lehn and C. J. Pedersen, who were awarded the Nobel Prize in 1987 "for their development and use of molecules with structure-specific interactions of high selectivity".[1] Since then, supramolecular chemistry has been developing in an astounding pace. Different fields, such as molecule-based electronics, molecular machines, supramolecular photo- and nanochemistry, semiochemistry (signaling devices) have grown out of it. Leading chemical review journals dedicate special issues to supramolecular chemistry frontiers almost every year, and a number of publications dealing with supramolecular systems and their applications tends to grow. Moreover, another Nobel Prize was given to J.-P. Sauvage, F. Stoddart, and B. Feringa in 2016 for the work in the field of molecular machines. These facts indicate that supramolecular chemistry is a growing area with a lot of existing and potential applications. But what is traditionally meant under the term "supramolecular chemistry"?

One of the founders of the field, Jean-Marie Lehn, has given this field a strict definition "chemistry of molecular assemblies and of their intermolecular bonds". Some other modern definitions that are important for the present work are "chemistry beyond the molecule" and "chemistry of non-covalent bond".[2]

The term "non-covalent bond" is understood nowadays as interactions and effects that play a crucial role in stability of supramolecular complexes. The most important non-covalent bond are listed below:

- hydrogen bond

- ion–ion, ion–dipole, and dipole–dipole interactions
- interactions involving π-electrons of aromatic systems: π–π, cation–π, anion–π
- solvatophobic effect
- Van der Waals and London dispersion interactions
- halogen bond[3]

Typical supramolecular complex must include at least one large molecule known as "host" and a small molecule — "guest" — that are held together with the help of non-covalent bonds. As expected, complexes with small guests such as cations, anions or water molecules were discovered first; nevertheless, these areas of supramolecular chemistry still remain interesting and present promising results mostly associated with sensing and transport in biological and environmental systems.

1.2. Recognition of cations and anions

Complexes of Schiff bases with cations obtained in 1960s were historically the first supramolecular systems.[2] Similar compound had already been used previously in coordination chemistry, but the synthesis of closed structures — macrocycles — allowed scientists to obtain metal complexes with significantly higher binding constants due to the chelate and macrocyclic effects. In the next few years first crown ethers have been synthesized and their outstanding binding properties have been discovered. After that, the area of cation recognition developed very fast producing different analogues of crown ethers, as well as new classes of receptors, some of which provided even higher affinity and selectivity towards a particular cation. Selected examples of classic and modern cation receptors are presented in Fig. 1.1.[2,4,5]

As the knowledge about cation recognition has grown, it has become clear that designing a selective host for a desired cation is a complicated task because there are many factors that influence selectivity. For example, one must consider the complementarity between the cation size and the host's cavity, solvation energies of a host and a guest, relative position of binding sites in the host, kinetics and thermodynamics of the equilibrium.

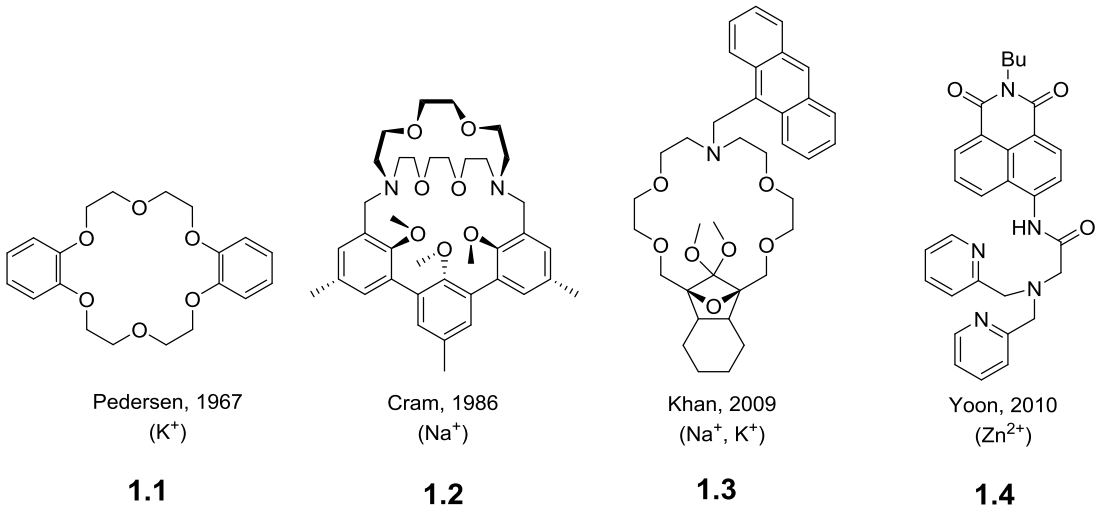

Figure 1.1: Selected examples of synthetic receptors for cations.

Most of the cations are Lewis acids, therefore, they easily interact with lone pairs of nitrogen and oxygen atoms that are often present in organic molecules. Thus, there are a lot of alternatives for the host design. Anions, on the other hand, are negatively charged and have a complete electron shell, which makes complexation with oxo- and azamacrocycles unfavorable. Moreover, even simple inorganic anions are relatively large compared to isoelectronic cations and have a variety of shapes and geometries (Fig. 1.2). This fact raises problems to design a host with a complementary geometry for a desired anion.

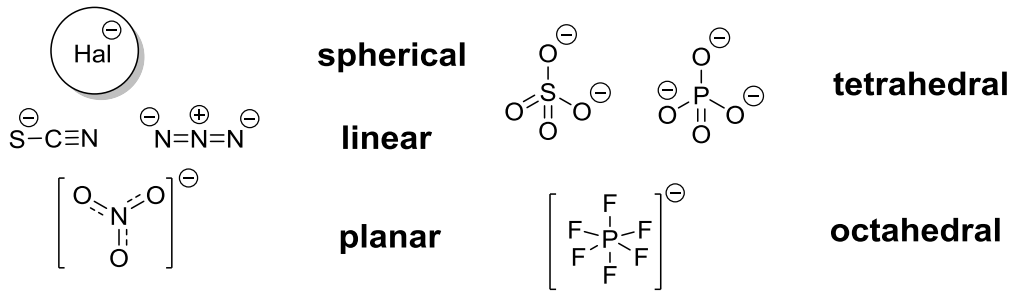

Figure 1.2: Typical geometries of inorganic anions.

Another difficulty one has to face in anion recognition is higher energies of solvation compared to cations. For example, $\Delta G_{\text{hydration}}$ (F^-) = −465 kJ/mol^{-1}, $\Delta G_{\text{hydration}}$($K^+$) = −295 kJ/mol^{-1}, whereas the sizes of these ions are similar. It means that the energy of binding must be high enough to compete with solvation. This fact becomes even more important, if the recognition process takes place in highly competitive medium, such as pure water or aqueous mixtures.

Anions are usually coordinated through hydrogen bonds, different ion–ion or π–ion interactions. Electrostatic forces are widely used in metal- or ammonium-based receptors to trap a guest molecule. In the case of metal-based receptors, a metal complex can additionally perform a function of a reporter group, whose photochemical or redox response is changed upon binding of an anion. Metal-based receptors for sulfate are briefly discussed in Chapter 2.1.4. Ammonium-based receptors were the first discovered receptors for anions. In 1968 Park and Simons found that certain macrobicyclic amines encapsulate halide ions when protonated.[6] Since that time, many efforts have been put into designing selective polyammonium receptors for anions, mostly for halogens and tetrahedral anions such as sulfate and phosphate.[7]

Receptors utilizing hydrogen bonding are often used for recognition of anions. Anions play role of hydrogen bond acceptors; therefore, a potential receptor must contain multiple sites with hydrogen bond donors. A number of different fragments of organic molecules are suitable for this role, for example, amides, pyrroles, (thio)ureas, squaramides. All of these motifs have attracted much attention and corresponding anion receptors have been studied extensively.[8–12] Selected examples of anion receptors containing these fragments are depicted in Fig. 1.3.

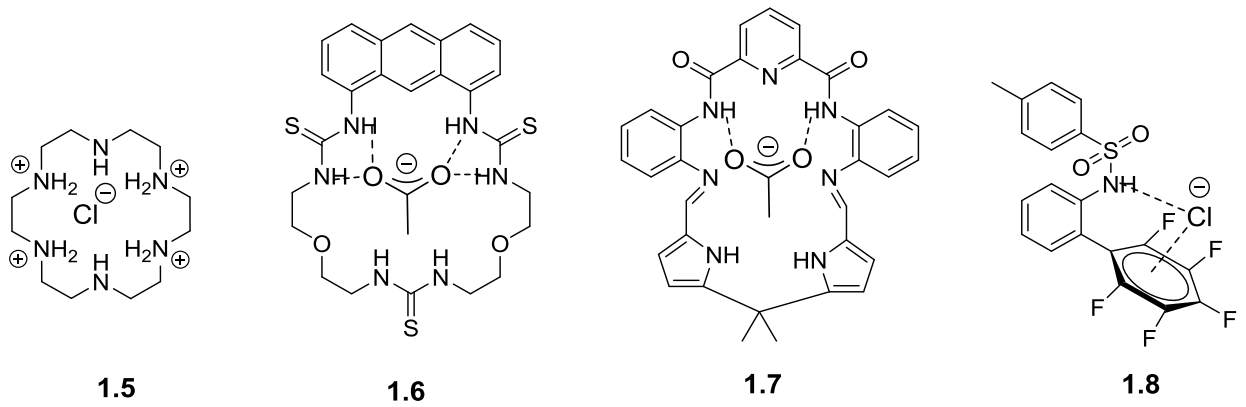

Figure 1.3: Examples of anion receptors employing different non-covalent interactions: electrostatic (**1.5**),[13] hydrogen bonds (**1.6**, **1.7**),[14,15] anion–π interactions (**1.8**)[16].

1.3. Methods for determination of binding constants and stoichiometry of complexes

In supramolecular chemistry, the important parameter of a host–guest complex is the strength of the interaction. The measure of this strength is a binding (association) constant, which is determined as an equilibrium constant between a host (H), a guest (G), and their complex:

$$H + G \rightleftharpoons HG$$

$$K = \frac{[\mathrm{HG}]}{[\mathrm{H}]\cdot[\mathrm{G}]}$$

Here, a host and a guest are bound in a 1:1 stoichiometry; however, many complexes with different host:guest ratio have been discovered. In this situation, equilibrium is described with stepwise and cumulative binding constants.

$$\mathrm{H} + \mathrm{G} \rightleftharpoons \mathrm{HG}$$

$$\mathrm{HG} + \mathrm{G} \rightleftharpoons \mathrm{HG_2}$$

Stepwise binding constants are:

$$K_{11} = \frac{[\mathrm{HG}]}{[\mathrm{H}]\cdot[\mathrm{G}]};\ K_{12} = \frac{[\mathrm{HG_2}]}{[\mathrm{HG}]\cdot[\mathrm{G}]}$$

The cumulative binding constant is:

$$\beta_{12} = \frac{[\mathrm{HG_2}]}{[\mathrm{H}]\cdot[\mathrm{G}]^2}$$

It follows from these two equations:

$$\beta_{12} = K_{11}\cdot K_{12};\ \log \beta_{12} = \log K_{11} + \log K_{12}$$

Some of the modern methods for determination of binding constants will be shortly discussed below.

1.3.1. Potentiometric titration

A number of classic host molecules, such as aza-macrocycles or cryptands (for example, **1.2**, **1.4**, **1.5**), can be protonated, and their pK_a values can be determined with the help of standard glass electrode via titration. Addition of a guest often influences the corresponding pK_a of a host, meaning that a host–guest complex possesses a different ability to accept or release a proton compared to the unbound host. Combining the data from both titrations (with and without guest) and analyzing them with available software (in this work we used Hyperquad[17]) will result in binding constants between the differently protonated forms of the host and the guest. The following problems should be taken into account: a) only hosts with suitable pK_a values may be analyzed; b) pure water or an aqueous medium with high water content is required; and c) the concentrations of the host and the guest must be at least 10^{-4} M–10^{-3} M.

1.3.2. NMR titration

NMR spectroscopic titration is one of the most commonly used techniques for the determination of binding constants in supramolecular chemistry. Compared with other

spectroscopic methods, NMR provides more details about non-covalent interactions involved in the formation of host–guest complex. For example, the protons of a host that are shifted the most during the titration experiments, are very likely involved in hydrogen bonding with a guest. The interaction equilibrium can be slow or fast on the NMR timescale. In the case of slow exchange, separate signals for the host and its complex appear in the spectrum (Fig. 1.4). Therefore, the binding constant can be determined (or at least, assessed) by simple integration of peaks from bound and unbound forms of the host. Unfortunately, such situations are very rare and most of the host–guest equilibria are fast on the NMR time scale.

If the exchange between the host and the host–guest complex is fast on the NMR time scale, then we observe shifts of the existing proton signals, usually the ones that participate in binding or are located close to the binding center. In this situation, changes in chemical shift are noted for different protons and different guest concentrations. After that, a titration curve ($\Delta\delta$ against added guest concentration) is plotted and analyzed with software such as EQNMR or HypNMR, which allows one to calculate binding constants.

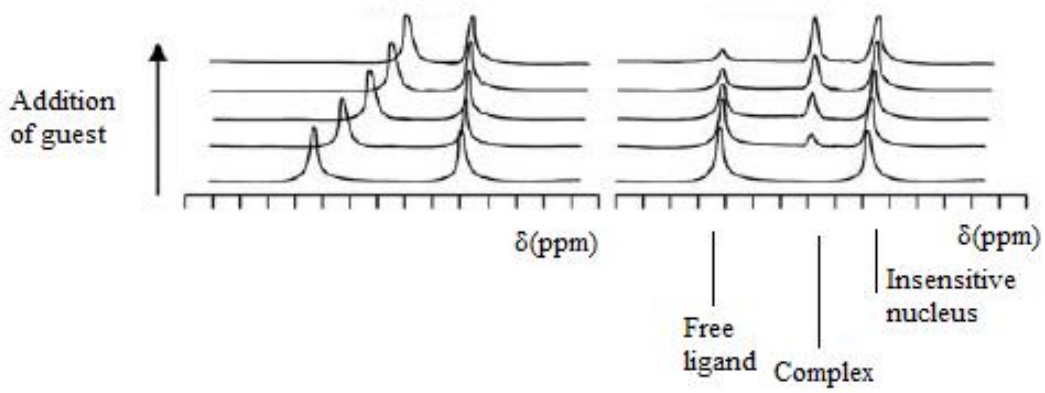

Figure 1.4: Changes in NMR spectrum in the cases of fast (left) and slow (right) exchange.[2]

1.3.3. UV-vis and fluorescence titration

UV-vis and fluorescence titrations imply monitoring the intensity of absorption or emission bands of a suitable component of a complex (typically, a host) upon titration with the other component. Both of these methods are more sensitive compared to NMR, therefore, a lower concentrations can be used (10^{-5} M and sometimes even less). In the case of UV-vis titration, an observation of at least one isobestic point is a good evidence for the complex formation. An isobestic point is a point in UV-vis spectra where absorbance remains constant at all time during titration (see example Fig. 1.5).

Detection of an isobestic point is uncommon during fluorescence titration; usually, simple enhancement or quenching of fluorescence is observed. These responses are called "turn-on" or "turn-off", respectively. However, in some cases fluorescence spectrum also can change a shape or shift in red or blue region, for example, when an excimer is formed.[18] Nowadays, an analysis of binding curves obtained from UV-vis of fluorescence titration is made by specific software, for example, Specfit or HypSpec. This software allows one to extract binding constants from titration data presuming that correct stoichiometry model is chosen.

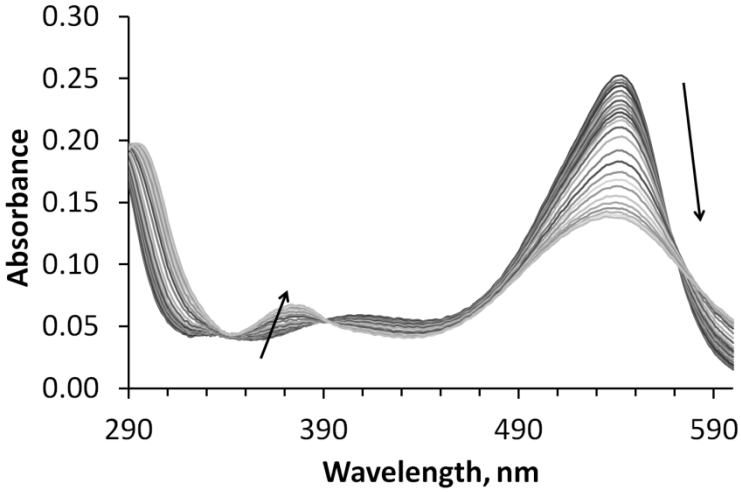

Figure 1.5: Typical changes in UV-vis spectrum of a host upon titration (shown with arrows); isobestic points are observed at 340, 390 and 570 nm.

1.3.4. Isothermal titration calorimetry

Isothermal titration calorimetry (ITC) is another popular method to describe supramolecular systems and obtain quantitative parameters. Moreover, not only binding constants may be obtained by this method, but also the enthalpy and entropy of the complex formation process. A standard calorimeter contains two identical cells, one is filled with pure solvent (reference) and another one containing one partner of a potential complex. The other component is added slowly through a syringe. Electric power heaters are connected with both cells, setting constant temperature for the reference cell and minimizing temperature difference between the cells. When small amount of the second component is added, the heat from the reaction affects temperature, which is detected by the regulator as it must maintain identical temperatures in both cells. As a result, the enthalpy is obtained directly by integration of an output plot, whereas the binding constant and the Gibbs energy come out as a result of fitting and therefore, strongly

depend on the correctness of the chosen model. Modern calorimeters can determine these parameters by installed software using nonlinear curve fitting.[19]

1.3.5 Methods for determination of stoichiometry

As discussed above, an appropriate stoichiometry model is often indispensable for correct studying of supramolecular systems. Several methods addressing this problem have been developed such as slope ratio method, mole ratio method, and the most popular continuous variation method, or the Job's method.[19] The idea of the last one is to monitor the concentration of a host–guest complex at different host–guest ratios, although the sum of concentrations must remain constant. Plotting the complex concentration against X = ([host]/([host] + [guest])) results in a graph, which is often referred to as the Job plot. X value corresponding to a maximum or a minimum can be converted into required stoichiometry, for example for 1:1 host:guest binding X would be 0.5, for 1:2 model — 0.33 and so on.

The first problem of the Job's method is the difficulty with the direct measurement of the complex concentration. Therefore, values proportional to it are normally used, for example, $[H]_0 \cdot (\delta - \delta_h)$ for NMR experiments when the exchange is fast (δ and δ_h are chemical shifts observed for the host–guest complex and for the pure host, respectively; $[H]_0$ is the host concentration in the sample).[19] Such curves, where a proportional value is plotted instead of the complex concentration, are known as modified Job plots. Another and more serious question about the Job plot has been recently brought up by Ulatowski et al.[20] It was pointed out that this method is based on the assumption of only one major complex forming, whereas a mixture of complexes exists in reality. Applying the Job's method to such systems would most probably lead to the maximum somewhere between points corresponding to the both complexes (for example, between 0.33 and 0.5 for the mixture of 1:2 and 1:1 complexes). Moreover, a maximum near 0.5 doesn't necessarily mean that only 1:1 complex is forming unless the plot is very sharp.

The persuasive arguments and conclusions in this paper led to the postulate of the Job plot's death for practical supramolecular chemistry published in the review by Hibbert and Thordarson.[21] Ulatowski et al suggested a residual plot as an alternative to the Job's method. A residual plot is a difference between observed and calculated analytical signals. When such plot has a sinusoidal form, this may be a sign of incorrect stoichiometry model. However, this method doesn't suggest the right model, therefore, the best approach is to try all possible fittings

and then compare the obtained data. The method was used in this work especially when the results of the Job plot were difficult to interpret (see Chapter 2).

1.4. Methods for visualization of binding processes and underlying mechanisms

Visualization of a binding event is very important, especially for monitoring the concentrations of essential molecules or ions in biological systems. Nowadays there is a great demand for molecules that are able to selectively recognize and detect small species.[22] A number of methods for visualization of binding process have already been developed and reviewed.[5,23–26] In principle, there are two different approaches: a) indicator–spacer–receptor (ICR) design, where a chromophore or a fluorophore is covalently linked to a receptor, and b) indicator–displacement assay (IDA), where an indicator is bound reversibly to a receptor (Fig. 1.6). The ICR approach is more popular for the design of chemosensors.

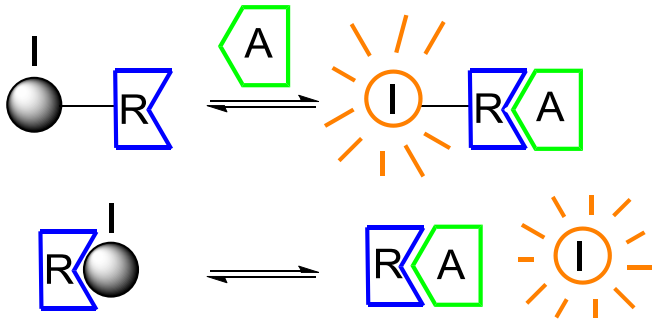

Figure 1.6: Schematic representation of the ICR (top) and IDA (bottom) approaches. R, I, A — receptor, indicator, analyte, respectively.[27]

These approaches have been used to study different mechanisms of a signal transduction. Following mechanisms in fluorescent receptors can be summarized: photoinduced electron transfer (PET), internal charge transfer (ICT) and twisted internal charge transfer (TICT), dynamic quenching, fluorescence resonance energy transfer (FRET), excimer/exciplex formation, excited-state intramolecular proton transfer (ESIPT), aggregation-induced emission (AIE), metal-ligand charge transfer (MLCT), through-bond energy transfer (TBET), and electron energy transfer (EET). In this chapter, we will shortly describe IDA and the mechanisms of a signal transduction that are the most common and/or represent special interest for the present work. The examples will be taken from the area of anion recognition, as it is the subject of our research.

1.4.1. Indicator–displacement assay (IDA)

IDA approach consists of two parts: first, an indicator is allowed to bind reversibly with a receptor, and after that, an analyte (guest) is added, which causes a displacement of the indicator and signal modulation. Therefore, the strongest requirement for IDA is a similar affinity between the pairs receptor–indicator and receptor–analyte. The most widespread types of interactions between the indicator or analyte and the receptor are hydrogen bonding, ion–ion interactions or complexing with metal centers.[27] Indicators can generate either a colorimetric or a fluorescent signal, based on this principle IDAs are classified as colorimetric or fluorescent ones.

IDAs have been developed for both cations and anions; however, nowadays this method is mostly used to sense anions,[28] including biologically important ones such as nucleotides,[29–31] citrate,[32] and cyanide.[33] A simple and elegant example of a colorimetric IDA have been developed by Gale et al. for halides detection by calix[4]pyrrole **1.9** (Fig. 1.7).[34] 4-Nitrophenolate **1.10** was used as an indicator (UV-vis active compound). When calix[4]pyrrole was added to a solution of **1.10**, the intense yellow color of the indicator disappeared. Afterwards the color was retrieved upon addition of fluoride or chloride anions because of the displacement of 4-nitrophenolate from the complex.

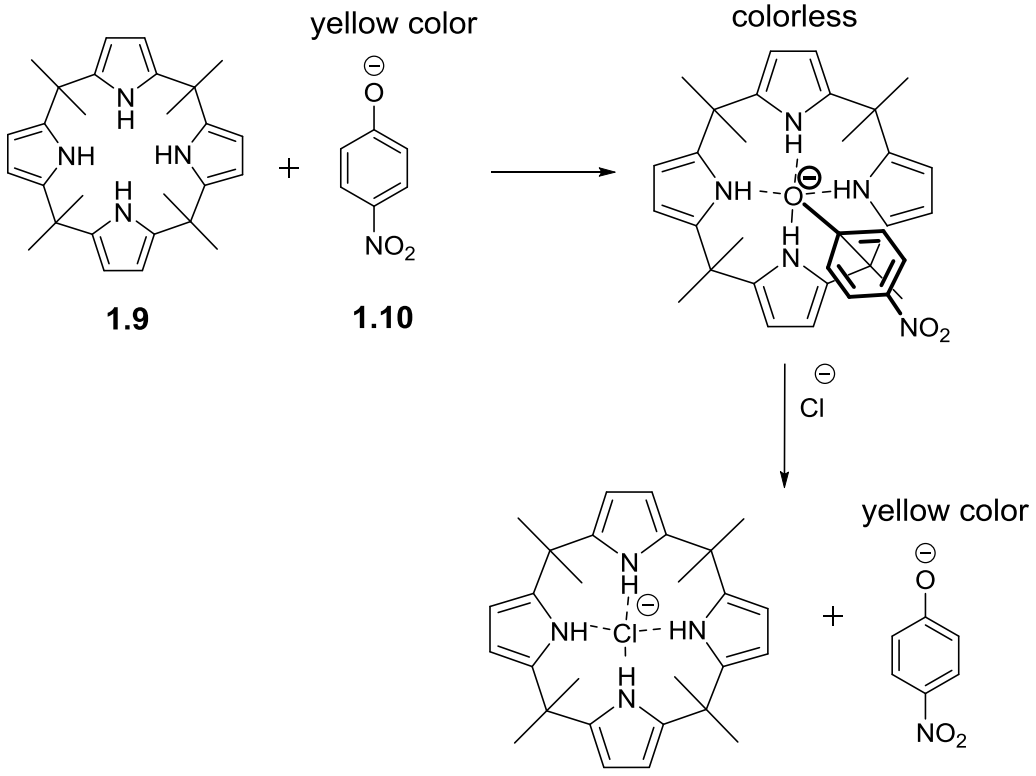

Figure 1.7: IDA used by Gale for halides detection.[34]

1.4.2. Photoinduced electron transfer (PET)

PET is probably the most common mechanism used in the design of sensors for cations and anions. A great number of reviews has been devoted to PET sensors.[24,25,35–37] PET can occur when the orbital from a part of the molecule that is close to a fluorophore has an energy level between the highest occupied molecular orbital (HOMO) and the lowest unoccupied molecular orbital (LUMO) of the fluorophore. When this "neighbor" orbital is full, an electron can be transferred to the HOMO orbital of the fluorophore after a light absorption. An electron from the LUMO orbital moves to the external orbital, and as a result, the fluorophore comes to its ground state (Scheme 1.1). This process causes partial or full quenching of fluorescence.

A typical example of "turn-off" PET sensors for anions has been developed by Gunnlaugsson et al. (**1.11**, Scheme 1.2).[38] It contains anthracene as an indicator, and thiourea as a hydrogen bond donor — anion binding site. Upon addition of anions, such as F^-, OAc^- and $H_2PO_4^-$ in dimethyl sulfoxide significant quenching of the emission (50% or higher) was observed. The authors ascribed this behavior to a PET process caused by the anion binding, and suggested that the "neighbor" orbital, which caused quenching, belonged to the bound anion.

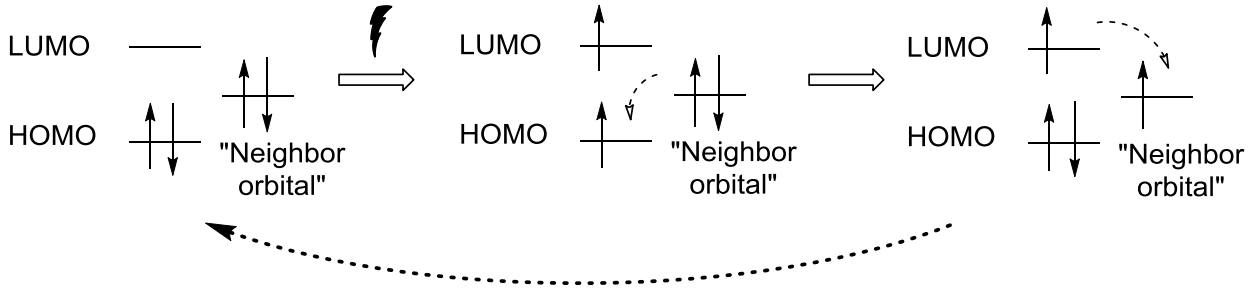

Scheme 1.1: Mechanism of PET quenching.

In spite of the fact that a PET process inevitably means quenching, and that turn-off sensors are still more widespread, turn-on PET sensors are of great interest and demand. The first specially designed sensor of that kind was reported by Czarnik in 1989 (**1.12**, Scheme 1.2).[39] The receptor's fluorescence is enhanced upon an addition of anions such as phosphate and sulfate at pH 6. The following mechanism was proposed to describe the mechanism of the fluorescence response for phosphate: at this pH all amines except for the benzylic one are protonated, therefore, the anion is coordinated by the receptor through ion–ion and hydrogen bond interactions; this leads to a protonation of the benzylic nitrogen because of an intracomplex proton transfer, which in turn leads to a fluorescence increase, as the lone pair of benzylic nitrogen is not able to quench anthracene fluorescence anymore (Scheme 1.2). An evidence in

support of this theory was the fact that emission of **1.12** also increases upon lowering the pH, which means that protonation of the benzylic nitrogen hinders PET. An alternative explanation of the "turn-on" behavior includes the formation of a hydrogen bond between the benzilic nitrogen and OH-group of phosphate, which would also inhibit the PET process.[25]

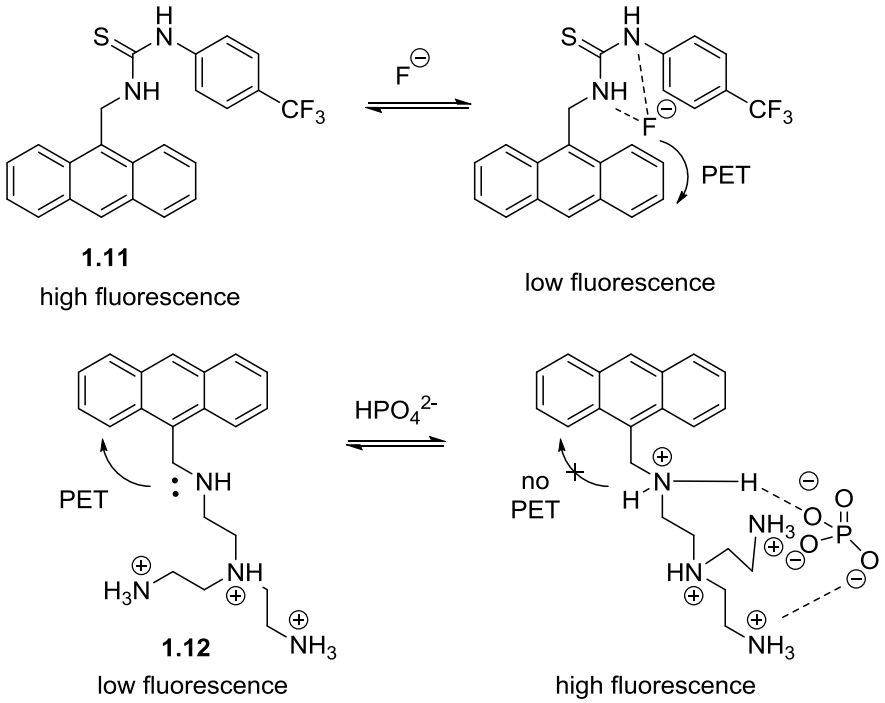

Scheme 1.2: Mechanisms of anion sensing with by "turn-off" (top) and "turn-on" (bottom) PET probes.

Czarnik's work is of great importance for the present study, because it proved that "turn-on" PET probes for anions are possible in principle. At the same time, this study raises a number of questions, such as how can we govern the selectivity of the receptor and what anions can enhance emission by hindering PET? Our contribution to this area will be discussed in Chapter 2.

1.4.3. Dynamic quenching of fluorescence

Dynamic quenching was first observed by Stokes in 1869. He noticed that emission of quinine significantly decreased upon addition of chloride.[40] This quenching can be explained in terms of electron transfer mechanism from halogen ion to the excited state of quinolinium fragment, which happens after a bimolecular collision. The process is called dynamic quenching because it is governed by a diffusional process. The property of an anion to dynamically quench the fluorescence of a dye depends on its oxidation/reduction potential, i.e. the ability to donate

electrons. Therefore, reducing anions such as I^-, Br^- or NCS^- have higher tendency to this mechanism, than NO_3^- or HSO_4^-, for example. The dynamic quenching is described by Stern–Volmer equation:

$$\frac{I_0}{I} = 1 + k_q * \tau_0 * [A] = 1 + K_{SV} * [A]$$

where k_q is the quenching constants, τ_0 is the lifetime of the excited fluorophore, K_{sv} — Stern–Volmer constant, [A] — concentration of the quencher, for example, iodide.

However, in real systems two parallel processes — dynamic and static quenching — often occur simultaneously. Static quenching is a result of host–guest complex formation. In this case, a modified Stern–Volmer equation can be applied:

$$\frac{I_0}{I} = (1 + K_{SV} * [A]) * (1 + K_{ass} * [A])$$

where K_{ass} is the association constant mentioned above. Parabolic behavior will be observed in coordinates: I_0/I–[A].

1.4.4. Fluorescence (Förster) resonance energy transfer (FRET)

FRET is a mechanism involving an energy transfer between two fluorophores in close proximity (from 10 to 100 Å). Other requirements concern a relatively high quantum yield of the donor, and a substantial overlap between the donor emission spectrum and the acceptor absorbance spectrum. FRET can be considered as a spectroscopic ruler because of the dependence on a distance between fluorophores. Due to this ability it has been applied not only to supramolecular chemistry, but also to biological problems such as analysis of DNA and protein structures, function analysis and immunoassays.[41]

Addition of an analyte can have an influence on the ratio of donor and acceptor emission bands, and this is a standard mechanism for applying FRET to sensing. The feature of FRET-based receptors is that a concentration of an analyte can be determined directly by measuring this emission ratio. For example, a FRET-based probe selective for ATP has been described recently (**1.13**, Fig. 1.8), using naphthalimide and rhodamine as donor and acceptor, respectively.[42] Clear linear dependence was obtained by plotting the emission ratios I(580)/I(530) against the concentration of ATP.

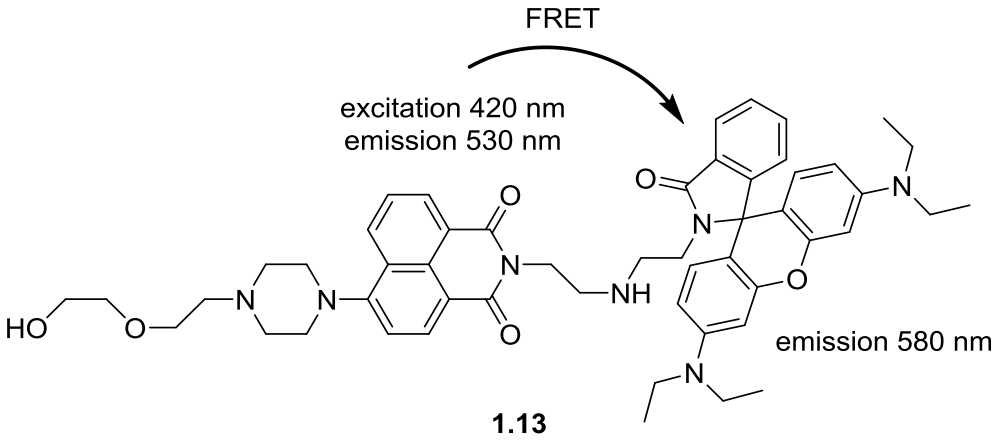

1.13

Figure 1.8: FRET-based sensor for ATP.

1.5. Motivation

Summarizing all methods and examples described above, we can conclude that supramolecular chemistry of anions is now a separate and mature field of science. Over the past two decades anion sensing has attracted much attention mostly because of the immense perspective it opens for biology and other life sciences. It is remarkable that over 70% of all cofactors and biology substrates are of anionic nature and therefore, monitoring their concentration would definitely help to control and treat many diseases. While the anion sensing has greatly developed recently, there are still numerous challenges in this field, especially concerning recognition and sensing of anions in water.

This work consists of two main parts addressing several problems of the modern supramolecular chemistry of anions. The "central" anion of the first part (Chapter 2) is sulfate. Sulfate has attracted much less attention in the literature than phosphate, which has similar ion radius and geometry. Therefore, the number of receptors that can selectively recognize and bind sulfate in aqueous solution is limited. Moreover, these receptors are often "one-of-a-kind", i.e. there is no functioning concept that would allow one to modify structures in order to improve their binding properties. The sulfate receptors from Kubik's group discussed in the next part represent an exception. Another important requirement for modern anion receptors is their applicability to real-time sensing, which can be achieved by designing a colorimetric or a turn-on fluorescent probe. Very small number of receptors for sulfate satisfy all of the mentioned requirements. Thus, the goal of Chapter 2 was to challenge this problem, and to create novel fluorescent turn-on receptors for sulfate that can function in solutions with high water content.

The second part (Chapter 3) of this thesis deals with the recognition of nucleoside triphosphates by Zn(II)-based receptors bearing aromatic dyes. However, this part is focused not on modification of the receptors, but on understanding of non-covalent interactions between the aromatic dyes and nucleobases. Dispersion interactions of such type are of great interest for chemistry and biology. These interactions are usually considered as very weak in aqueous solution, and, therefore, hard to assess and describe. In chapter 3 we address this problem and present different theoretical and experimental methods that allowed us to quantify dispersion interactions in water. Using these methods, the selectivity of different dyes towards nucleobases can be assessed, and this knowledge can be used in the design of new target receptors for nucleotides.

2. Novel fluorescent receptors for sulfate

2.1. State of the art

2.1.1. Importance of sulfate anion

Sulfate plays a significant role in different areas. Because of its abundance in biosphere, it is found in human and animal bodies, as well as in many agricultural fertilizers and industrial raw materials. High levels of sulfate can be harmful for rain, ground and surface waters; it is also worth mentioning that hazardous acid rains contain sulfuric acid as one of the main components.[43] Therefore, tap water samples are regularly controlled by the government in order to prevent increase of sulfate concentration, which causes bitter taste of water and digestion problems: diarrhea and diarrhea-induced dehydration, and intestinal pain, especially for babies.[44] On the other hand, sulfate is indispensable for some processes in human body. For example, there are a number of sulfated polysaccharides that are highly important for the normal functioning of the organism. The most well-known one is heparin, a common blood thinner. Another polysaccharide heparan sulfate is suspected to play a role in progression of Alzheimer and Parkinson's diseases. Apparently, sulfate monitoring can also be helpful for patients with diabetes: it has been shown that high concentration of sulfate in urine is associated with lower risk of renal disease progression.[45]

One more problem associated with sulfate is the radioactive waste remediation. A possible solution is a vitrification process that convert the crude waste into glass. Unfortunately, this process is highly sensitive to variation in the chemical parameters of the system. Sulfate, in particular, have been shown to influence and complicate the vitrification process.[15]

To sum up, sulfate can be considered biologically and environmentally relevant anion, and therefore, the development of new methods for sulfate sensing and recognition is highly desirable.

2.1.2. Current methods for the determination of sulfate

There are several traditional methods for sulfate determination: gravimetric, volumetric, turbidimetric, and ion-exchange chromatography. Except for the last one, all these methods are based on the reaction between barium cation and sulfate forming insoluble barium sulfate. Ion

exchanged chromatography is usually employed for biological purposes,[45,46] because it is more expensive.

Gravimetric method is based on exact mass determination of the precipitated barium sulfate. It is probably the most precise method, and it is used as a reference when other methods give contradictory results. However, it is more tedious than, for example, volumetric methods, and also requires more time.

There are several volumetric methods for sulfate determination. The standard one includes the precipitation of barium sulfate, which afterwards dissolves in excess of added EDTA. Quantity of the unreacted EDTA is measured by titration with magnesium salt in the presence of Eriochrome Black T as an indicator. A simpler method is based on a titration of a sulfate-containing solution with a barium salt, whereas excess of barium can be noticed with the help of special indicators such as nitrchromaso or chlorphosphonaso.[47]

Turbidimetry is the process of measuring the decrease in light intensity due to the suspended particles. Applying to sulfate determination, it means that barium sulfate suspension must be obtained under controlled conditions. Glycerin and sodium chloride are added to stabilize the suspension. The resulting turbidity is determined by a spectrophotometer and the results are compared to a curve obtained from standard sulfate solutions.[48]

All described methods have proven their reliability and are used nowadays. However, each of them has advantages and disadvantages. The obvious disadvantages for all methods except for the ion chromatography is long time required for analysis and necessity to use toxic barium salts. Detection with the help of fluorescence spectroscopy can be a good alternative to ion chromatography, as it is fast and has high sensitivity.

2.1.3. Metal-free receptors for sulfate

The earliest era, when sulfate recognition and binding was studied, is associated with polyazamacrocycles, which were the first class of compounds known to bind anions. For example, Lehn and co-workers in 1981 synthesized a number of aza- and oxoazamacrocycles such as **2.1** (Fig. 2.1) and studied their binding properties in fully protonated state.[49] It was found that there was no selectivity for sulfate among three macrocycles with different sizes and the number of nitrogens as well as there was very small difference in binding of sulfate and other dianions such as oxalate or malonate. This fact reflected purely electrostatic charge-dependent principle of binding for these compounds. However, the macrobicyclic effect was found to play a

role in binding: cryptand-type compound **2.2** bound sulfate stronger than its macrocyclic analogue **2.1**.[50] Similarly to the first example, compounds **2.3**[51] and **2.4**[52] showed significant affinity to sulfate in polyprotonated forms, whereas no selectivity between sulfate and selenate was observed for **2.3**.

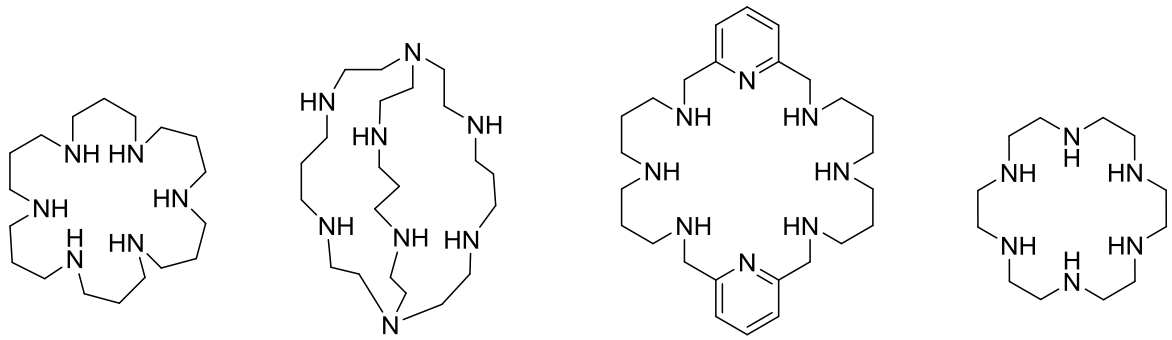

Figure 2.1: Selected examples of polyammonium receptors for sulfate.

Binding constants were determined with the help of potentiometric titrations and calorimetry. Additional NMR studies provided valuable information about binding properties of receptors. For example, it was found that methylene groups close to nitrogen underwent significant shift in ^{1}H NMR upon protonation of the nitrogen. Therefore, titrations of a ligand with an acid could give information about protonation patterns, and knowing a number of protons in the complex, one could find out the location of the protonated nitrogen that participates in binding.

Interestingly, stoichiometry of binding was a rather complicated issue. For example, one group reported complexes with **2.4** and sulfate with stoichiometry 1:1 and 1:2 (the 1:2 complex contained ligand in tetraprotonated form),[52] whereas other researchers found only 1:1 complexes for the same compound in various protonation states.[53]

Analysis of the literature leads to the conclusion that polyammonium receptors can hardly discriminate between similar tetrahedral anions, such as sulfate and selenate. Nevertheless, some efforts have been made to establish, if it is possible to achieve sulfate/phosphate selectivity using cyclic polyamines. Due to the high acidity of the sulfuric acid, sulfate is present exclusively as a dianion in a broad pH region (>2.5). Opposite to sulfate, phosphate can exist as mono-, di- or trianion depending on the pH of the medium. At low pH values phosphate is present as a mixture of mono- and dianions. Hence, a protonated receptor may have higher affinity towards sulfate rather than phosphate because at low pH values a receptor has more positive charges. Indeed, this behavior was observed for some polyaza cryptands.[54–56] However, such behavior cannot be considered as a universal pattern, as some compounds were found to be selective for sulfate or

phosphate in the whole pH range. Interestingly, receptor **2.4** demonstrated completely different selectivity at various pH values: for phosphate at low pH, for sulfate at higher pH.[53]

Simultaneously with the development of polyammonium receptors, the structure of the active center of the sulfate-binding protein (SBP) was determined. It was found that sulfate was bound in SBP exclusively by hydrogen bonds, but the association constant of the complex is nevertheless very high: 10^6 M^{-1} in pure water.[57,58] This discovery has inspired many scientists to search for neutral receptors that could also bind sulfate through hydrogen bonding. Many receptors have been created on the basis of fragments known to form strong hydrogen bonds, such as amides, sulfanilamides, ureas and thioureas, pyrroles and sqaramides (derivatives of squaric, also called quadratic acid). However, this approach has some disadvantages: first, such compounds tend to have low solubility in water, so their properties could only be studied in organic solvents. Another problem concerning specifically sulfate recognition is that the "pure" hydrogen-bond receptors are usually unable to discriminate between HSO_4^- and $H_2PO_4^-$ as they both have the same tetrahedral geometry. For example, compound **2.5** (Fig. 2.2) presented by Bowman-James et al formed a 2:1 sandwich complex with sulfate in the solid state. In chloroform solution, the receptor showed a 1:1 binding mode and similar binding constants for sulfate and phosphate, log K = 4.50 and 4.66, respectively.[59] Tris(2-aminoethyl)amine (tren), and its derivatives found a lot of applications in the recognition of anions, especially, tetrahedral anions.[60] Compound **2.6** is an urea-containing tren derivative that binds sulfate (non-selectively over phosphate) in DMSO via seven hydrogen bonds,[61] the binding constant is similar to that observed for **2.5**.

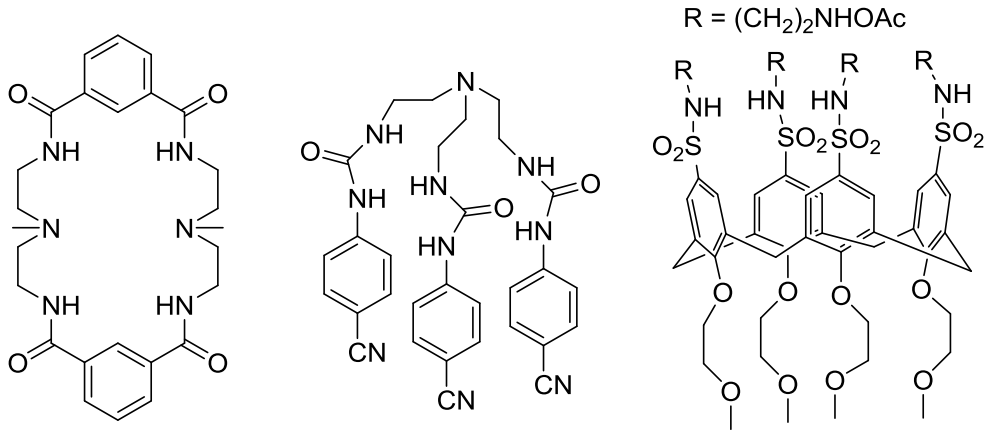

2.5 **2.6** **2.7**

Figure 2.2: Selected examples of receptors for sulfate functioning in organic solvents.

However, rationally constructed receptors based on hydrogen bonds can successfully discriminate between sulfate and, for example, halogens, perchlorate or nitrate. Compound **2.7**, calix[4]arene with amides and sulfonilamides have binding constants with hydrogen sulfate exceeding $10^5\ M^{-1}$ in chloroform, whereas the constant for nitrate is below $10^3\ M^{-1}$.[62]

The examples of receptors that bind sulfate in organic solvents discussed above, represent a very small and arbitrary chosen part of the great number published recently. For additional examples of receptors for sulfate one could refer to specific reviews concerning recognition of tetrahedral oxoanions.[63,64] Only sulfate receptors that can function in water or at least in water–organic solvent mixture with water content ≥10% will be discussed in the section below. Such receptors are more difficult to design because of high solvation energy of sulfate. However, these receptors are more interesting in terms of real applications.

Molecules containing only hydrogen-bonding sites were studied in different organic solvent–water solutions with 10–50% of water. Prevailing groups in this receptors are ureas, thioureas and squaramides.[65–71] Addition of water led in most of the cases to minor changes in properties of such compounds. For example, it was found that some complex equilibria present in DMSO disappeared in 9:1 DMSO–water mixture.[66] Also a gradual diminishing of binding constants was observed along with increasing water content. Thus at 50% of water the receptor with four urea groups had a binding constant with sulfate only 47 M^{-1}, whereas at 10% of water the constant exceeded $10^4\ M^{-1}$.[70] Nevertheless, few compounds demonstrated sufficient selectivity for sulfate over dihydrogen phosphate,[71] for example, a receptor containing benzothiazole binding sites.[72]

A very important contribution in the field of sulfate recognition was made by S. Kubik and his group. He presented a new class of peptide receptors that combines several important features: a number of hydrogen bond donor groups and excellent solubility in such competitive solvents as water or methanol. The first compound of this family **2.8** (Fig. 2.3) showed affinity towards halogens, sulfate and tosylate.[73] The binding properties were studied by ESI-MS, NMR and X-ray analysis. It was found that the stability of the halide complexes decreased in the order $Cl^- < Br^- < I^-$ and that the receptor tended to form 2:1 "sandwich" complexes, where the anion (halides or sulfate) located between two molecules of the host. Selectivity towards iodide was attributed to a good match between the size of the cavity and the radius of the anions. The fact that **2.8** bound sulfate more strongly than, hydrogen phosphate or hydrogen carbonate, was

explained by the propensity of sulfate to form multiple hydrogen bonds with NH fragments of the receptor.

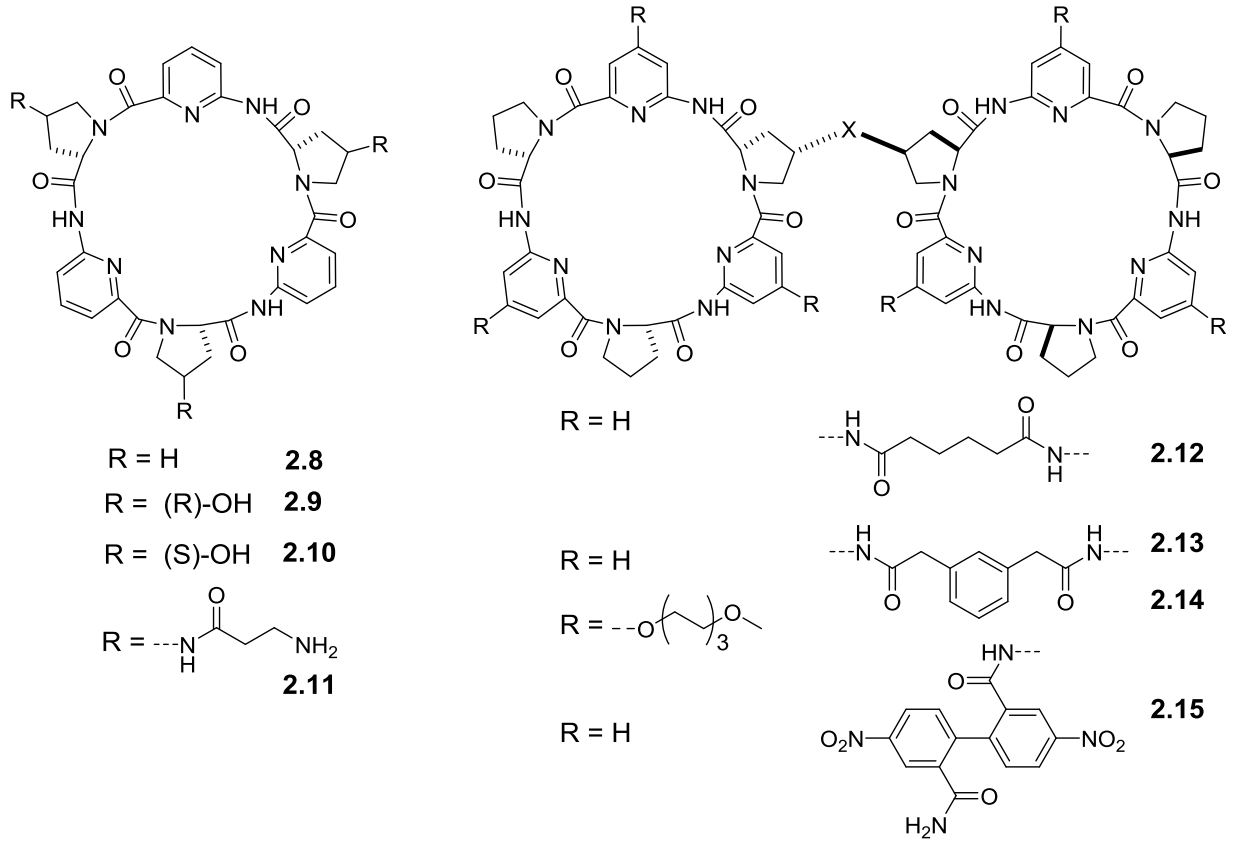

Figure 2.3: Sulfate receptors created by Kubik's group.

Due to the limited solubility of **2.8** all measurements were made in the system 8:2 water–methanol. In order to increase the water content proline was replaced by hydroxyproline, which resulted in compounds **2.9** and **2.10**.[74] Interestingly, such a modification prevented the formation of 2:1 complexes and only 1:1 complexes were found for **2.9** with the binding constants 14 M^{-1} for iodide and 52 M^{-1} for sulfate in pure water. CD spectra demonstrated that conformation of **2.9** resembled the one of **2.8,** which made the compound suitable for anion binding. However, the change of hydroxyproline configuration (compound **2.7**) led to drastic difference in conformation and, therefore, in properties. The solubility of **2.10** in water–methanol mixtures was lower than that of **2.8** or **2.9**; moreover, at room temperature it existed as a mixture of two conformers. These facts complicated quantitative evaluation of anion binding properties of **2.10**.

Complexes with the stoichiometry different from 1:1 are usually more difficult to analyze. Therefore, two hexapeptides **2.8** were connected with different linkers (compounds **2.12**–**2.15**).

Adipinic acid was chosen first to connect macrocycles as a result of molecular modeling of iodide complexes.[75] Indeed, compound **2.12** bound halogens, nitrate and sulfate in a 1:1 manner. However, the solubility of **2.12** allowed one to study binding properties only in a 1:1 methanol–water mixture. In this solvent system, a particularly high affinity and selectivity for sulfate was observed: K(sulfate) = $3.55 \cdot 10^5$ M^{-1}, K(iodide) = $8.9 \cdot 10^4$ M^{-1}. The results of this study motivated researchers to investigate the influence of the linker on binding properties.[76] It was found that compound **2.13** demonstrated higher affinities towards sulfate ($9.33 \cdot 10^5$ M^{-1}). The solubility of **2.13** in water, however, remained limited, therefore, solubilizing triethyene glycol residues were appended giving **2.14**.[77] This modification didn't induce a decrease in the binding constant with sulfate comparing to **2.13** in a 1:1 methanol–water. An improved solubility of **2.14** made possible to study binding properties in the systems containing up to 95% of water. As expected, higher amounts of water led to weaker binding, i.e. reducing the binding constant for sulfate to $5 \cdot 10^4$ M^{-1}. Thus, the selectivity between sulfate and iodide observed for **2.12** and **2.13** was completely lost in 95% of water and binding with iodide became even stronger than that with sulfate. The reason for this could be a higher solvation energy of sulfate, which is more pronounced when the solutions has higher water content.

2,2′-Dinitrobiphenyl fragment (compound **2.15**) was also among the tested linkers. Although its binding properties towards sulfate were not the best ones in that study,[76] it possessed luminescent properties. Fluorescence of compounds with such linkers depends on the dihedral angle between two aryl rings. Upon the binding of sulfate this angle changed significantly, which induced quenching of the fluorescence.[78] Binding constant with sulfate remained high (log K = 4.12, 1:1 water–methanol) even in the presence of 100 equiv of chloride.

More receptors for sulfate were obtained from dynamical combinatorial libraries by using reversible disulfide chemistry.[79,80] The building blocks can react reversibly with each other. An addition of a guest shifts the equilibrium and favors the formation of the most effective receptor for this guest. This approach allowed the authors to find a receptor with exceptionally high binding constant for sulfate (log K = 8.67) in the mixture 2:1 acetonitrile–water.

Unfortunately, structural modification of compounds like **2.8** apart from the introduction of hydroxyproline and its derivatives is synthetically very challenging. Therefore, a number of analogues containing 1,2,3-triazole unit instead of proline were obtained.[81,82] In the case of 1,5-disubstituted triazoles, the pseudopeptide compound indeed showed high affinity towards sulfate, although the maximum water content during measurements reached only 33%.[81]

Interestingly, when a similar 1,4-disubstituted triazole was studied, it demonstrated very low solubility (only in DMSO or organic solvents with at least 5% of DMSO), and stoichiometry of the anion complexes was different from the one observed for **2.8** or 1,5-disubstituted pseudopeptide.[82] The triazole-containing linker was also used to design a cage-like receptor, which consisted of triply linked pairs of hexapeptides.[83] The sulfate complex of this cage was one order of magnitude more stable than that of the analogue with only one linker.

The most prominent receptor created by Kubik's group for sulfate binding in water was synthesized by substitution of proline's hydrogens in **2.8** to the residue of β-alanine, compound **2.11**.[84] The solubility of this receptor was excellent, so it was possible to perform all measurements in pure water. Moreover, due to the high protonation constants of primary amines, it existed almost completely in a triprotonated form up to pH 7. Interestingly, the ability of **2.11** to discriminate between sulfate and iodide, which was a typical competitor for such compounds, is unclear, as it was not mentioned in the article. The properties of **2.11** were studied in different phosphate and acetate buffers with pH values 2.3–7.0. The highest constant (log K = 4.20) was observed in the acetate buffer. As expected, the presence of similarly-structured phosphate hindered the binding, but even in the phosphate buffer (pH 7) the constant was significant (log K = 2.44). These results demonstrate that combining electrostatic interactions with hydrogen bonding is a very promising approach for sulfate binding.

Other researchers have also employed this approach. Thus, compound **2.16** (Fig. 2.4) containing squaramides and positively charged ammonium groups demonstrated moderate selectivity for sulfate over oxalate and good selectivity over phenylphosphate in the system 9:1 methanol–water.[85] Indicator displacement assay (IDA) approach was used to provide fluorescent recognition. First, addition of **2.16** to fluorescein produced non-fluorescent complex, which was destroyed upon addition of sulfate anion, causing an enhancement of fluorescence. Furthermore, this method was applied for a similarly-structured acyclic compound to develop a new method for simultaneous determination of sulfate and phosphate. In that study two different receptor–dye complexes provided different affinity towards anions.[86] Another squaramide-based system for sulfate recognition was created using boehmite nanoparticles.[87] With binding constant log K = 4.98 for sulfate and 40-fold selectivity over phosphate, this system remains one of the most efficient sulfate receptors in pure water described so far

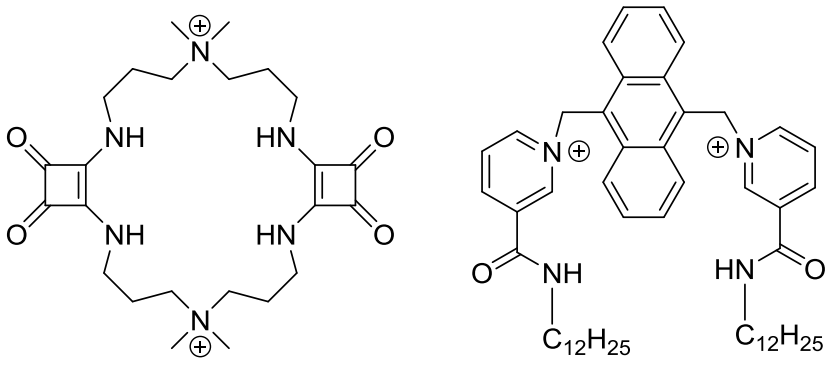

2.16

2.18

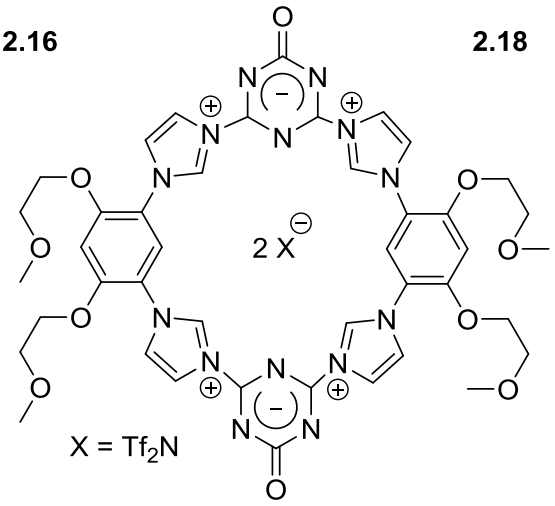

2.17

Figure 2.4: Examples of sulfate receptors.

In 2013 Zhou et al reported fluorescent tetrakisimidazolium macrocycle **2.17** with high affinity and selectivity for sulfate dianion over monoanions.[88] Four methoxyethoxy chains provide good solubility of the receptor in pure water. The receptor binds sulfate in a 2:1 stoichiometry with binding constant β_{12} = 8.6 × 10^9 M^{-2}. The stability of the complex was attributed to strong electrostatic interactions between imidazoliums and sulfate, suitable geometry of cavity, and π–π stacking interactions. Addition of sulfate caused approx. a 3-fold increase in fluorescence, while other anions induced only small fluorescence changes.

In a recent study by Saini and Kumar[89] compound **2.18** and an analogous amide without dodecyl substitutes were described. On the one hand, **2.18** demonstrated excellent selectivity for sulfate over all kinds of anions including phosphate in a 9:1 water–DMSO mixture. Moreover, a 16-fold increase in fluorescence was observed after addition of only 5 equiv of sulfate. On the other hand, there are some intriguing questions that arise in connection with this study. First of all, one can find hydrogen sulfate in the list of "failed" anions, for which this receptor is not selective. This is rather surprising, as hydrogen sulfate cannot exist in HEPES buffer at pH 7.4,

which was used in the study, rather it exists in a dinegative form at this pH. Thus, the data presented in this work cannot be considered as reliable.

Indolium derivative **2.19** (Fig. 2.5) can serve as an example of a hydrogen sulfate receptor based on reversible aggregation.[90] Here, in particular, a formation of H-aggregates inducing hypsochromic shift was observed in 1:1 water–ethanol. Aggregation was accompanied by dramatic changes in UV-vis and fluorescence spectra, and the color of solution became bright yellow instead of red. Authors suggested that hydrogen sulfate was firstly bound with **2.19**, and afterwards the complex aggregated in a head-to-tail fashion. Interestingly, sulfate dianion didn't lead to any changes in the receptor's properties, so the selectivity can be at least partially provided by high acidity of hydrogen sulfate dianion. For the similarly-structured compound **2.20**, an aggregation-induced emission was observed upon addition of both sulfate and hydrogen sulfate.[91] Sulfate-induced aggregation and crystallization of receptors/dyes attracted much attention in recent years.[92–94]

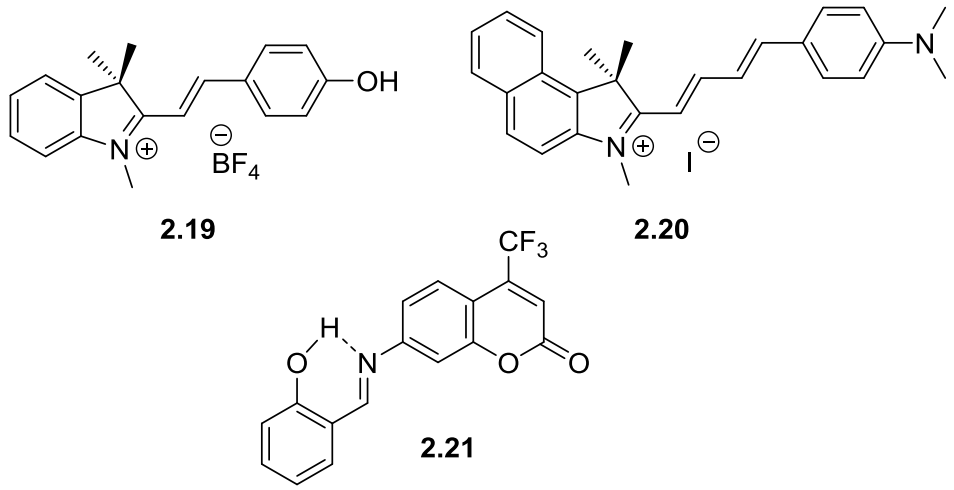

Figure 2.5: Selected examples of hydrogen sulfate or sulfate receptors.

A number of receptors for sulfate or hydrogen sulfate described so far contain a salicylimine fragment, compound **2.21** can serve as an example.[95] This receptor, in particular, demonstrated high selectivity for hydrogen sulfate over other monoanions including dihydrogen phosphate in a 1:1 water–acetonitrile mixture. Fluorescence intensity of **2.21** increased 10-fold upon addition of hydrogen sulfate. In this study, it was suggested that a turn-on behavior is due to the suppression of PET process, which was initially caused by the 6-membered ring with intramolecular hydrogen bond (hydroxyl group–imine). Another work explained the changes in fluorescence upon addition of hydrogen sulfate in terms of tautomerization of azophenol to quinone-hydrazone.[96] The selectivity for sulfate and quenching of fluorescence was assigned to an

inhibition of ESIPT (excited state intramolecular proton transfer) process.[97] These examples demonstrate that salicylimine-based compounds might be perspective for sulfate recognition, but a clear understanding of the binding mechanism is still lacking.

Some colorimetric receptors for hydrogen sulfate based on rhodamine B have been described in the literature.[98,99] One of the receptors was used to modify cellulose paper giving a selective sensor for hydrogen sulfate functioning in 100% water with a turn-on response.[98] A buffer was not used in this study, and it is not clear in which protonation form sulfate was present in solution. It is known that spirolactam ring of the rhodamine B derivatives is influenced by pH: at basic pH values the ring closed and is colorless and non-fluorescent; at acidic pH values the ring is open, and the solution is pink and fluorescent. Therefore, if pH of the solution is not kept constant, addition of hydrogen sulfate decreases the pH value, which leads to pink color and high fluorescence emission. Thus, acidic properties of hydrogen sulfate may be the reason for the selectivity. For example, in one study it was shown directly that hydrogen sulfate preference was provided by the ability of the anion to hydrolyze an imine, which, in turn, was very likely influenced by acidity of the medium.[100]

Finally, some approaches have been found to provide applications for compounds with low water solubility but presumable affinity towards sulfate. Anion-selective electrodes have been created on the basis of urea- and thiourea-containing molecules.[101,102] The formation of nanoparticles helped to develop hydrogen sulfate selective systems.[103–105] The studies on nanoparticles require more research, because the origins of sulfate selectivity are usually unclear; moreover, different methods used for preparation of nanoparticles increase a number of parameters to be taken into consideration.

2.1.4. Metal-based receptors for sulfate

Receptors for sulfate containing metal ions are less common compared to metal-free receptors. Different ferrocene-based receptors for anions have been developed by P. Beer and his group (Fig. 2.6). This class of receptors have proven its effectiveness in transforming interactions between a host and a guest into measurable changes of the redox potential of the ligand. For example, it was found that aminoamide **2.22** had a preference for hydrogen sulfate over phosphate and chloride in chloroform and acetonitrile.[106] The authors recognized the role of acidic properties of hydrogen sulfate in the binding process. Two different binding modes were proposed for **2.22**: the first one included only hydrogen bonds from amine and amide

groups; the second one was based on both electrostatic interactions between the protonated amine and hydrogen bonds. The last mode was observed for hydrogen sulfate and bromoacetic acid. The cathodic shift for sulfate was the highest among all anions, closely followed by phosphate. Later, macrocyclic polyaza ferrocene receptors were synthesized and their properties were studied by potentiometry in THF–water solution.[107] Similar to non-metallic polyaza macrocycles, the sulfate/phosphate selectivity was strongly influenced by pH. Thus, some of the studied receptors demonstrated a selectivity for sulfate at acidic pH values, and some of them — for phosphate at neutral and basic values. However, the absence or presence of such selectivity pattern seems to be strongly dependent on the structure of the receptor. The same group has recently described a new [3]rotaxane, which forms 1:1 complex with sulfate in the system containing 10% of water with stability constant $>10^4$ M^{-1}.[108]

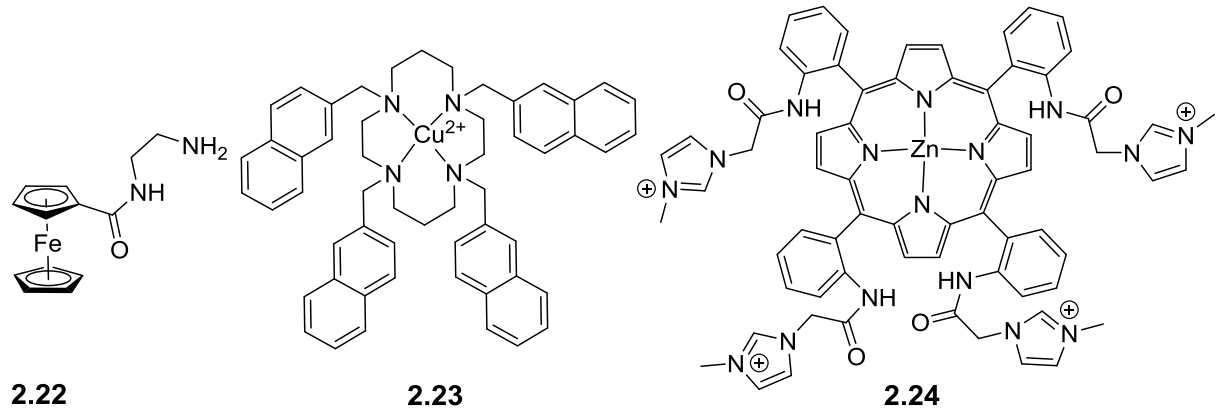

2.22 **2.23** **2.24**

Figure 2.6: Metal-based receptors for sulfate and hydrogen sulfate.

The copper complex of cyclam **2.23** demonstrated interesting fluorescent behavior in the presence of anions.[109] Thus, at acidic pH values (<5) addition of hydrogen sulfate caused approx. 5-fold enhancement of fluorescence, whereas phosphate induced only small increase, and halogens didn't influence fluorescence at all. The probable reason for the enhancement as suggested by authors was a competition between the metal ion and sulfate for coordination with **2.23**. However, the selectivity for sulfate observed in the system 7:3 THF–water was lost in the mixture of THF and acetonitrile, where **2.23** demonstrated an increase in fluorescence upon addition of phosphate.

Synthetic zinc porphyrin **2.24** presented by Beer et al was studied in organic and semiaqueous solvents.[110] It was found that **2.24** showed more pronounced affinity for sulfate than for phosphate in DMSO and DMSO–water mixtures. The binding constants with sulfate were estimated to be $>10^6$ M^{-1} in this solvents. Perturbations in UV-vis spectra of **2.24**, namely a

bathochromic shift and intensity changes were attributed to axial ligation of the anion to the Lewis acidic zinc centre. Interestingly, the analogous compound without imidazolium fragments demonstrated no affinity for hydrogen sulfate. Thus, the combination of attractive electrostatic charges and potential imidazolium methine hydrogen bond donating groups of **2.24** resulted in a selective receptor for hydrogen sulfate.

2.2. New sulfate receptor containing 1,2-phenylenediamine fragment

A. M. Agafontsev, T. A. Shumilova, P. A. Panchenko, S. Janz, O. A. Fedorova, E. A. Kataev, *Chem. - A. Eur. J.* **2016**, *22*, 15069–15074. Utilizing a pH-sensitive dye in selective fluorescent recognition of sulfate.

The synthesis and characterization of the described compounds was conducted jointly by T. Shumilova, A. Agafontsev and S. Janz. The binding studies were performed by T. Shumilova..

2.2.1. Design of the receptor

Dipyrrolylmethane-based compounds are known to be excellent anion receptors due to an ability of pyrroles NH fragments to form strong hydrogen bonds. Such receptors have been described, among others, by P. Gale and by our group.[111–113] For example, the 2,2'-bisamidodipyrrolylmethane receptor **2.25** (Fig. 2.7) containing two aniline fragments is highly selective for fluoride in DMSO-d_6 solution.[112] However, the selectivity of the receptor changes dramatically towards dihydrogen phosphate when D_2O (25% vol.) is added. Thus, the core structure of **2.25** was a good starting point for the design of a new receptor with the selectivity for tetrahedral oxoanions in aqueous medium. It has been recently described by our group that 2,2'-dipyrrolylmethane binding motif with propyl substituents in the *meso*-position demonstrates better selectivity for tetrahedral oxoanions than the one with dimethyl substituents, because the sterically large groups favor the pyrrole rings to orient towards the anion.[113]

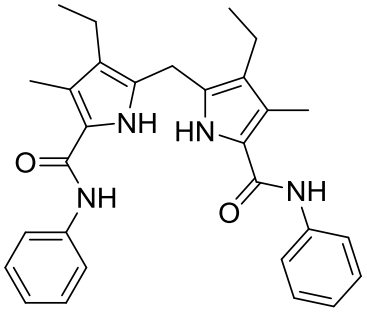

2.25

Figure 2.7: The receptor for oxoanions in aqueous solution reported by Gale.

The free amino groups were introduced in the *ortho*-position to the amides with the goal to form hydrogen bonds and electrostatic interactions (when amines are protonated) with anions. The pK_a values of the aniline group are typically 4–5. As discussed above, in a number of studies polyaza receptors show selectivity for sulfate over phosphate at low pH values.[56,109] Therefore,

we expected sulfate selectivity at pH values below 5, at which aniline amino groups are protonated.

A naphthalimide dye was introduced to obtain a fluorescent receptor. Preliminary experiments demonstrated that compounds with an aniline fragment at the amide end of naphthalimide and a methoxyethoxy substituent at 8th position change their fluorescence intensity depending on the pH. Namely, at low pH values an enhancement of fluorescence was observed, while at neutral and basic conditions there were no changes in spectra. These results are in agreement with those obtained for classical PET probes. When the amine and amide groups are in *ortho*-position, the naphthalimide fragment could be introduced in *para*-position to one of them, and *metha*-position to other one, depending on a synthetic approach (compounds **2.26**, **2.27**, Fig. 2.8). The position of the dye was not important to us, so we developed synthetic strategies for both compounds.

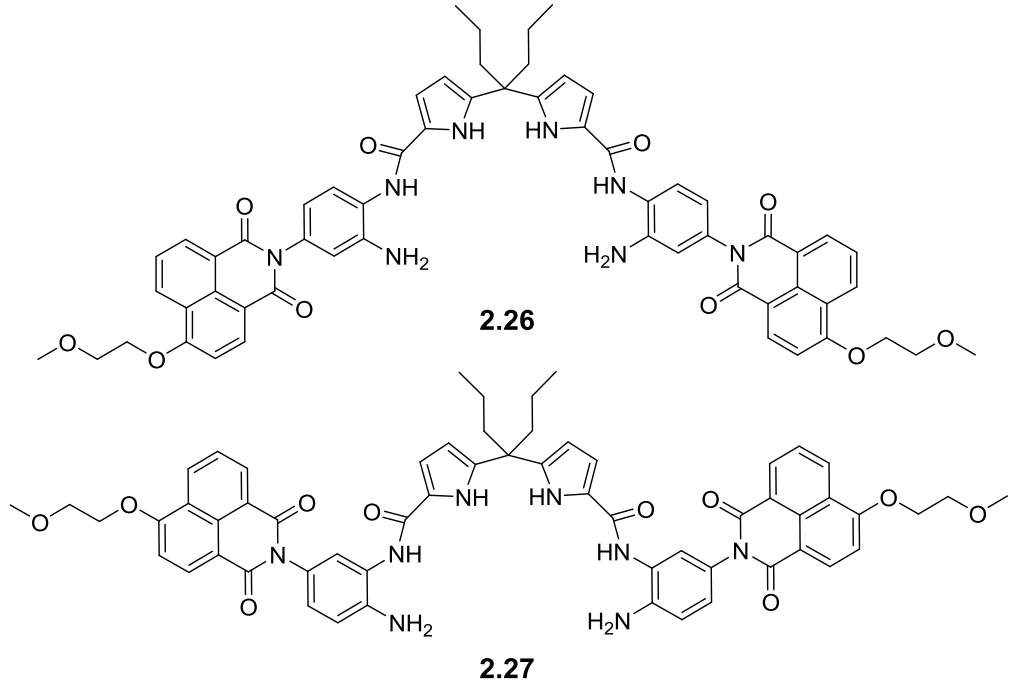

Figure 2.8: Possible structures of the target receptor.

2.2.2. Synthesis of the target receptor

The first step in synthesis of **2.26** and **2.27** consisted in preparation of the substituted naphthalimide. First, 1,8-bromonaphthalimide reacted with 2-nitro-1,4-phenylenediamine as described in the literature resulting in compound **2.28**.[114] Substitution of bromide was performed in 2-methoxyethanol, which served both as a reagent and a solvent (Scheme 2.1).[115]

A synthetic path leading to isomer **2.26** began with an acylation of **2.29** with the diacid obtained from *meso*-substituted dipyrrolylmethane (**2.30**, corresponding dichloride **2.31**). Compounds **2.30** and **2.31** were synthesized as described previously.[113] However, the reaction between nitroamine **2.29** and diacid **2.30** in the presence of different coupling reagents (see Scheme 2.2) proceeded with very low conversion. Acylation with dichloride **2.31** in THF led to the same result. There are two main factors causing low conversion: extremely low solubility of **2.29** in organic solvents except for DMF (at elevated temperature), and the fact that the nitro-group in *ortho*-position decreases the reactivity of the amino group.

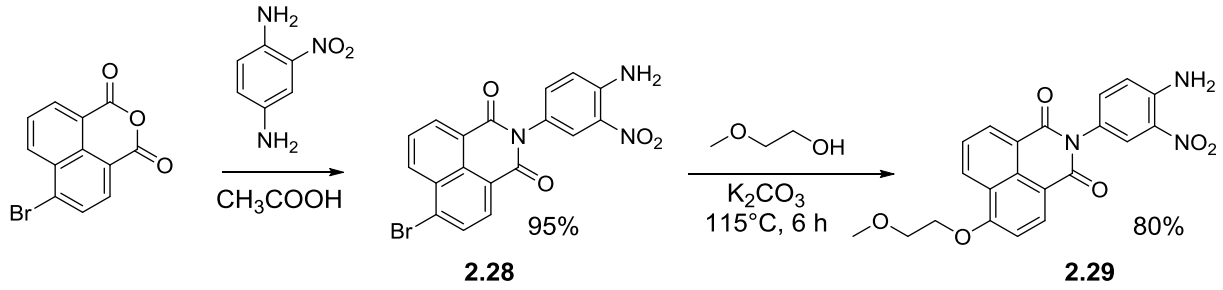

Scheme 2.1: Modification of the naphthalimide fragment.

Thus, attempts of direct acylation of **2.29** were not successful. Therefore, we focused on preparation of compound **2.27**. The chosen synthetic path included the protection of the amino group of **2.29**, followed by reduction of the nitro group and coupling with dipyrromethane derivatives **2.30** or **2.31**. Finally, the deprotection of the amino group was supposed to lead to the target compound **2.27**.

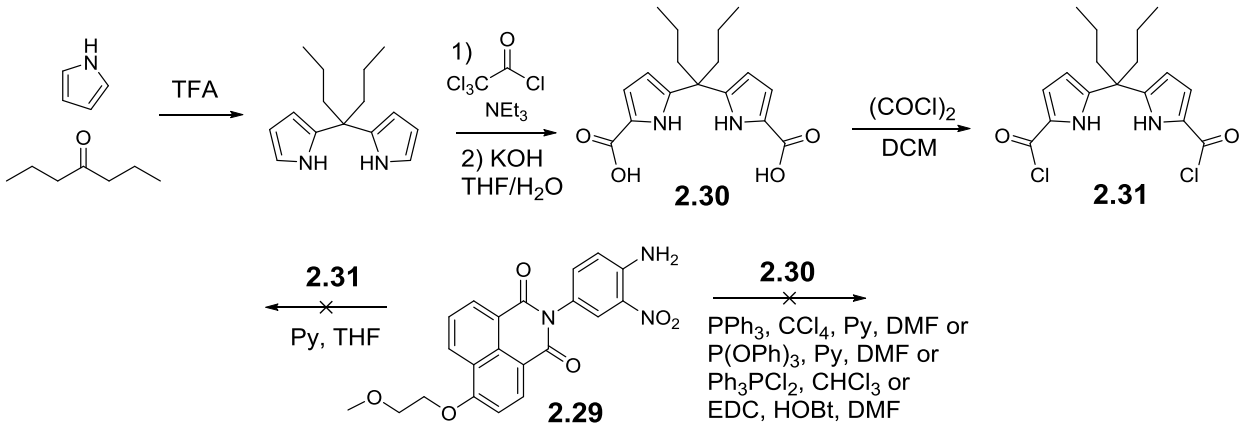

Scheme 2.2: Preparation of dipyrrolylmethane derivatives and attempts of direct acylation.

Numerous protecting groups for amines are described in the literature. Our first choice was an amide-based trifluoracetyl protecting group. It was successfully introduced by the reaction of

2.29 with trifluoroacetic anhydride in dichloromethane (product **2.32a**, Scheme 2.3). Hydrogenation with tin (II) chloride in ethanol produced amine **2.33a**. Acylation of the product with dichloride **2.31** resulted in protected precursor of **2.27** — compound **2.34a**. Unfortunately, the last deprotection step was the most difficult, because none of the traditional systems used for removing of trifluoracetyl protective group were effective for **2.34a**. A complex mixture of products was obtained in all cases. Basic conditions employed for deprotection led to destruction of the target molecule due to hydrolysis of the amide bonds. Thus, we decided to try tert-butyloxycarbonyl (Boc) protecting group, because it can be removed under acidic conditions.

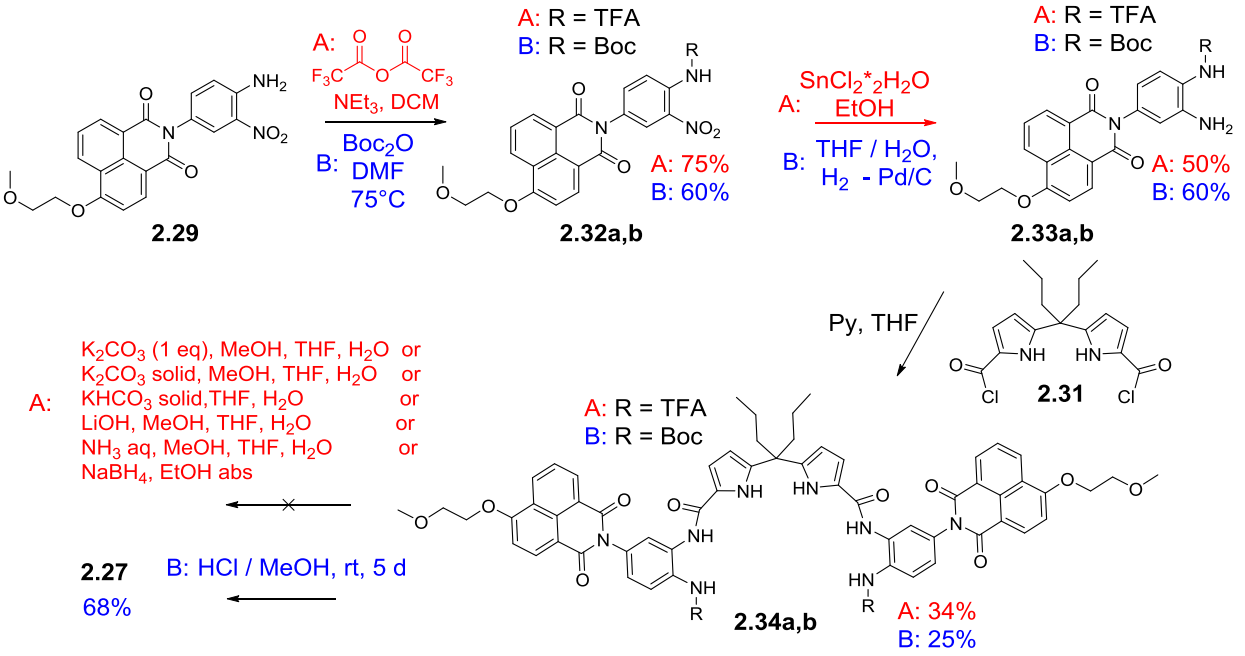

Scheme 2.3: Synthesis of target receptors.

Classical Boc-protection conditions were not appropriate for **2.29**. The reaction of the nitroamine with Boc_2O yielded a di-Boc derivative. Similar reactions are described in the literature.[116] Thus, we developed a new method, which involved heating of **2.29** in DMF in the presence of tert-butyloxycarbonyl anhydride. This reaction conditions allowed us to prepare protected nitroamine **2.32b** in a 60% yield. The reduction by hydrogen in the presence of Pd/C and subsequent coupling with diacid dichloride **2.31** proceeded smoothly and resulted in precursor **2.34b**. Finally, deprotection of **2.34b** by hydrochloric acid in methanol produced target compound **2.27** in 68% yield after column chromatography. To study the influence of the dipyrrolylmethane fragment on binding properties of receptors, we also prepared diamine **2.35** by reduction of the nitro group of **2.29** (Scheme 2.4).

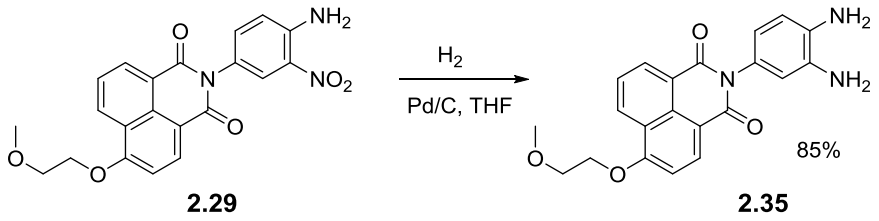

Scheme 2.4: Preparation of reference compound **2.35**.

2.2.3. Anion binding properties

Conformation of a receptor often plays a crucial role for its binding properties. To establish the conformation of **2.27** a $^{1}H–^{1}H$ ROESY experiment was carried out in DMSO-d_6. The observed cross signals (between the propyl CH and the pyrrole CH, the pyrrole NH and the amide NH, the amide NH and the amine group) proved that **2.27** adopts a *cis*-conformation relative to amino groups, as shown in Fig. 2.9. Hence, the receptor is already preorganized for the binding of an anion.

Next, we needed to choose appropriate conditions to study binding properties. NMR method requires concentration of the receptor more than 10^{-4} M. This concentration could be achieved by using 25% of water content in DMSO. To prepare a stock solution for the titration, we mixed a receptor solution in DMSO and aqueous phase containing 0.6 M $NaClO_4$ to fix the ionic strength, and added 2 equiv of $HClO_4$ to protonate the receptor. According to the measurements, the solution had pH 3. Titration experiments with $TBAHSO_4$, $TBAH_2PO_4$ and TBAOAc were carried out using these conditions. Protons appended to nitrogen atoms such as amine, amide or pyrrole NHs cannot be seen by NMR in aqueous mixtures due to exchange with deuterium. However, these protons are usually very important as they can directly participate in hydrogen bonding with anions and, theoretically, should have the strongest changes in chemical shifts. CH protons typically give lower changes but can also deliver information about the binding process.

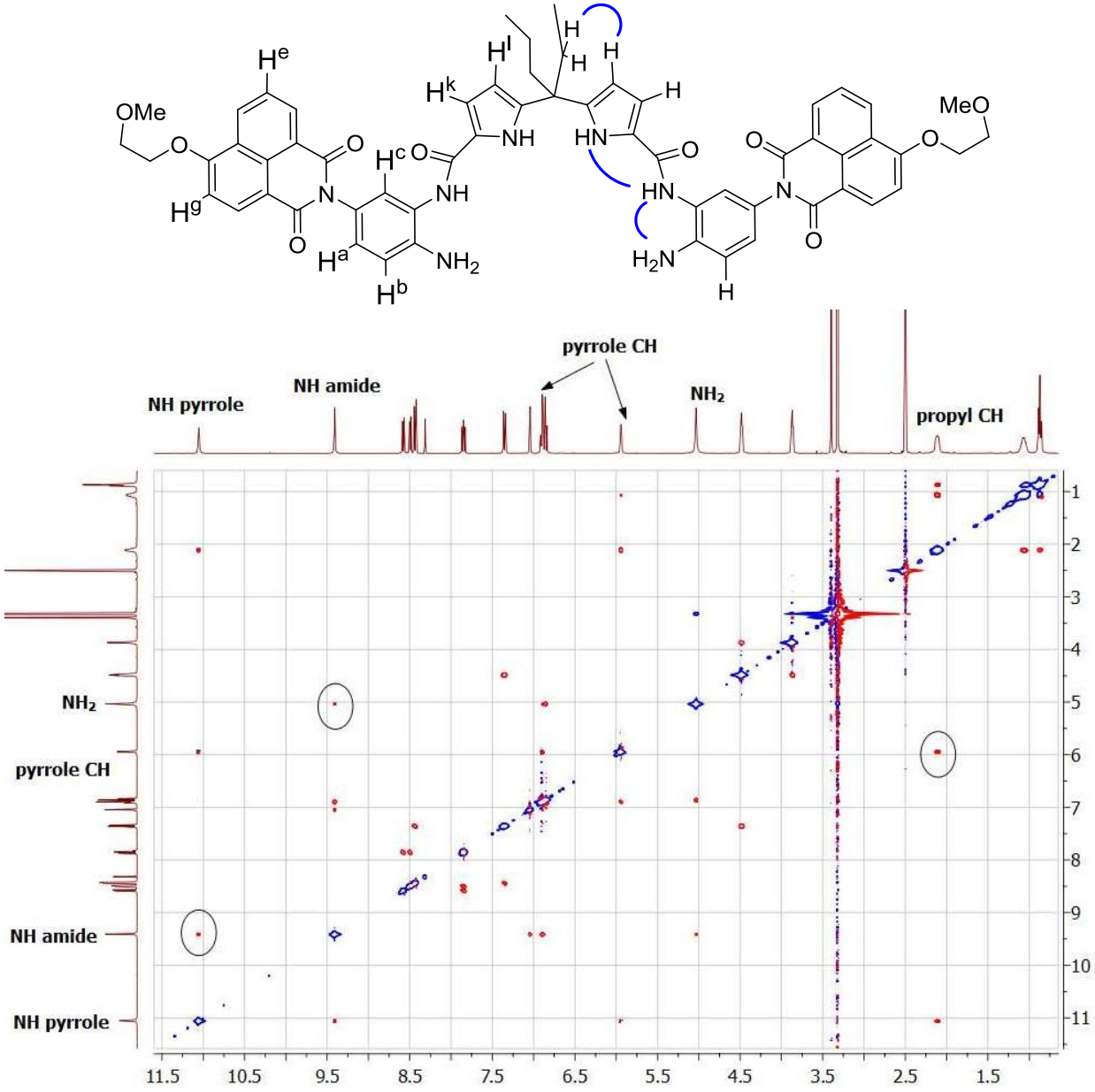

Figure 2.9: Through-space interactions in **2.27** (above); ^{1}H–^{1}H ROESY NMR for **2.27** in DMSO-d_6 (below).

According to the titration experiments, sulfate was bound stepwise in a 1:2 fashion with the first binding constant log K_{11} > 4 as fitted by using most chemical shifts in the aromatic region by HyperNMR program (Fig. 2.10). The second binding event was also accompanied by shifts to lower field, but it was too weak to be accurately accessed.

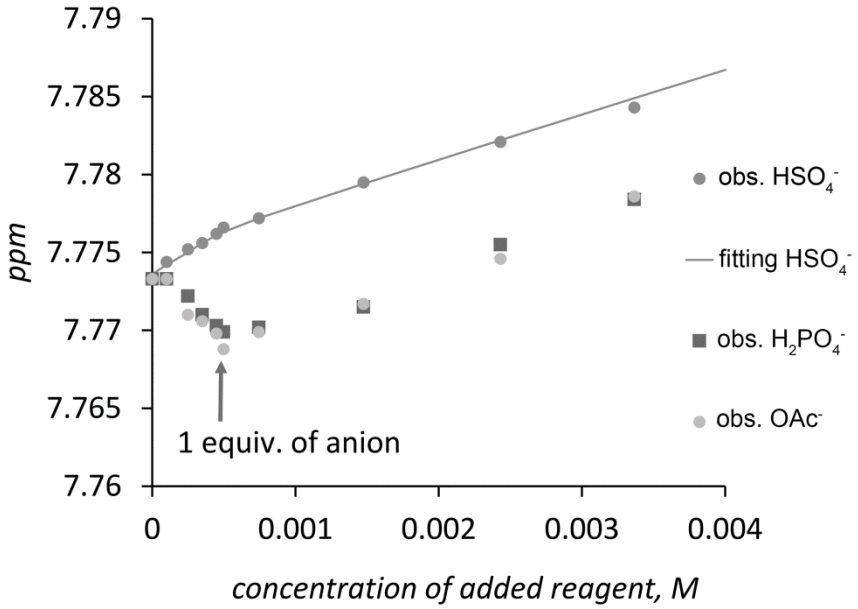

Figure 2.10: Observed chemical shifts of proton H^e in **2.27** during the addition of different anions and the fitting curve for sulfate.

Interestingly, addition of acetate and phosphate to the protonated receptor induced shifting of signals to a higher field until one equivalent, opposite to hydrogen sulfate, which caused shifts only to lower field. Moreover, addition of acetate and phosphate led to drastic changes in the region of phenyl ring protons (6.90–7.10 ppm) located close to the amino group. We suggested that these anions caused deprotonation of the receptor, because the changes were opposite to those observed during addition of perchloric acid to the neutral **2.27** (Fig. 2.11). Namely, after addition of an exactly one equivalent of acetate or phosphate to the protonated receptor, the signal pattern in the area of interest became identical with the one of the neutral receptor. Therefore, NMR experiments revealed that at low water content sulfate formed a complex with **2.27**, whereas phosphate and acetate substantially led to deprotonation of the receptor.

Next, we studied fluorescence properties of receptor **2.27** and reference diamine **2.35**. At a concentration of 10^{-5} M, which is suitable for fluorescence measurements, the DMSO content could be decreased until 10% retaining a good solubility of the compounds.

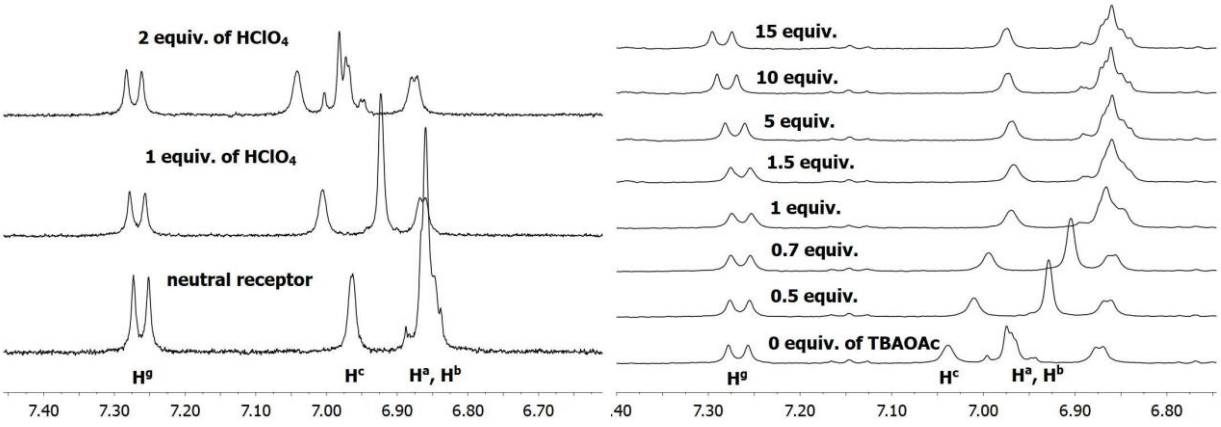

Figure 2.11: Changes in the NMR spectrum of **2.27** upon addition of $HClO_4$ (left); changes upon addition of TBAOAc to the solution of **2.27** containing 2 equiv of $HClO_4$ for protonation (right).

The influence of pH on the fluorescence of compounds **2.27** and **2.35** was determined first. It was expected that fluorescence would be high at acidic pHs and low at basic pHs due to hindering and realization of PET process, respectively. pH values of the solutions was set with hydrochloric acid and sodium hydroxide. Hydrochloric acid was chosen because of its strength and expected weak interactions of the counteranion — chloride with the studied compounds. Indeed, the decrease of fluorescence intensity was observed simultaneously with the increased pH of the solution (Fig. **2.12**). The calculated apparent pK_a values for diamines **2.27** and **2.35** were 2.8 and 4.5 respectively.

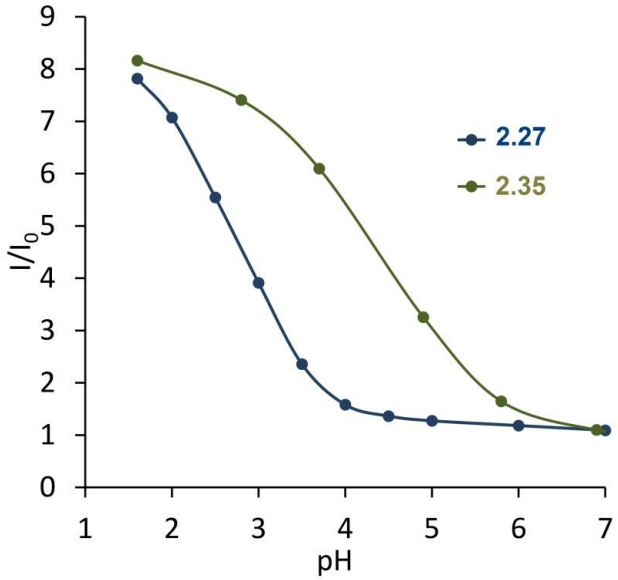

Figure 2.12: Influence of the pH on fluorescence intensity of compounds **2.27** and **2.35**.

At pH values more than 4.0, the receptor is not protonated and is not able to coordinate anions via only hydrogen bonds provided by dipyrrolylmethane subunits. For example, addition of anions in a 10% (vol.) DMSO–acetate buffer mixture (50 mM, pH 5.5) resulted in no changes in fluorescence of the studied compounds. We suggested that anion binding measurements should be carried out at pH values 2.5–4.0, because in this region the receptor of interest **2.27** is protonated and the pH curve has the strongest slope. Therefore, we chose a 50 mM acetate buffer at pH 3.6 containing 10% (vol.) DMSO. Acetate anion should not compete with other anions, as inferred from the NMR studies in a 4:1 DMSO–water mixture. According to the fluorescence titrations, the receptor demonstrated a fluorescence increase upon an addition of Na_2SO_4 (Fig. 2.13). Most of the other anions did not lead to changes in fluorescence intensity, except for bromide and iodide.

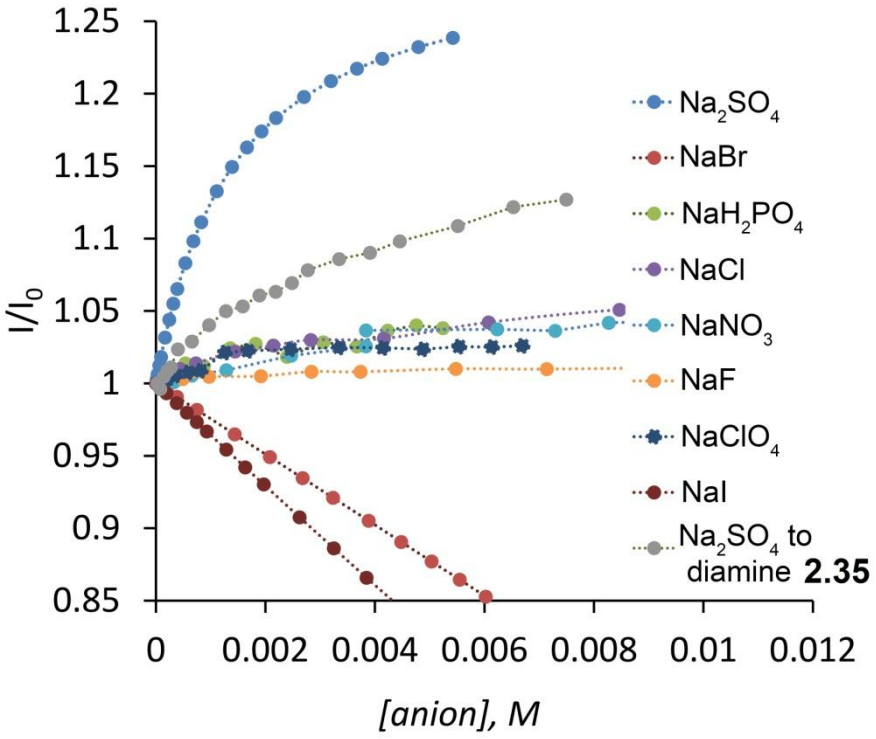

Figure 2.13: Fluorescence changes at 460 nm of the $1.4 \cdot 10^{-5}$ M solution of **2.27** in 10% DMSO–acetate buffer (50 mM, pH 3.6) upon the addition of different salts. "Na_2SO_4 to diamine **2.35**"corresponds to fluorescence changes of diamine **2.35** during the addition of sodium sulfate, measured under the same conditions. Excitation at 360 nm, emission 420–500 nm.

Addition of biologically important phosphates, such as pyrophosphate or adenosine mono-, di-, and triphosphate also did not induce any changes in the fluorescence of **2.27**.The receptor binds sulfate with a 1:1 stoichiometry and association constant 1025 ± 20 M^{-1} as obtained from the fitting by HypSpec program. Interestingly, bromide and iodide showed relatively strong

quenching efficiency because of the dynamic quenching with Stern–Volmer quenching constants 27 ± 1 M^{-1} and 46 ± 1 M^{-1}, respectively. The control titration experiment of diamine **2.35** with sulfate revealed also a fluorescence increase, albeit with lower I/I_0 ratio and flatter slope. Fitting of the curve yielded association constant 57 M^{-1}. Therefore, the dipyrrolylmethane binding motif present in **2.27** plays an important role in binding of sulfate.

Selectivity of the receptor was studied by a competitive binding. This experiment is designed to understand, how the presence of competitive anions (here, all anions except for sulfate) influence the fluorescence response of the receptor–sulfate complex. Fluorescence changes upon addition of 100 equiv of Na_2SO_4 to a solution of **2.27** in the presence of 10 equiv of competing anions were measured (Fig. 2.14). Most of the anions only slightly influenced the fluorescence response observed for sulfate. Sodium iodide and bromide showed the strongest variation in the emission intensity because of the dynamic quenching process.

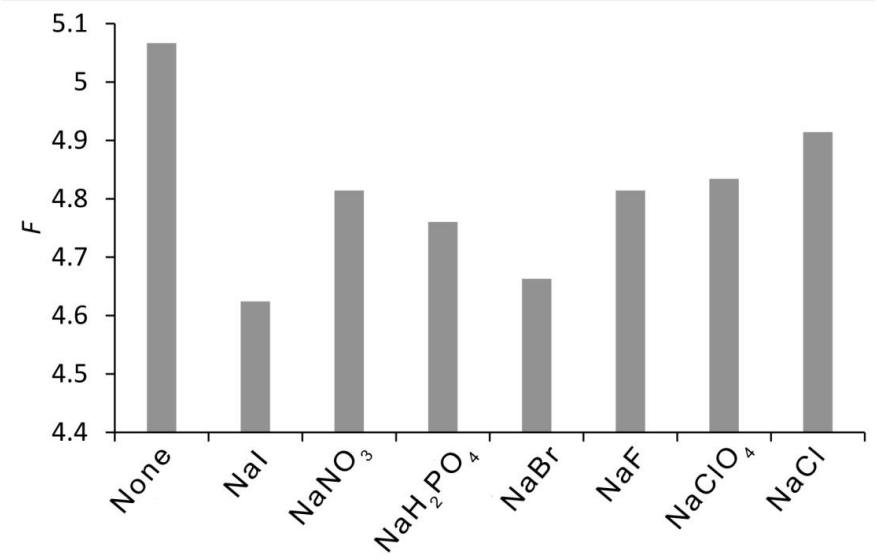

Figure 2.14: Fluorescence changes upon addition of 100 equiv of Na_2SO_4 to a solution of **2.27** (14 μm) in10% (vol.) DMSO–acetate buffer (50 mM, pH 3.6) in the presence of 10 equivalents of competing anions.

Additionally, the sulfate complex formation was proved by ESI-TOF MS analysis. The acetonitrile–water solution of **2.27** in the presence of 10 equiv of tetrabutylammonium hydrogen sulfate gave the signal at 1173.3388, which was in accordance with cation [**2.27** H^++HSO_4^-+K^+ $]^+$. The potassium cation came from the calibration solution. The same experiment with tetrabutylammonium dihydrogen phosphate did not give the signal for the corresponding anion complex.

In summary, receptor **2.27** bearing two amino groups and amidopyrroles as hydrogen bond donor bindings sites has been synthesized. Receptor **2.27** represents an example of a rational design of a turn-on fluorescent probe for the anion by utilizing a PET process. The amino groups can be protonated in aqueous medium and, along with hydrogen bonds, provide electrostatic interactions for anion coordination. The fluorescence of the naphthalimide dye is sensitive to protonation of the amino groups because the latter process blocks the PET quenching. The receptor has been shown to possess high selectivity for sulfate binding and sensing in a 50 mM acetate buffer at pH 3.6 (10 vol. % DMSO).

2.2.4. Experimental part

Instruments and materials

The solvents and other chemicals for synthesis were purchased from commercial suppliers and used without purification, unless mentioned otherwise. Column chromatography was performed on silica gel 60 Å (230–400 mesh). For fluorescence measurement analytical grade organic solvents and high purity water (conductivity 0.055 μS/cm, Barnstead ™ Smart2Pure ™) were used. Analytical grade salts were used for NMR and fluorescence titrations.

NMR spectra were recorded by UNITY NOVA NMR spectrometer (400 MHz) from Varian at room temperature (23 °C) if not mentioned otherwise. The following frequencies were used: 399.92 MHz for ^{1}H spectra, 100.57 MHz for ^{13}C spectra. The NMR spectra were referenced to trace solvent peak (7.24 ppm for $CDCl_3$, 2.50 ppm for DMSO-d_6, 4.79 ppm for D_2O), the spectroscopic solvents were purchased from Deutero. Mass spectra were recorded with Finnigan MAT SSQ 710 A (CI) and Finnigan MAT 95 (HRMS). Melting Points were determined on Büchi SMP or Lambda PhotometricsOptiMelt MPA 100. Absorption spectra were recorded on Varian Cary BIO 50 UV/VIS/NIR. PH measurements were performed with G20 compact titrator from Mettler Toledo, equipped with a DG115-SC pH electrode. Buffer solutions with pH values 4.01, 7.00, 9.21 purchased from Mettler Toledo were used for calibration of the electrode. Fluorescence spectra were recorded on a FluoroMax® Spectrofluoremeter from Horiba Scientific. For elemental analysis the device CHNOS elementar Vario MICRO cube was used.

Synthesis

Compound **2.28** (2-(4-amino-3-nitrophenyl)-6-bromo-1*H*-benzo[de]isoquinoline-1,3(2*H*)-dione)

4-Bromo-1,8-naphthalic anhydride (5.00 g, 18.12 mmol) and 2-nitro-1,4-phenylenediamine (5.06 g, 33.06 mmol) were boiled in 65 mL of acetic acid for 4 h. After cooling the mixture to the room temperature, precipitation was observed. The green solid was filtered off, washed with ethanol, and finally dried in vacuum. Yield 7.06 g, 95%. ^{1}H NMR (DMSO-d_6), δ [ppm]: 7.13 (d, 1H, ^{3}J = 9.2 Hz); 7.42 (dd, 1H, ^{3}J = 9.2 Hz, ^{4}J = 2.4 Hz); 7.63 (s, 2H), 8.03–8.07 (m, 2H); 8.27 (d, 1H, ^{3}J = 8.4 Hz); 8.36 (d, 1H, ^{3}J = 8.4 Hz); 8.61 (dd, 2H, ^{3}J = 7.8 Hz, ^{4}J = 2.4 Hz). ^{13}C NMR (DMSO-d_6), δ [ppm]: 163.44, 163.39, 146.1, 136.7, 132.8, 131.7, 131.5, 131.0, 130.0, 129.7, 129.2, 128.9, 128.8, 125.9, 123.5, 123.1, 122.8. M. p. 348.3–50.7 °C. Anal calcd (%): C 52.45, H 2.45, N 10.19. Found C 51.07, H 2.42, N 10.29.

Compound **2.29** **(**2-(4-amino-3-nitrophenyl)-6-(2-methoxyethoxy)-1*H*-benzo[de]isoquinoline-1,3(2*H*)-dione)

Potassium carbonate (1.86 g) and nitroamine **2.28** (0.5 g, 1.2 mmol) were mixed in 26 mL of 2-methoxyetthanole. The mixture was heated for 6 h at 115ºC. After cooling the solution to the room temperature the precipitate formed and it was collected by filtration, followed by washing with water and ethanol. The green product (85%, 0.42 g) was dried in vacuum. ^{1}H NMR (DMSO-d_6), δ [ppm]: 3.40 (s, 3H); 3.87 (t, 2H, ^{3}J = 4.2 Hz); 4.50 (t, 2H, ^{3}J = 4.0 Hz); 7.11 (d, 1H, ^{3}J = 8.8 Hz); 7.37–7.41 (m, 2H); 7.61 (s, 2H); 7.87 (t, 1H, ^{3}J = 7.80 Hz); 8.02 (d, 1H, ^{4}J = 2.0 Hz); 8.46 (d, 1H, ^{3}J = 8.4 Hz); 8.52 (dd, 1H, ^{3}J = 7.2 Hz, ^{4}J = 0.4 Hz); 8.61 (dd, 1H, ^{3}J = 8.0 Hz, ^{4}J = 0.4 Hz). ^{13}C NMR (DMSO-d_6), δ [ppm]: 164.1, 163.4, 159.6, 145.9, 136.9, 133.3, 131.2, 129.7, 129.1, 128.4, 126.4, 125.8, 123.4, 122.9, 122.5, 119.2, 114.8, 106.9, 70.1, 68.5, 58.4. M. p.: 306.2–308.0 °C. Anal calcd (%): C 61.91, H 4.21, N 10.31. Found C 61.47, H 4.01, N 10.05. ESI-MS calcd for MH^{+}: 407.1117. Found 407.1114.

Compound **2.32b** (tert-Butyl *N*-{2-nitro-4-[8-(2-methoxyethoxy)-2,4-dioxo-3-azatricyclo-[7.3.1.05,13]trideca-1(12),5,7,9(13),10-pentane-3-yl]phenyl}carbamate)

Nitroamine **2.29** (2.05 g, 5 mmol) was dissolved in DMF (70 mL) by heating the solution. The temperature of the solution was fixed to 75 °C and Boc_2O was added (1.08 g, 5 mmol). The solution was stirred at this temperature for ca. 12 h. The completion of the reaction was controlled by TLC in a 10:1 $CHCl_3$–CH_3CN solvent mixture (Rf of the product is 0.8). DMF was evaporated and 100 mL of $CHCl_3$ were added and heated to reflux. The hot solution was filtered from the insoluble starting material. The chloroform solution was evaporated and the product was purified by column chromatography yielding 55% of the pure product. ^{1}H NMR (DMSO-d_6), δ [ppm]: 1.48 (s, 9H); 3.40 (s, 3H); 3.88 (m, 2H); 4.50 (m, 2H); 7.39 (d, 1H, ^{3}J = 8.5 Hz);

7.72 (m, 2H); 7.89 (t, 1H, ^3J = 7.8 Hz); 8.11 (d, 1H, ^4J = 2.1 Hz); 8.48 (d, 1H, ^3J = 8.3 Hz); 8.54 (dd, 1H, ^3J = 7.3 Hz, ^4J = 1.1 Hz); 8.62 (dd, 1H, ^3J = 8.4 Hz, ^4J = 1.0 Hz); 9.78 (s, 1H). ^{13}C NMR (DMSO-d_6), δ [ppm]: 163.8, 163.1, 159.7, 152.4, 141.0, 135.1, 133.3, 132.3, 131.5, 131.1, 129.1, 128.6, 126.4, 126.1, 124.2, 122.9, 122.3, 114.5, 106.9, 80.6, 70.0, 68.5, 58.4, 27.8. M.p. 173–177 °C ESI-MS calcd for M + Na^+: 530.1534, found 530.1529.

Compound **2.33b** (tert-Butyl *N*-{2-amino-4-[8-(2-methoxyethoxy)-2,4-dioxo-3-azatricyclo-[7.3.1.05,13]trideca-1(12),5,7,9(13),10-pentaen-3-yl]phenyl}carbamate)

Boc-protected nitroamine **2.32b** (2.35 g, 5 mmol) was dissolved in dry THF (100 mL). In another flask, Pd/C 10% (0.230 g) was dissolved in THF (100 mL) and saturated with hydrogen during 30 min. The dissolved Boc-nitroamine and water (25 mL) were added to the catalyst and the resulted solution was stirred for 12 h. The completion of the reaction was controlled by TLC. The reaction mixture was filtered from the catalyst and evaporated. The product was purified by column chromatography in a 10:1 $CHCl_3$–CH_3CN mixture and then washed with a 10:1 $CHCl_3$–CH_3OH mixture. The purification yielded 50% of the yellow-green powder. ^{1}H NMR (DMSO-d_6), δ [ppm]: 1.49 (s, 9H); 3.40 (s, 3H); 3.87 (m, 2H); 4.49 (m, 2H); 5.00 (s, 2H); 6.48 (dd, 1H, ^3J = 8.3 Hz, ^4J = 2.3 Hz); 6.61 (d, 1H, ^4J = 2.3 Hz); 7.30 (d, 1H, ^3J = 8.4 Hz); 7.37 (d, 1H, ^3J = 8.5 Hz); 7.86 (dd, ^3J = 7.4 Hz, ^3J = 8.4 Hz); 8.44 (br.s, 1H); 8.44 (d, 1H, ^3J = 8.4 Hz); 8.51 (dd, 1H, ^3J = 7.3 Hz, ^4J = 1.2 Hz); 8.59 (dd, 1H, ^3J = 8.4 Hz, ^4J = 1.2 Hz). ^{13}C NMR (DMSO-d_6), δ [ppm]: 163.7, 163.1, 159.5, 153.6, 141.5, 133.1, 132.5, 131.0, 128.9, 128.3, 126.3, 124.4, 123.4, 122.9, 122.4, 116.6, 115.9, 114.6, 106.9, 78.8, 70.0, 68.5, 58.3, 28.1. M.p. 212–217 °C. ESI-MS calcd for MH^+: 478.1973, found 478.1979.

Compound **2.35** (3-(3,4-diaminophenyl)-8-(2-methoxyethoxy)-3-azatricyclo-[7.3.1.05,13]trideca-1(12),5,7,9(13),10-pentaene-2,4-dione). Nitroamine **2.29** (1.53 g, 3.75 mmol) and 10% Pd/C powder (0.15 g) were mixed in THF (300 mL) and saturated with hydrogen gas for 2 h. Then water (50 mL) was added, and the reaction mixture was stirred under hydrogen atmosphere at r.t. overnight. The catalyst was filtered off and the solution was evaporated. The product was purified by column chromatography in mixtures $CHCl_3$–CH_3CN 10:1, then $CHCl_3$–MeOH 100:2, 100:5. The product was obtained in 85% yield (1.2 g) as an orange powder. ^{1}H NMR (DMSO-d_6), δ [ppm]: 3.40 (s, 3H); 3.86 (t, 2H, ^3J = 4.2 Hz); 4.47 (t, 2H, ^3J = 4.2 Hz); 4.58 (s, 2H); 4.62 (s, 2H); 6.29 (dd, 1H, ^3J = 8.2 Hz, ^4J = 2.2 Hz); 6.39 (d, 1H, ^4J = 2.0 Hz); 6.57 (d, 1H, ^3J = 8.0 Hz); 7.34 (d, 1H, ^3J = 8.4 Hz); 7.83 (t, 1H, ^3J = 7.8 Hz,); 8.42 (d, 1H; ^3J = 8.4 Hz); 8.48 (dd, 1H, ^3J = 7.2 Hz, ^4J = 0.8 Hz); 8.56 (dd, 1H, ^3J = 8.40 Hz, ^4J = 1.2

Hz). ^{13}C NMR (DMSO-d_6), δ [ppm]: 164.1, 163.4, 159.4, 135.2, 134.8, 133.1, 131.1, 128.9, 128.2, 126.4, 125.3, 122.9, 122.6, 117.2, 114.9, 114.6, 113.9, 106.9, 70.1, 68.5, 58.4. Elemental analysis calcd (%): C, 66.83; H, 5.07; N, 11.13; found C, 66.74; H, 5.24; N, 10.88. M.p. 152.2–153.6 °C. ESI-MS calcd for M + Na^+: 402.1424, found 402.1418.

Compound **2.27** (5,5'-(heptane-4,4-diyl)bis(*N*-(2-amino-5-(6-(2-methoxyethoxy)-1,3-dioxo-1*H*-benzo[de]isoquinolin-2(3*H*)-yl)phenyl)-1*H*-pyrrole-2-carboxamide)). The dipyrrolylmethane diacid dichloride **2.31** was prepared according to the previously published procedure.[113] The solution of **2.31** in CH_2Cl_2 (0.6 equiv) was added to the solution of Boc-diamine **2.33b** (0.477 g, 1 mmol) in dry THF (25 mL), 0.025 g of 4-dimethylaminopyridine and pyridine (0.4 mL) under nitrogen atmosphere and cooled to 0 °C with an ice bath. The resulted mixture was stirred under this temperature for 30 min. and then overnight under room temperature. The reaction mixture was poured into water (150 mL) and extracted with $CHCl_3$ (3 x 40 mL). The chloroform solution was dried under sodium sulfate and evaporated. The product was purified by column chromatography using silica gel in a $CHCl_3$–CH_3OH (from 100:2 to 100:10) eluent. The crude product was dissolved in MeOH–$CHCl_3$ mixture (100 mL, 3:2 vol.) and concentrated hydrochloric acid (2 g) was added. The mixture was stirred for 5 days under room temperature. After that, the reaction mixture became unclear. Saturated $NaHCO_3$ solution was added until pH 7, and the product was extracted with $CHCl_3$ (3 x 40 mL). The chloroform solution was dried under sodium sulfate and evaporated. The solid compound was purified by column chromatography using silica gel in a $CHCl_3$–CH_3OH (100:2 and 100:10) solvent mixtures. The product was obtained in 30% overall yield as a yellow powder. ^{1}H NMR (DMSO-d_6), δ [ppm]: 0.87 (t, 3H, ^3J = 7.2 Hz); 1.07 (m, 2H); 2.11 (m, 2H); 3.40 (s, 3H); 3.87 (m, 2H); 4.48 (m, 2H); 5.05 (s, 2H); 5.94 (t, 2H, ^3J = 3.1 Hz); 6.87 (m, 3H); 7.04 (d, 1H, ^3J = 2.2 Hz); 7.35 (d, 1H, ^3J = 8.5 Hz); 7.85 (t, 1H, ^3J = 8.3 Hz); 8.43 (d, 1H, ^3J = 8.3 Hz); 8.49 (dd, 1H, ^3J = 7.3 Hz, ^4J = 1.1 Hz); 8.57 (dd, 1H, ^3J = 8.4 Hz, ^4J = 1.1 Hz); 9.43 (s, 1H); 11.10 (s, 1H). ^{13}C NMR (DMSO-d_6), δ [ppm]: 164.0, 163.4, 159.5, 159.1, 143.1, 141.8, 133.1, 131.1, 129.0, 128.3, 126.6, 126.5, 126.4, 125.2, 124.5, 123.5, 122.9, 122.6, 116.0, 114.8, 111.7, 106.9, 106.4, 70.1, 68.5, 58.4, 16.8, 14.4. M.p. 255–258 °C ESI-MS calcd for M + Na^+: 1059.4012, found 1059.4022.

Anion binding studies

NMR titrations were performed as following. 5.0 mg of receptor **2.27** were dissolved in 482 mkL of DMSO-d_6, to an NMR tube were added: 35 mkL of the stock solution, 490 mkL of DMSO-d_6, 175 mkL of 0.6 M solution of $NaClO_4$ in D_2O, 2 mkL of 0.35 M $HClO_4$ solution in

D_2O. Thus, the resulted concentrations in the NMR tube containing 25% vol. of D_2O and 75% vol. of DMSO-d_6 were: $5 \cdot 10^{-4}$ M of receptor **2.27**, 10^{-3} M (2 equiv) of $HClO_4$, 0.15 M of $NaClO_4$. For NMR titrations 0.0875 M solutions of tetrabutylammonium hydrogen sulfate, dihydrogen phosphate and acetate were prepared in DMSO-d_6 (4 mkL of the solution corresponding to 1 equiv of the receptor in NMR tube). To the prepared receptor solution small aliquots of the salt solutions were added, total added volume 60 mkL (15 equiv). After addition of every aliquot ^1H NMR spectrum was recorded. The results were fitted using HyperNMR program.

For the experiment with $HClO_4$ addition to the receptor, $5 \cdot 10^{-4}$ M solution of the receptor was prepared as described above, excluding addition of $HClO_4$. Small aliquots of the $HClO_4$ solution (0.35 M) in D_2O were added to the receptor solution, namely 1 mkL (1 equiv), 2 mkL (2 equiv).

Fluorescence titrations were performed as following. Stock solution of the receptors was prepared in DMSO, and then diluted with acetate buffer (50 mM, pH 3.6) in order to obtain $1.4 \cdot 10^{-5}$ M concentration of **2.27** or **2.35** and 10% vol. of DMSO in the final solution. Sodium salts were dissolved in the diluted solution of the receptor to keep its concentration constant during titrations. Small aliquots of the salt solutions were added to the receptor solution, and a fluorescence spectrum was recorded after each addition. Parameters of fluorescence measurements for **2.27** and **2.35**: excitation 360 nm, emission 420–500 nm. For the competitive binding experiment (Fig. 2.14) the diluted solution of **2.27** was prepared as described; 100 equiv of sodium sulfate solution were added first to the receptor solution, and the fluorescence spectrum was measured. After that, 10 equiv of different sodium salts were added to the solution containing the receptor and sodium sulfate (for the each competing anion a new portion of solution was needed), and changes in fluorescence response were recorded.

2.3. New sulfate receptors containing piperazine fragment

T. A. Shumilova, T. Rüffer, H. Lang, E. A. Kataev, *Chem. - A. Eur. J.*, **accepted for publication**. Straightforward design of fluorescent receptors for sulfate: study of non-covalent interactions contributing to host-guest formation.

2.3.1. Design of the receptors

In the previous study about the sulfate receptor containing 1,2-phenylenediamine fragment, an enhancement of fluorescence was observed upon addition of sulfate. We suggested that sulfate can increase a degree of protonation of the receptor's amine group, which would result in hindering of the PET process. Such a phenomenon has been observed, for example, by Czarnik for dihydrogen phosphate[39] (see detailed discussion in Section 1.4.2) and pyrophosphate.[117] However, these anions carry protons at neutral pH values and, therefore, they can form hydrogen bonds with amines, and thus, partially protonate amino groups. According to our knowledge, such an effect has not yet been described for the sulfate anion. As a next step, we wanted to provide an experimental evidence that this phenomenon is possible and can be used for detection of sulfate by fluorescence.

Molecular probes containing piperazine ring attached to a naphthalimide subunit at 4th position has become very popular in the recent five years. They have found applications as sensors for different metal ions, such as mercury,[118,119] aluminum,[120] chromium,[121,122] lead,[123] as well as for cysteine and histidine,[124,125] and even for pyrophosphate[126] and ATP.[42] Interestingly, similar compounds have been utilized as intra- and extracellular pH sensors (Fig. 2.15).[127–129] For example, Sessler and Kim used such type of compounds as pH sensors for mitochondria.[129] For these compounds, the pK_a value of the non-aromatic piperazine nitrogen in pure water was determined to be 6.18 ± 0.049. Thus, the design of receptors in our work was based on the naphthalimide–piperazine fragment.

Anion binding sites were also an important part of the receptors design. Covalent bonding between piperazine and hydrogen bond donor fragments was provided by the ethylamine linker. Four different anion binding sites capable of multiple hydrogen bonding were chosen: bis-(dipyrromethane)amide (compound **2.36**)[130], tris-thiourea fragment (compound **2.37**),[131–133] 2,6-pyridinedicarboxamide (compound **2.38**),[70] 1,3-benzenedicarboxamide (compound **2.39**)[8] (Fig. 2.16). Reference compound **2.40** containing only one piperazine–naphthalimide fragment

was designed to determine the smallest sufficient number of positive charges in a potential sulfate receptor.

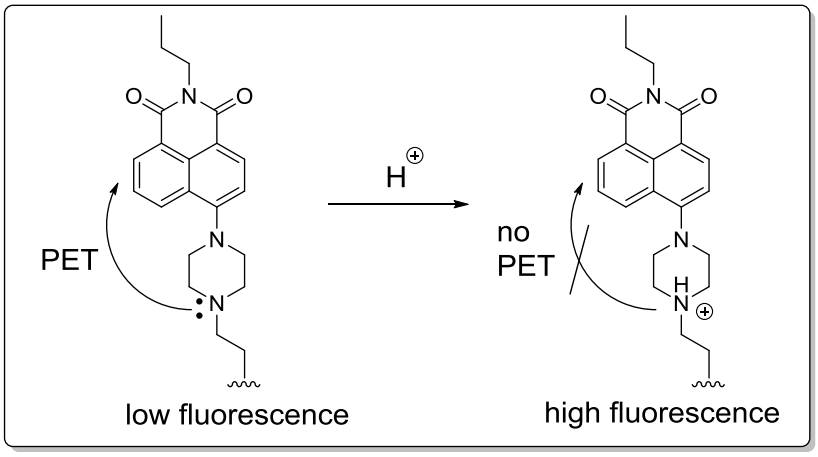

Figure 2.15: Principle of a PET pH probe functioning in water.

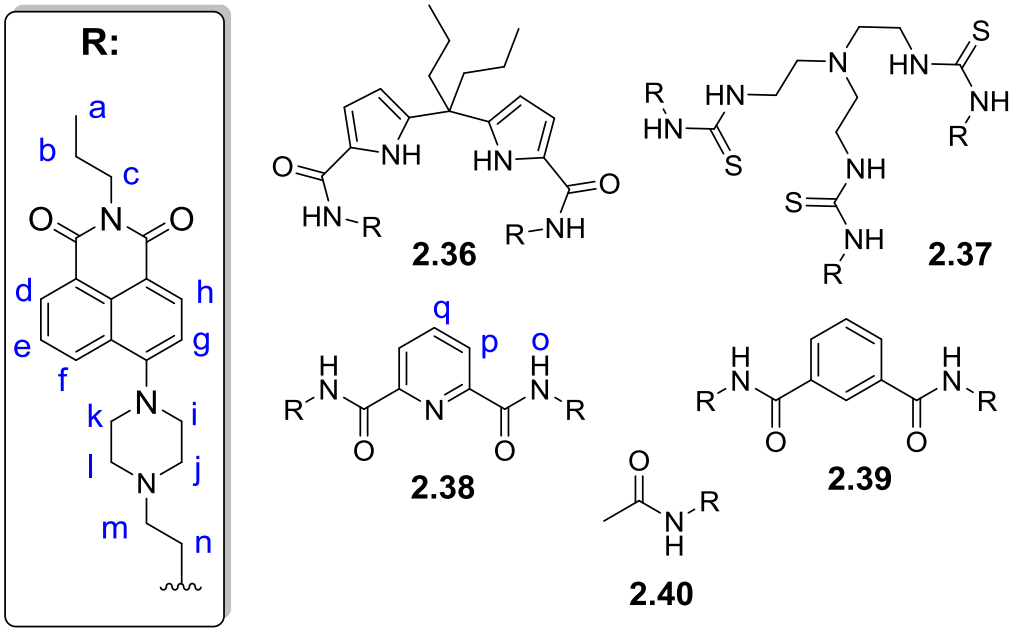

Figure 2.16: Structures of the developed receptors.

For the potential complex of diprotonated **2.38** and sulfate DFT calculations were performed. We wondered, apart from overall stability of the sulfate complex, if the flexibility of the ethylamine linker could allow two naphthalimide dyes to form π–π interactions in the complex with sulfate. The conformational search yielded three minima with structures shown in Fig. 2.17. Structure I has the lowest energy and displays stacking interactions between two naphthalimide rings. The sulfate anion is "wrapped" by the receptor and forms hydrogen bonds with amide NH,

NH^+, and CH fragments. Structure II is 3 kcal/mol less stable and was generated by the rotation of the naphthalimide ring by 180°. In structure III, naphthalimide rings do not stack, which leads to 18 kcal/mol higher energy of the complex relative to I. Thus, DFT calculations provided an evidence of a good complementarity for the host–guest complex.

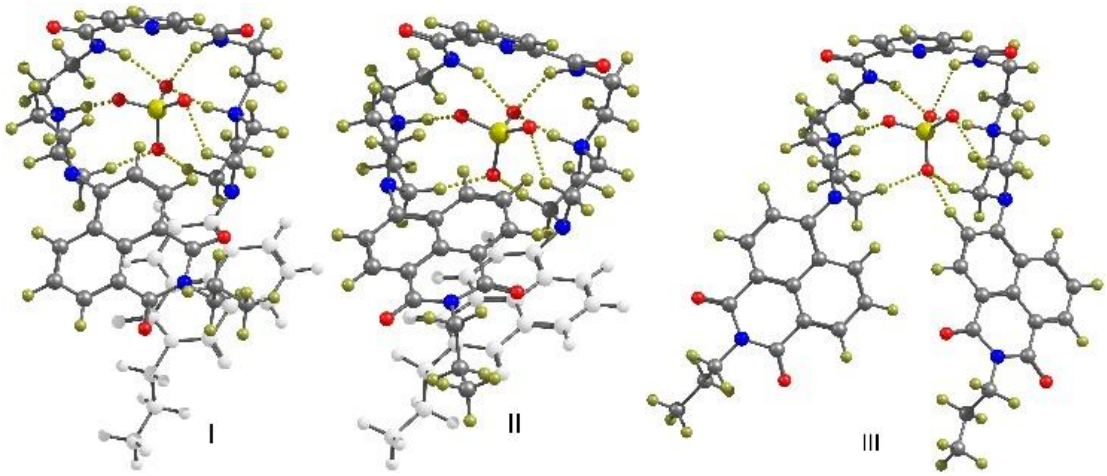

Figure 2.17: Optimized structures I–III of **2.38**·H_2SO_4. In structures I and II, the lower stacking naphthalimide ring is shown in pale colors for clarity.

2.3.2. Synthesis of the receptors

First steps of the synthesis included substitution of the bromo-substituent in N-propyl-4-bromonaphthalimide (compound **2.41**) as described in the literature,[134] followed by the nucleophilic substitution in Boc-protected 2-bromoethylamine, which resulted in compound **2.43** (Scheme 2.5). Deprotection by using hydrochloric acid in methanol smoothly led to dichloride **2.44**. This precursor was used to obtain most of the target receptors in one-step. Thus, compounds **2.38** and **2.39** were synthesized by acylation of **2.44** with corresponding diacid dichlorides. Similarly, reference compound **2.40** was obtained by the reaction of **2.44** with acetic anhydride.

Attempts to synthesize the thiourea-containing receptor by a one-pot synthesis were unsuccessful. Therefore, we decided to isolate tris-(2-isothiocyanate-ethyl)amine by the reaction of tris(2-aminoethyl)amine and carbon disulfide in the presence of DCC,[135] and then complete the same acylation-type reaction as for **2.38** and **2.39**. This approach resulted in receptor **2.37**.

The receptor with dipyrrolylmethane unit was synthesized by coupling of **2.44** with diacid **2.31** in the presence of peptide-coupling reagents: 1-ethyl-3-(3-dimethylaminopropyl) carbodiimid (EDC), and 1-hydroxybenzotriazol (HOBt). As a result, yellow product precipitated from the DCM solution. Unfortunately, the substance appeared to be almost insoluble in organic

solvents in a non-protonated form. Thus, a ^{1}H NMR spectrum of this compound was measured in the mixture of DMSO-d_6 and CD_3COOD, which confirmed the structure of **2.36**. However, we were unable to carry out anion binding studies because of extremely low solubility of the receptor. In summary, we synthesized three potential receptors for sulfate **2.37**–**2.39** and reference compound **2.40**.

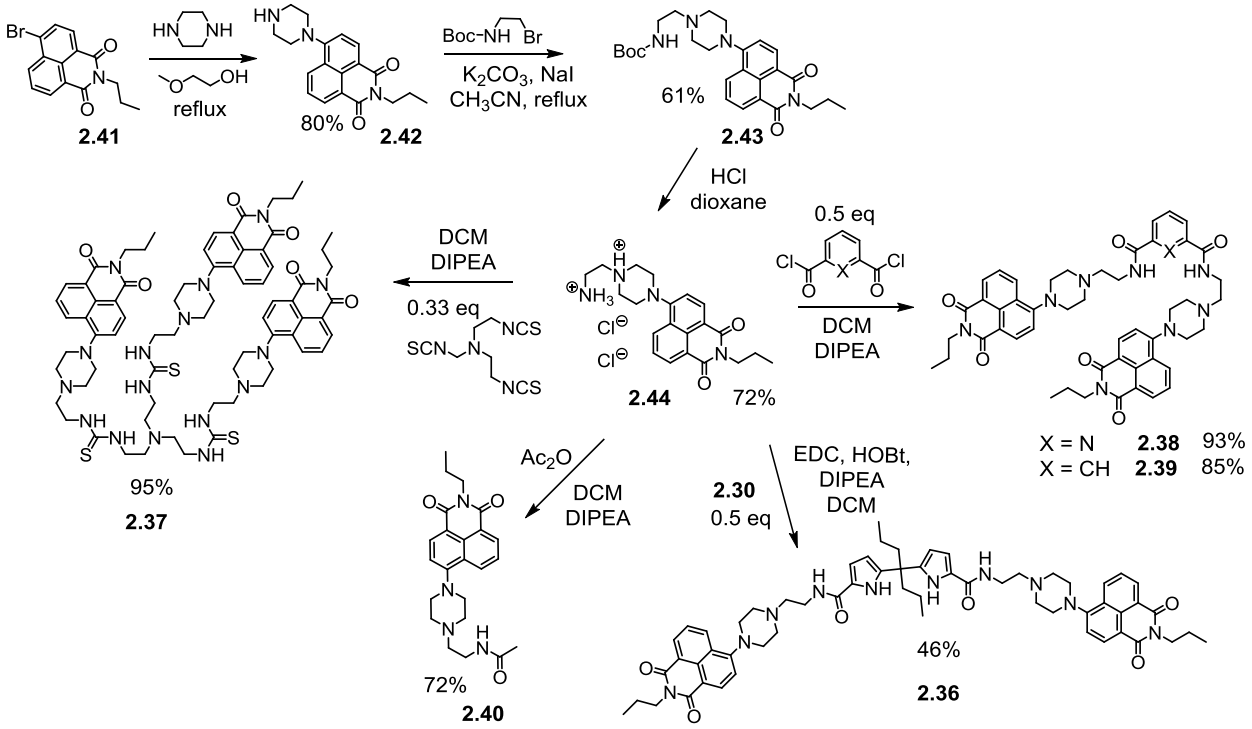

Scheme 2.5:. Synthesis of the target receptors.

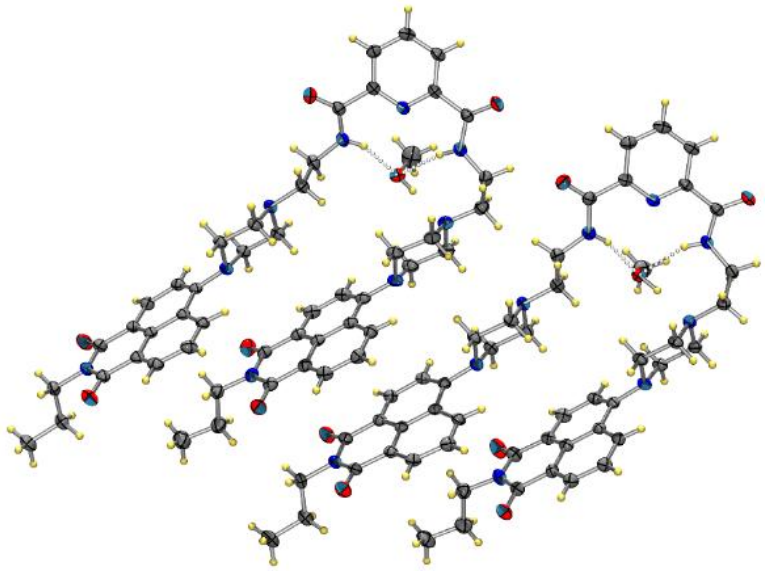

Figure 2.18: Single crystal X-ray structure of receptor **2.38**.

Receptor **2.38** was successfully recrystallized from the mixture of dioxane and methanol, and the crystals suitable for the X-ray analysis were obtained. According to the X-ray data, **2.38** has parallel oriented naphthalimide rings, which display CH–π interactions with the piperazine ring (Fig. 2.18). Stacking π–π interactions were found between the molecules. The receptor coordinates one methanol molecule through hydrogen bonds with amide-NHs.

2.3.3. Dependence of fluorescence of receptors on pH

The first step towards studying the binding properties consisted of choosing a suitable pH region of the solution. To analyze the dependence of fluorescence on pH, we prepared 50 mM acetic acid solutions in water and adjusted the pH with sodium hydroxide to reach a certain pH value. Three sets of solutions with pH values from 3 to 7 were prepared: first contained only 50 mM acetate, second and third contained additionally 10 mM of sulfate and dihydrogen phosphate, respectively. Phosphate-containing solution was used to understand the selectivity between sulfate and phosphate anions. Solubility of compounds **2.37–2.40** didn't allow us to perform experiments in pure water. Thus, the water content in THF was varied from 70% at 1 μM concentration to 50% at 0.1 mM for **2.38**. We decided to use higher concentration (0.1 mM) in all experiments including fluorescence in order to keep the content of THF approximately constant for all methods, namely 50% vol. for fluorescence, UV-vis, and potentiometry. A UV-vis dilution experiment confirmed that no aggregation occurs at 0.1 mM (Fig. 2.19).

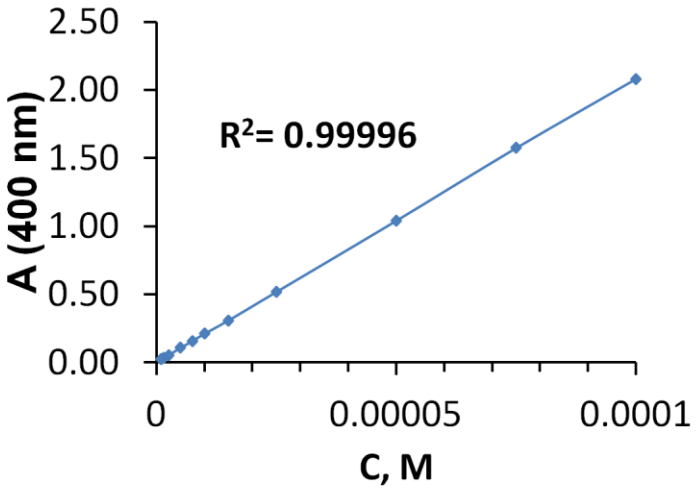

Figure 2.19: UV-vis dilution experiment for receptor **2.38** in a 1:1 THF–50 mM acetate buffer (pH 4.1).

For the simplicity of the experiment, we did not measure the pH values of all the THF–buffer mixtures. It should be mentioned, however, that the actual pH values of these semiaqueous mixtures are higher than those for the buffers. For example, the resulting pH of the 1:1 mixture THF–acetate buffer (pH 4.1) was found to be 5.6. All the pH values that we refer to in the following are the pH values of the buffers.

Typical curves "fluorescence–pH" obtained as described above are shown in Fig. 2.20. Changes between the "acetate" curves and the "phosphate" curves are minimal for all compounds. For reference compound **2.40** all curves look very similar (Fig. 2.20d). Therefore, it is unlikely that this compound will show any fluorescent changes upon titrations with sulfate or phosphate. At the same time, we observed a significant shift of the curve to higher pH values for receptors **2.37–2.39**, when sulfate was added to the solution. Such a shift indicates that the complexes of the receptors with sulfate have higher pK_a values than the receptors in an unbound state. In other words, the receptors become more protonated upon addition of sulfate, and this protonation induces a fluorescent increase (shown with an arrow for receptor **2.38**). We observed similar pK_a shifts for some pyrophosphate receptors in our previous work.[136]

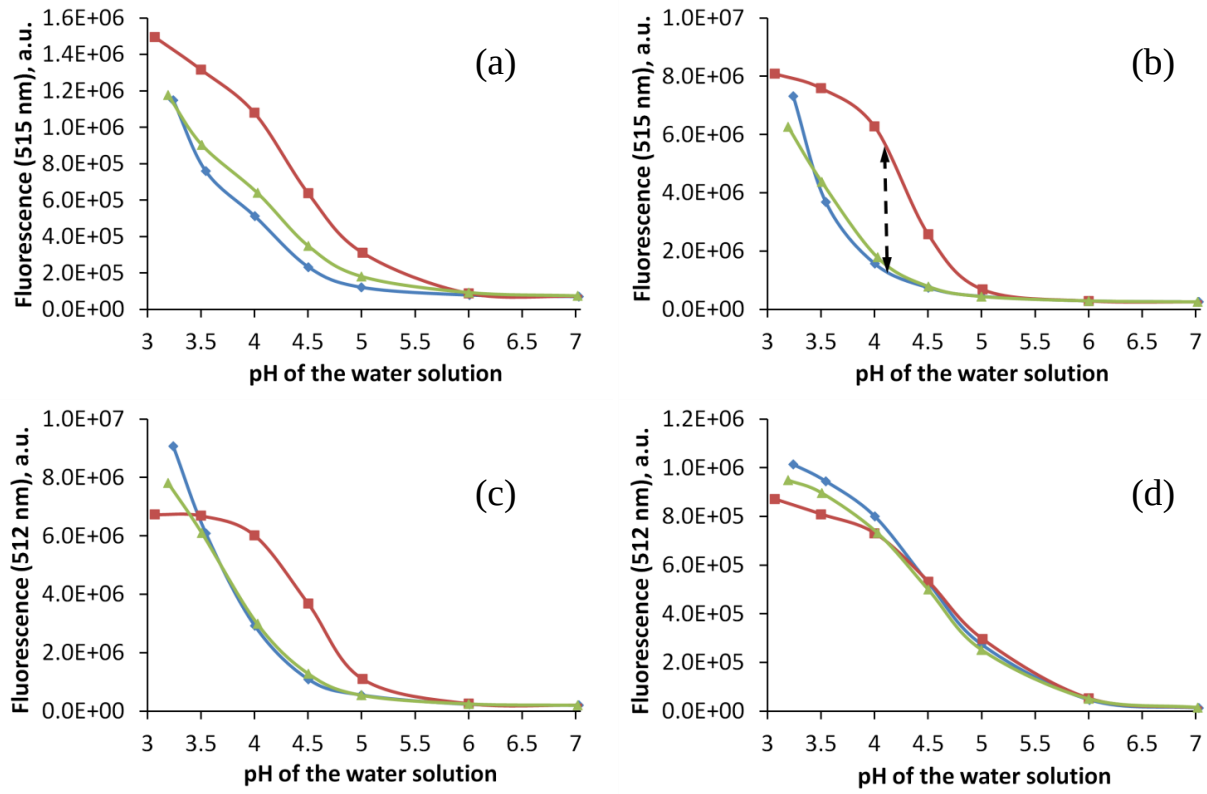

Figure 2.20: Fluorescence vs. pH for receptors **2.37** (a), **2.38** (b), **2.39** (c), **2.40** (d). The blue curves represent solutions containing 25 mM of acetate, the green curves—containing additionally 5 mM of dihydrogen phosphate, the red curves—containing additionally 5 mM of sulfate.

An experiment using the same water solutions was conducted for compound **2.38** with the help of UV-vis spectroscopy (Fig. 2.21). Obtained results were consistent with the ones from fluorescence. Namely, protonation of the receptor led to strong hypsochromic shift both in the presence and in the absence of sulfate, but in the presence of sulfate smaller amount of acid sufficed to induce shifts, than in the case of just acetate.

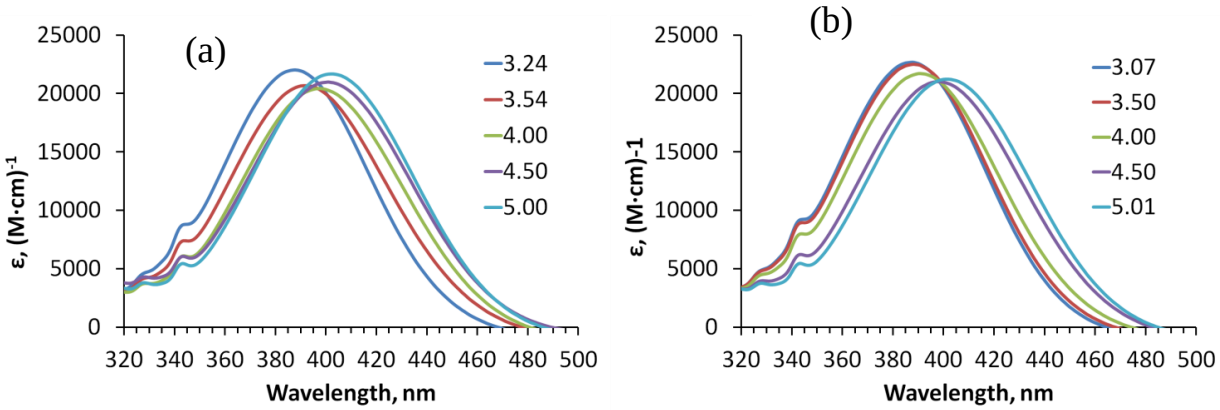

Figure 2.21: UV-vis spectra of **2.38** depending on the pH.. (a) Receptor solutions contain 25 mM of acetate. (b) The solutions contain 25 mM of acetate and 5 mM of sulfate.

Thus, at pH 5.0 the highest absorbance is observed at 401 nm both in the presence and in the absence of sulfate. When pH is lowered up to 4.0 the sulfate solution (Fig. 2.21b) has maximum at 391 nm, reaching 11 nm shift. At the same time the acetate solution (Fig. 2.21a) "achieves" 11 nm shift only at pH 3.5. This result indicates that the presence of sulfate favors protonation of **2.38**. In other words, sulfate induces pK_a shift in this receptor.

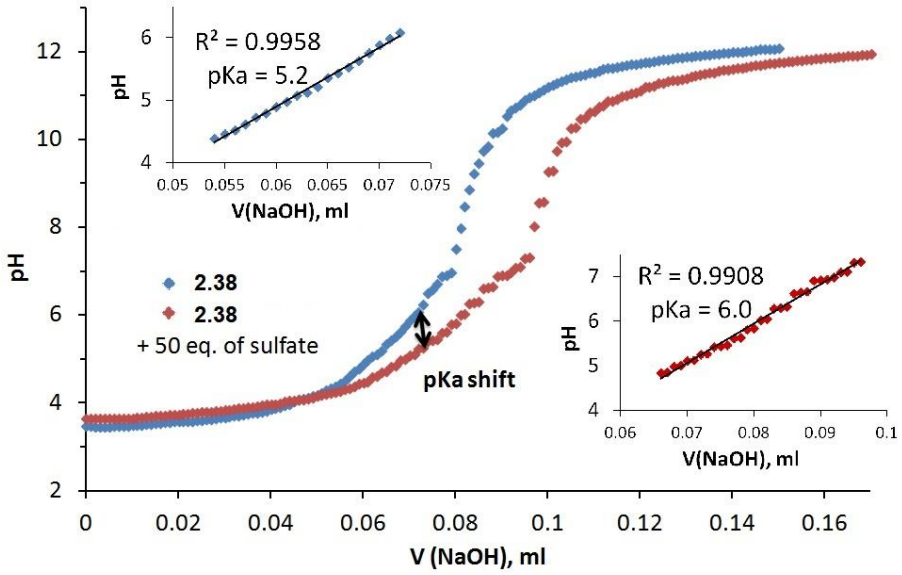

Figure 2.22: Potentiometric titration of **2.38** in the presence (red curve) and in the absence (blue curve) of sulfate.

We used potentiometric titration to determine pK_a values for **2.38** and its complex with sulfate (Fig. 2.22). The chloride salts of the receptors were prepared and titrations with NaOH were performed. 0.05 M NaCl was used to provide a constant ionic strength of solutions. As revealed from the experiments, chloride does not compete with sulfate under the titration conditions. Difference in pK_a values for the receptor and the complex can be observed both qualitatively and quantitatively. Linear regions of the titration curves (R^2> 0.99) were chosen to assess pK_a values, which appeared to be 5.2 and 6.0 for unbound receptor **2.38** and its sulfate complex, respectively. Thus, the pK_a shift of the amine groups, caused by the coordination of sulfate to a receptor, was confirmed by three different methods: potentiometry, fluorescence and UV-vis spectroscopy.

2.3.4. Anion binding studies

Receptor **2.38** containing 2,6-pyridinedicarboxamide fragment was the most promising receptor, as it showed the largest pK_a shift in pH–fluorescence studies upon addition of sulfate (Fig. 2.20b). To establish the optimal pH value for anion binding studies we prepared 50 mM acetate buffers within pH values between 4.1 and 4.7, and carried out fluorescent titrations of **2.38** with sodium sulfate (Fig. 2.23).

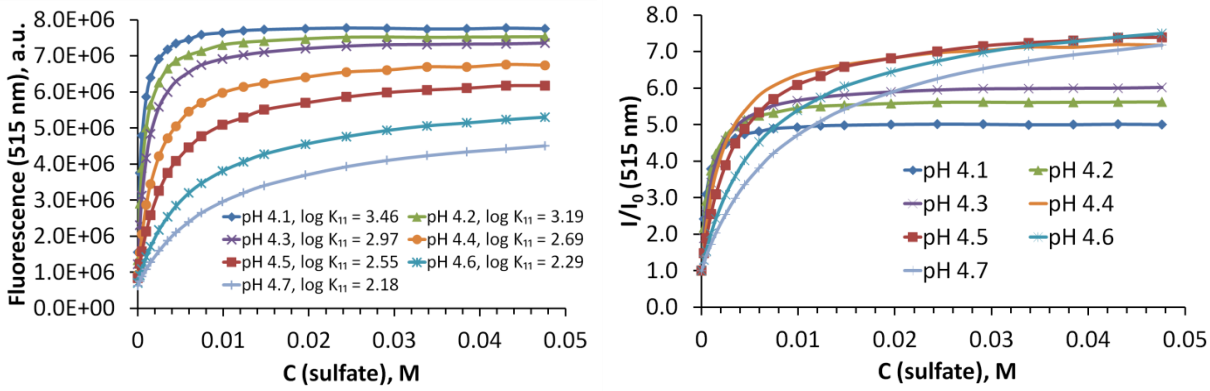

Figure 2.23: Fluorescent titrations of **2.38** with sulfate using acetate buffers with different pH values.

The most remarkable result that was extracted from the obtained data is a significant decrease in binding constants even after a small change of the pH value. For instance, at pH 4.1 the binding constant K_{11} is 2880 M^{-1}, but it diminishes to 930 M^{-1} when pH value is 4.3. The largest increase of fluorescence was observed at pH 4.4 (approx. 7-fold, see Fig. 2.38 right). The

binding constant at this pH is, unfortunately, rather small. Therefore, the pH value 4.1 was chosen for the following anion binding studies, because the strongest binding and the sufficient fluorescence enhancement were observed at that point.

A comprehensive study of anion binding properties was carried out in a 1:1 THF–acetate buffer (pH 4.1) mixture at for **2.38** and **2.39**, and in a 2:3 THF–acetate buffer (pH 4.1) mixture for **2.37** and **2.40**. The latter compounds have a slightly higher solubility in water mixtures. Common monoanions including those present in the environmental water were chosen for the study together with oxalate as an additional dianion present under studied pH values. As expected from the pH–fluorescence dependencies (Fig. 2.20d), reference compound **2.40** did not show significant fluorescent increase upon addition of sulfate. Only small bathochromic shift accompanied by minor quenching was observed (Fig. 2.24a). In contrast, compounds **2.37**–**2.39** showed remarkable selectivity for sulfate over monoanions, including tetrahedral dihydrogen phosphate. Iodide induced dynamic quenching of fluorescence, which is a well-known phenomenon (see Section 1.4.3).

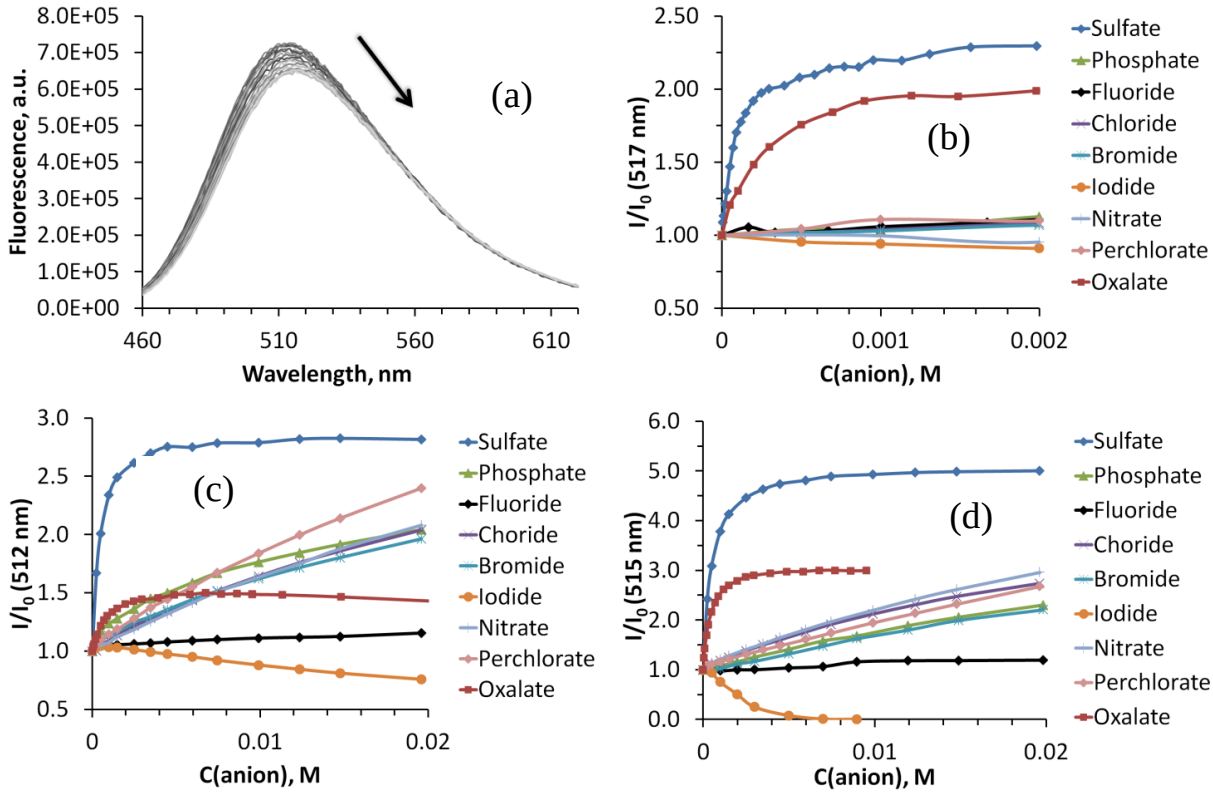

Figure 2.24: Fluorescence titrations of receptors **2.37**–**2.40** with different anions in THF–50 mM acetate buffer pH 4.1. (a) Changes in fluorescence spectrum of **2.40** upon addition of sulfate. (b) Anion titrations for receptor **2.37**. (c) Anion titrations for receptor **2.38**. (d) Anion titrations for receptor **2.39**.

Receptor **2.38** demonstrated the highest 5-fold increase of fluorescence after addition of sulfate, whereas **2.37** and **2.39** showed 2.3 and 2.8-fold increase, respectively. Another dianion — oxalate — induced a significantly lower enhancement of fluorescence, but the binding constants with this anion were close to those with sulfate (see Table 2.1). This result is in agreement with the idea that the selectivity of the receptors is determined mostly by electrostatic interactions. Such a conclusion can be drawn from the fact that binding constants for tri-naphthalimide receptor **2.37** are higher than those for di-naphthalimide receptors **2.38** and **2.39**. Binding constants of **2.38** with sulfate determined by UV-vis spectroscopy were approximately the same as those obtained from fluorescence (Fig. 2.25). Limits of detection were found to be 0.37, 1.67, and 2.78 μM for **2.37**, **2.38**, and **2.39**, respectively.

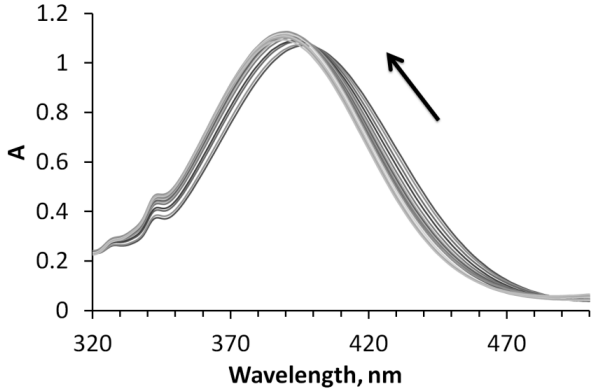

Figure 2.25: Changes in UV-vis spectrum of **2.38** upon addition of sulfate in 1:1 THF–50 mM acetate buffer pH 4.1, C (**2.38**) = $5 \cdot 10^{-5}$ M.

Some of the studied monoanions, especially perchlorate, caused considerable fluorescence increase, even though the calculated binding constants were rather low (< 50, see Table 2.1). The explanation to similar phenomena was provided by Fei et al.[137] The authors found that sterically large anions often suppress cation–anion interactions, which leads to an increase in fluorescence. In other words, acetate from the buffer could form ion pairs with partially protonated receptors causing quenching of naphthalimide fluorescence. When titrations with perchlorate were carried out, the amount of added anion was comparable with that of present acetate; therefore, perchlorate could displace acetate and form new ion pairs with higher emission as described in the literature.

Anion \ Log K[a]	**2.37**	**2.38**	**2.39**
$\boldsymbol{SO_4^{2-}}$	4.09 (K_{11}); 4.36 (K_{12}); 3.22 (K_{13})	3.46 (K_{11}), 2.38 (K_{12}); 4.02 (K_{11}), 2.92 (K_{12})[c]	3.36
$\boldsymbol{C_2O_4^{2-}}$	3.80[d]	3.40	3.10[d]
$\boldsymbol{H_2PO_4^-}$	1.26	1.28	1.89
$\boldsymbol{F^-}$	1.99	—[b]	1.82
$\boldsymbol{Cl^-}$	< 1	1.51	1.48
$\boldsymbol{Br^-}$	< 1	1.25	1.53
$\boldsymbol{I^-}$	1.59	—[b]	1.27
$\boldsymbol{NO_3^-}$	< 1	1.45	1.27
$\boldsymbol{ClO_4^-}$	< 1	1.03	1.15

Table 2.1: Binding constants of **2.37**–**2.39** with anions. a) Measurement error ≤ 10%, b) Equilibrium is slow, not possible to fit the data, c) UV-vis titration data, d) second binding is possible, log K_{12} <1.

Stoichiometry of binding was determined mostly by the best fit method.[20] Job plots experiments were carried out for compounds **2.37**–**2.39** (Fig. 2.26) and sulfate. However, a plausible value corresponding to 1:3 host–guest stoichiometry was obtained only for **2.37**, which was in agreement with the value obtained by the best fit. In other cases, a maximum of the Job plot curve located between values corresponding to 1:1 and 1:2 complexes. These results are in line with the recent findings about limited applicability of Job plot for supramolecular systems.[20,21]

Binding properties of receptor **2.38** were also studied with the help of ^{1}H NMR spectroscopy (Fig. 2.27). The content of tetrahydrofuran was increased only by 10% as compared to fluorescence studies. Chemical shifts of methylene groups belonging to piperazine (i–l) and the ethylene linker (n, m) moved towards low field upon addition of sulfate. These shifts confirmed the protonation of the amino groups upon binding of the anion. On the other hand, the pyridine protons (p, q) moved towards high field indicating the formation of hydrogen bonds between amide NH signals and the anion.

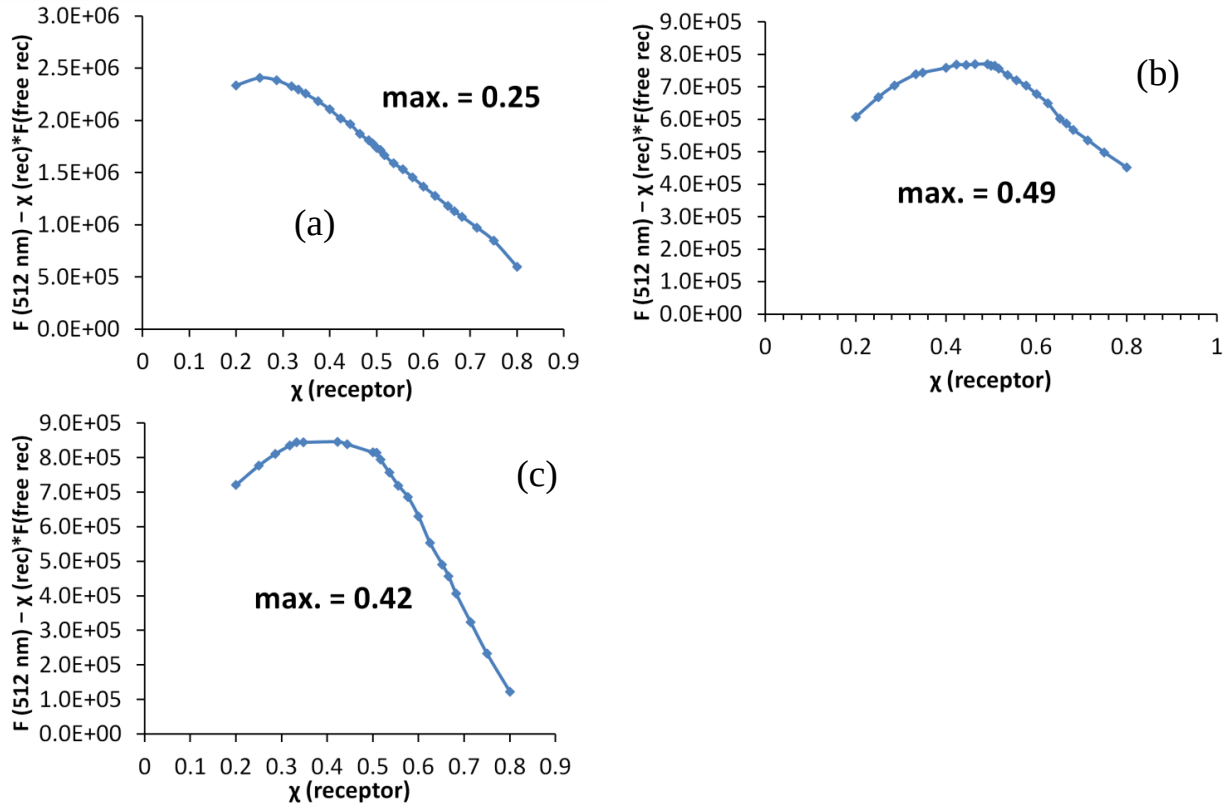

Figure 2.26: Job plots for compounds **2.37**–**2.39** (sulfate complexes) in THF–50 mM acetate buffer pH 4.1 (a) receptor **2.37**; (b) receptor **2.38**; (c) receptor **2.39**.

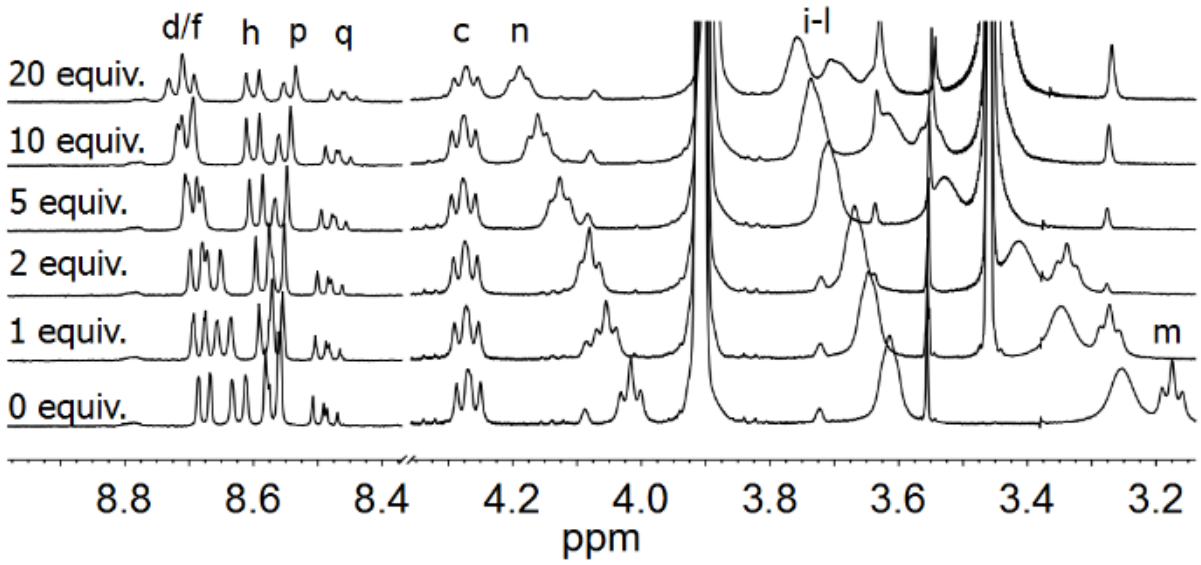

Figure 2.27: Changes in ^{1}H NMR spectrum of receptor **2.38** upon addition of $(NMe_4)_2SO_4$.

Next, we conducted ROESY measurements of receptor **2.38** in the absence and in the presence of sulfate to find out if stacking interactions are present in solution, as predicted by DFT calculations. Analysis of the spectra in Fig. 2.28 leads to the conclusion that the receptor in

acetate buffer exists presumably in the conformation with naphthalimide rings distant from each other. CH–π interactions found in the X-ray structure were not present. A number of new cross-signals in the ROESY spectrum appeared after addition of 20 equiv of $TBAHSO_4$ to the solution of **2.38**. These cross-signals unambiguously suggest π–π interactions between naphthalimide rings in the complex with sulfate. The proposed structure based on the ROESY experiment resembles the DFT predicted structure II (Fig. 2.17). Thus, stacking interactions between two dyes additionally contribute to the formation of the complex with sulfate. Such an arrangement of the anion-binding site through stacking interaction was reported recently for pyrophosphate sensing in acetone.[138]

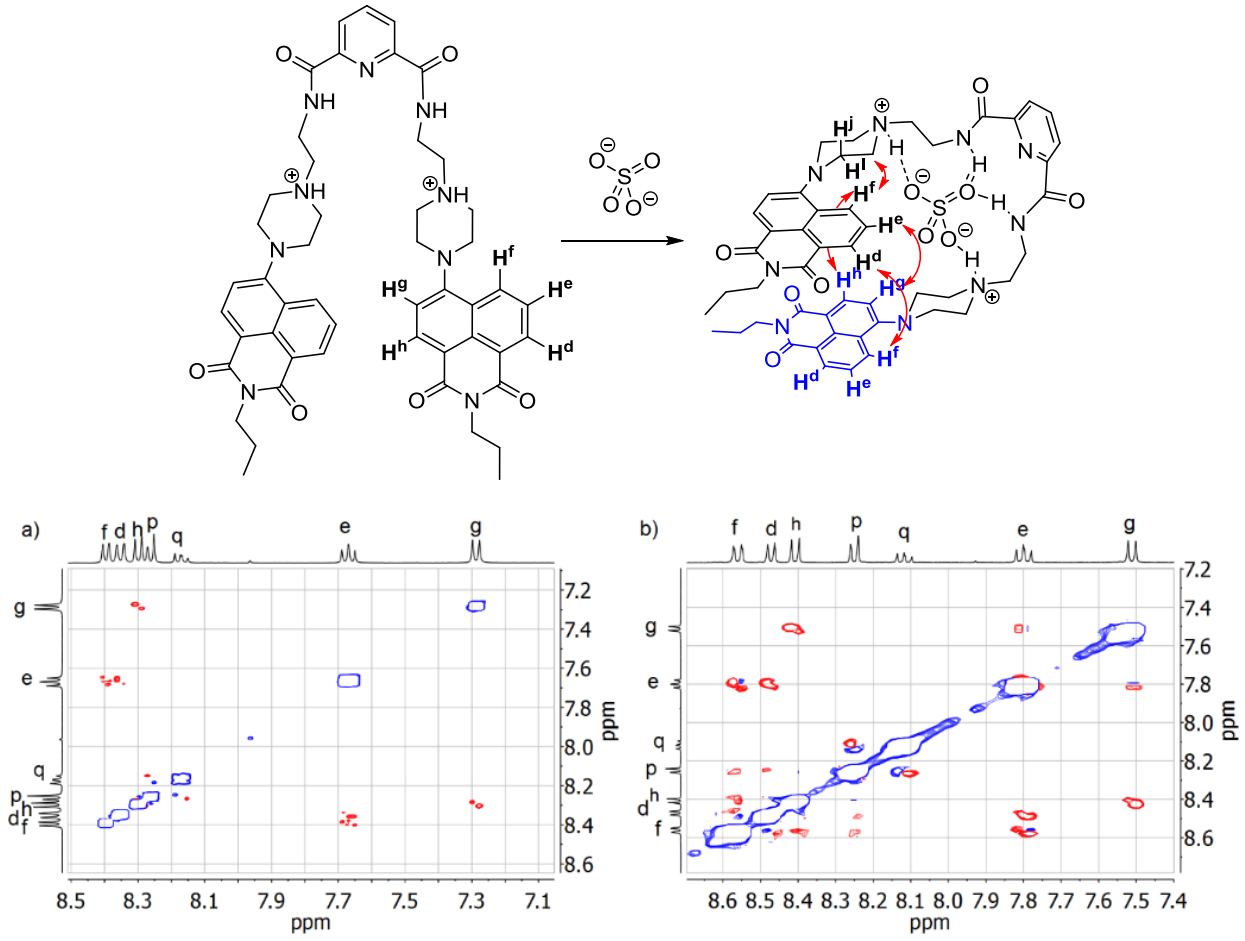

Figure 2.28: Proposed structure of the sulfate complex of receptor **2.38** (above); ROESY spectrum for **2.38** in the absence (a) and in the presence (b) of $TBAHSO_4$.

Competitive binding is a widely used approach to examine selectivity of a particular receptor, i.e. fluorescent response upon addition of a target anion in the presence of competitive ones. The blue bars in Fig. 2.29 show fluorescence response of receptors **2.37**–**2.39** upon addition of only 30 equiv of sulfate (bar "none") or upon addition of the same amount of sulfate in the presence of

100 equiv of other anions. An ideal receptor should show the same or very close results for all blue bars. The red bars represent response caused by 100 equiv of competitive anions alone. Again, in an ideal situation no response for competitive anions should be observed. The studied receptor show very good results for sulfate selectivity over all anions except for iodide (due to the dynamic quenching) and oxalate. Thus figure suggests that the presence of environmentally important anions in solution only slightly influence the response of the receptors.

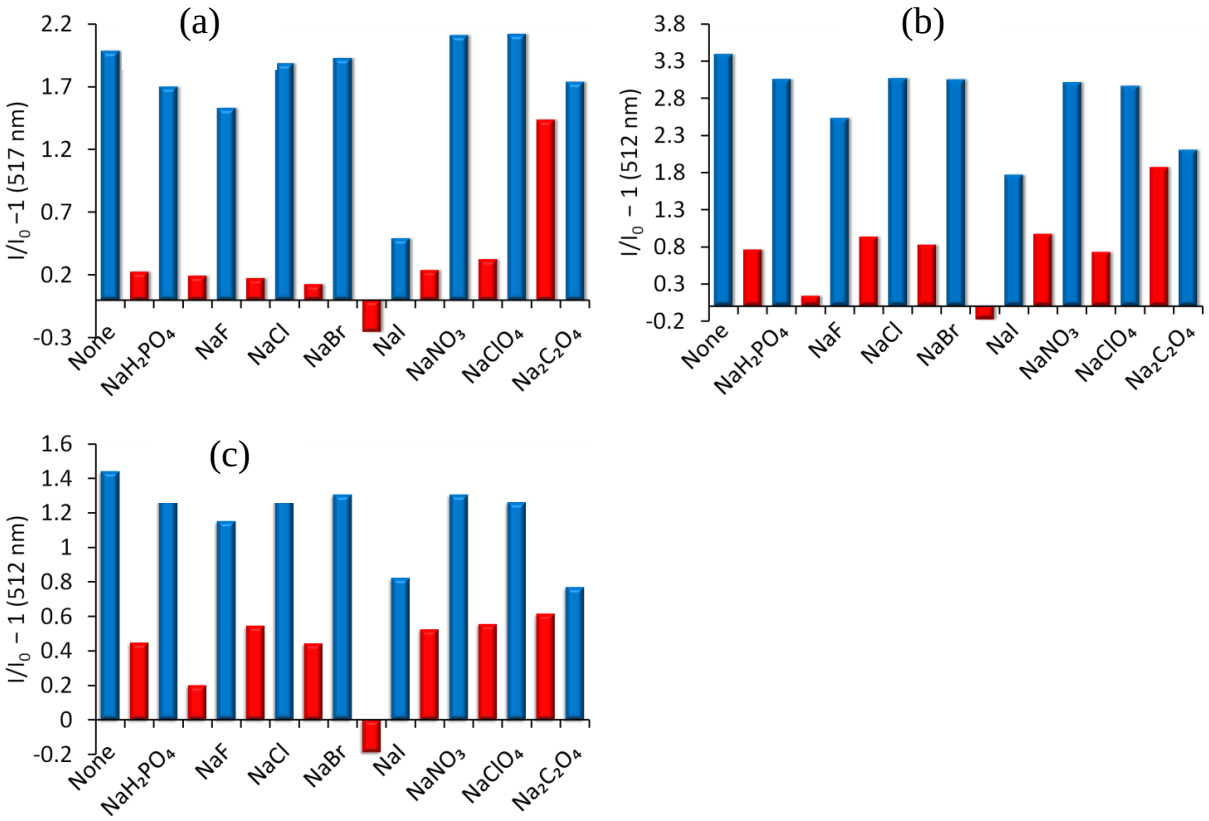

Figure 2.29: Competitive binding experiments for receptors in THF–50 mM acetate buffer (pH 4.1) **2.37** (a), **2.38** (b), **2.39** (c).

2.3.5. Role of hydrogen bonds

The formation of hydrogen bonds between an anion and a receptor in aqueous solutions can be hindered by strong solvation (water–anion and water–receptor interactions). Therefore, it was important for us to understand, whether amide NH sites indeed participated in sulfate recognition. To answer this question, we blocked NH sites in **2.38** with methyl groups. We decided to prepare Boc-protected 2-bromo-N-methylehylamine (**2.45**) in order to synthesize the methylated analogue of the compound **2.43**. Commercially available precursor for compound **2.45** is *N*-methylaminoethanol, which can be converted into the target compound in two steps:

the Boc-protection followed by bromination. First, we started with solvent-free Boc-protection of the alcohol, as described in the literature[139] (Scheme 2.6). However, the second step, Appel bromination, didn't result in the desired product. Therefore, we tried the reactions of Boc-derivative **2.46** with 4-toluenesulfonyl chloride and methansulfonylchlorid in order to obtain the corresponding tosyl- and mesyl-derivatives. Unfortunately, these reactions were also unsuccessful, because complex product mixtures were obtained. A different reaction order was employed, starting with the bromination of N-methylaminoethanol. Again, the first step proceed smoothly according to described method[140] and resulted in bromide **2.47**. An attempt to obtain **2.45** by treating the bromide with Boc_2O gave a single product. This was, surprisingly, not the target molecule, but 3-methyl-2-oxazolidinone (**2.48**), which could be distinguished from **2.45** by the chemical shifts of the methylene protons in ^1H NMR. Similar cyclization reactions for carbamates were found in the literature.[141,142] It was described that the methyl group plays a crucial role favoring the cyclization. The proposed mechanism of cyclization based on the literature data is shown in Scheme 2.6.

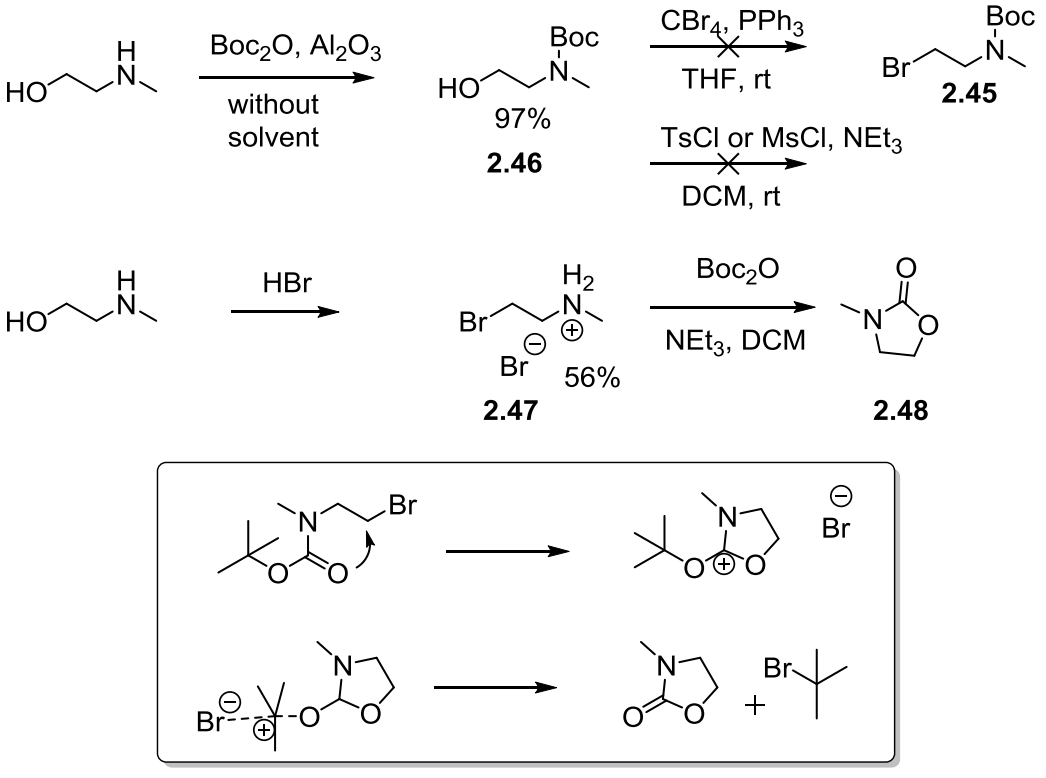

Scheme 2.6: Attempts to synthesize compound **2.45**, and the proposed mechanism of oxazolidinone formation.[141]

Since the target bromide **2.45** could not be obtained, we suggested two possibilities to perform the synthesis. The Mitsunobu reaction between amine **2.42** and alcohol **2.46** didn't result

in any product at all (Scheme 2.7). The reaction between **2.42** and unprotected amine **2.47** using the same conditions as for the non-methylated analogue resulted in **2.49** in a small yield.

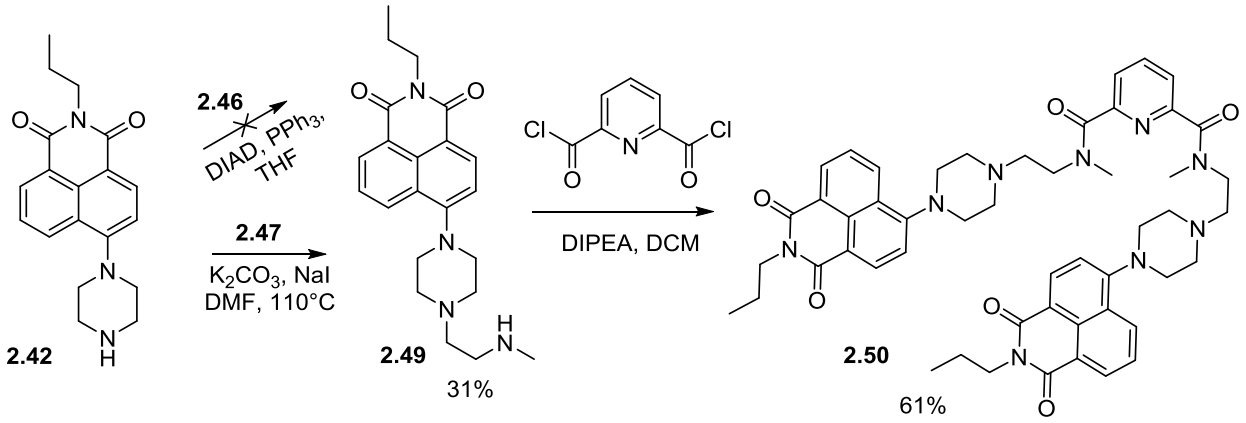

Scheme 2.7: Synthesis of receptor **2.50**.

The absence of the protection group was an impediment, as it favored polymerization of amines and formation of undesired products. Moreover, a 10-times excess of **2.47**, a change of solvent form acetonitrile to DMF and use of higher temperatures were necessary, and the reaction produced a complex mixture containing products and starting amine **2.42**. Luckily, this mixture was successfully separated on the column. The last step involved acylation of **2.49** with 2,6-pyridinedicarbonyl dichloride, which proceeded smoothly and resulted in compound **2.50**, a methylated analogue of receptor **2.38**. Receptor **2.50** exists as a mixture of conformers with slow exchange rate at room temperature. The structure of the receptor was unambiguously confirmed by NMR spectra measured at elevated temperature, at which the exchange rate between conformers is fast (Fig. 2.30).

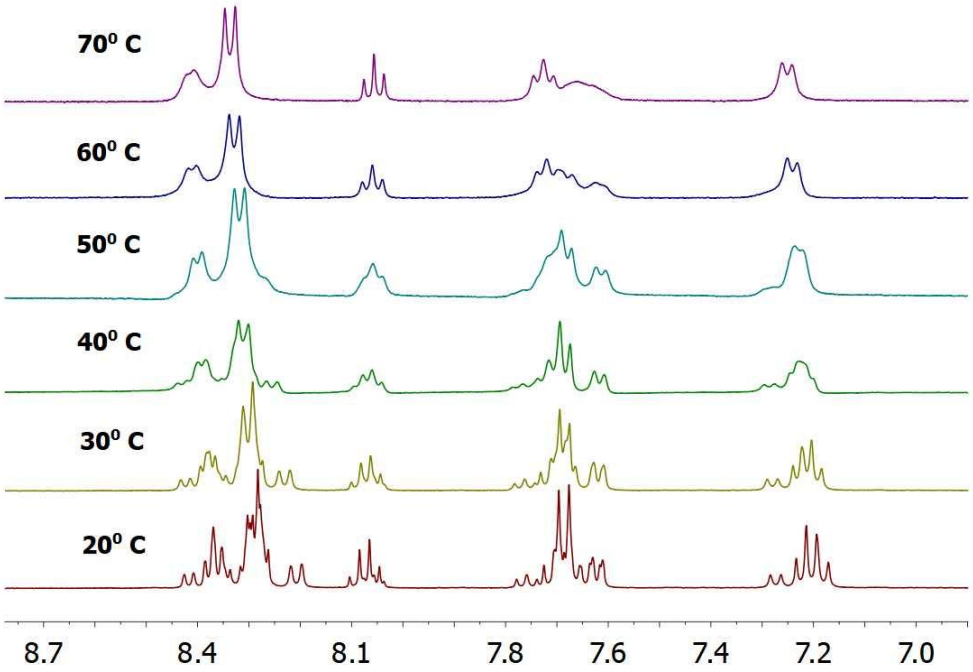

Figure 2.30: ^{1}H NMR spectra (aromatic protons region) of **2.50** in DMSO-d_6 at different temperatures.

Next, we performed all necessary experiments to determine anion binding properties of methylated receptor **2.50**. Thus, the pH scanning experiment (fluorescence–pH dependence) revealed that sulfate did induce pK_a shift for compound **2.50**, albeit a very small one compared to shifts of receptors **2.37**–**2.39** (Fig. 2.31a). This fact indicates that the fluorescent changes would not be large upon a titration with the anion. Job plot obtained for **2.50** with sulfate revealed a 1:1 binding stoichiometry (Fig. 2.31b). Fluorescent titrations for **2.50** demonstrated that the receptor had a clear binding preference for dianions (sulfate and oxalate) over monoanions (Fig. 2.31c). However, as can be seen in Table 2.2, the binding constants of **2.50** for dianions, especially for sulfate, are one order of magnitude lower than those observed for analogous receptor **2.38**. The affinity of the methylated receptor towards monoanions remains almost unchanged compared to non-methylated compound **2.38**. Competitive binding performed in the same conditions as for compounds **2.37**–**2.39** confirmed that selectivity for sulfate over monoanions is evidently higher for receptor **2.38** containing amide hydrogens than that for its methylated analogue **2.50** (Fig. 2.31d). Analysis of anion binding properties of receptor **2.50** suggests that hydrogen bonds between amide NH-groups and the bound anion indeed contribute to the selectivity of **2.38** for sulfate.

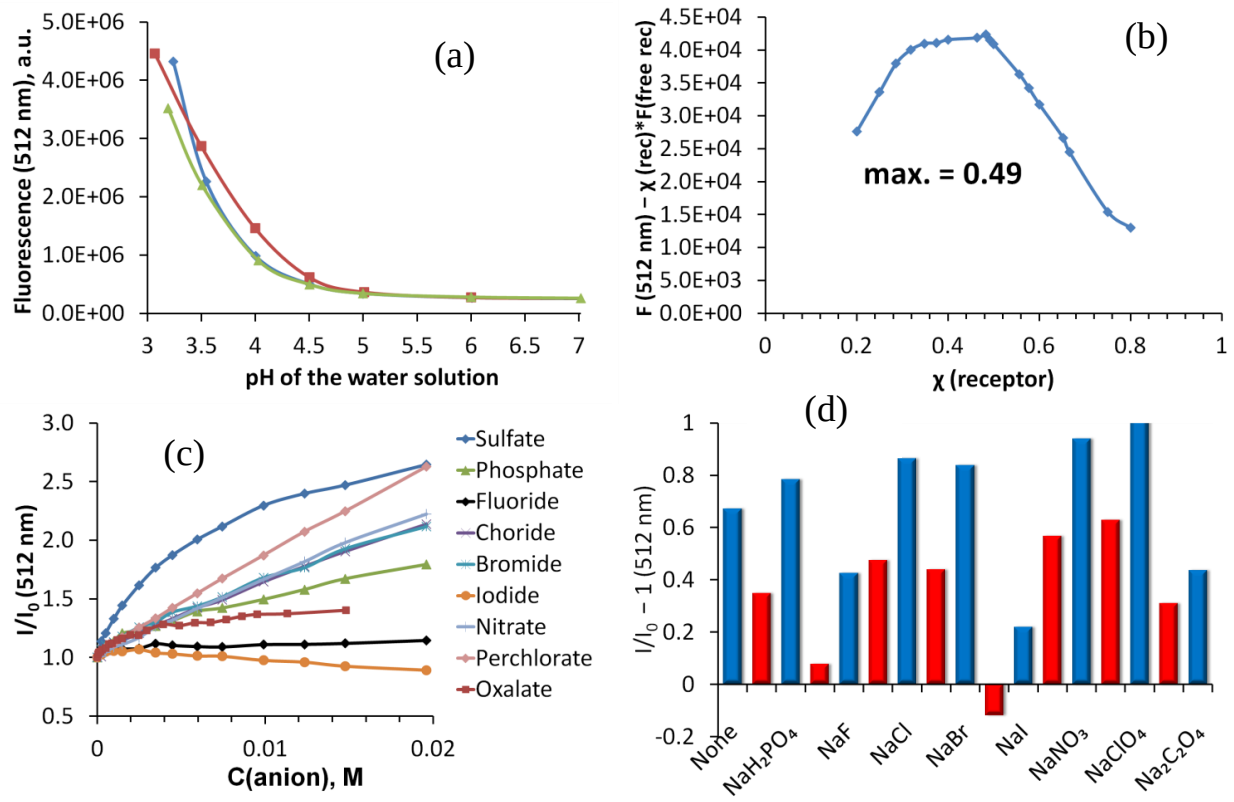

Figure 2.31: Binding properties of receptor **2.50** in THF–50 mM acetate buffer pH 4.1. (a) Fluorescence–pH dependence; (b) Job plot; (c) Fluorescent titrations with different anions; (d) Competitive binding.

Anion\ Log K[a]	SO_4^{2-}	$C_2O_4^{2-}$	$H_2PO_4^-$	F^-	Cl^-	Br^-	I^-	NO_3^-	ClO_4^-
2.38	3.46 (K_{11}) 2.38 (K_{12})	3.40	1.28	—[b]	1.51	1.25	—[b]	1.45	1.03
2.50	2.03	2.80 (K_{11}) 1.42 (K_{12})	1.45	—[b]	1.15	1.17	—[b]	<1	<1

Table 2.2: Binding constant of receptors **2.38** and **2.50** for selected anions. a) Measurement error ≤ 10%, b) Equilibrium is slow, not possible to fit the data.

2.3.6. Experimental part

Instruments and materials

See **2.2.4**

Synthesis

Compound **2.43** (tert-butyl (2-(4-(1,3-dioxo-2-propyl-2,3-dihydro-1*H*-benzo[de]isoquinolin-6-yl)piperazin-1-yl)ethyl)carbamate)

N-propyl-4-piperazine-1,8-naphthalimide (**2.42**) (1.233 g, 3.8 mmol) was dissolved in 70 mL of acetonitrile, *N*-Boc-2-bromoethylamine (1.109 g, 4.95 mmol), sodium carbonate (1.053 g, 7.62 mmol), and sodium iodide (0.857 g, 5.72 mmol) were added. The mixture was stirred at reflux for 5 h. After that, the solvent was evaporated, and the product was obtained with the help of gradient column chromatography (EtOAc–CH_3CN, from 95:5 to 90:10, Rf of the product 0.5 in the system EtOAc–CH_3CN 9:1). Yellow powder, yield 61%. ^{1}H NMR (DMSO-d_6), δ [ppm]: 0.90 (t, 3H, ^3J = 7.5 Hz); 1.39 (s, 9H); 1.63 (m, 2H); 2.47 (t, 2H, ^3J = 6.9 Hz); 2.71 (br. s, 4H); 3.11 (q, 2H, ^3J = 6.5 Hz); 3.22 (br. s, 4H); 3.98 (m, 2H); 6.70 (t, 1H, ^3J = 5.6 Hz); 7.31 (d, 1H, ^3J = 8.1 Hz); 7.78 (dd, 1H, ^3J = 7.4 Hz, ^3J = 8.3 Hz); 8.37 (d, 1H, ^3J = 8.1 Hz); 8.41 (dd, 1H, ^3J = 8.3 Hz, ^4J = 0.8 Hz); 8.44 (dd, 1H, ^3J = 7.3 Hz, ^4J = 0.8 Hz). ^{13}C NMR (DMSO-d_6), δ [ppm]: 163.6, 163.1, 155.7, 132.3, 130.7, 130.6, 129.1, 126.0, 125.3, 122.6, 115.5, 115.0, 77.7, 57.3, 52.7, 52.7, 28.3, 21.0, 11.4. M.p. 86–88 °C. ESI-MS calcd for MH^+: 467.2653, found 467.2686.

Compound **2.44** (1-(2-ammonioethyl)-4-(1,3-dioxo-2-propyl-2,3-dihydro-1*H*-benzo[de]isoquinolin-6-yl)piperazin-1-ium chloride)

Compound **2.43** (1.007 g) was dissolved in 110 mL of dioxane, 2.5 g of concentrated HCl were added (12 equiv), stirring was continued for 20 h. Yellow precipitate was filtered off and used without further purification. Yield 72%. ^{1}H NMR (D_2O), δ [ppm]: 0.94 (t, 3H, ^3J = 7.4 Hz); 1.56 (m, 2H); 3.69 (m, 14H); 7.16 (d, 1H, ^3J = 8.1 Hz); 7.56 (t, 1H, ^3J = 7.9 Hz); 7.99 (d, 1H, ^3J = 8.1 Hz); 8.06 (d, 1H, ^3J = 7.3 Hz); 8.17 (d, 1H, ^3J = 8.4 Hz). ^{13}C NMR (D_2O + DMSO-d_6), δ [ppm]: 166.7, 166.2, 155.6, 134.2, 133.1, 132.2, 130.0, 128.1, 126.5, 122.9, 117.5, 117.4, 54.5, 54.3, 51.3, 43.7, 35.4, 22.4, 12.4. M.p. 229–231 °C. ESI-MS calcd for MH^+: 367.2129; found 367.2143.

Compound **2.40** (*N*-(2-(4-(1,3-dioxo-2-propyl-2,3-dihydro-1*H*-benzo[de]isoquinolin-6-yl)piperazin-1-yl)ethyl)acetamide)

Compound **2.44** (0.05 g, 0.114 mmol) was dissolved in 7 mL of dry DCM, acetic anhydride (0.012 g, 0.114 mmol) and *N*,*N*-diisopropylethylamine (0.029 g, 0.228 mmol) were added. The mixture was stirred for 16 h at r. t. After that, the solution was washed with water (2 x 10 mL), dried under Na_2SO_4, and the solvent was evaporated. The product was purified with the help of gradient column chromatography (from pure $CHCl_3$ to $CHCl_3$–MeOH 100:5). Yellow powder,

yield 72%. ^{1}H NMR ($CDCl_3$), δ [ppm]: 0.99 (t, 3H, ^{3}J = 7.4 Hz); 1.73 (m, 2H); 2.00 (s, 3H); 2.63 (t, 2H, ^{3}J = 6.0 Hz); 2.78 (br. s, 4H); 3.28 (br. s, 4H); 3.42 (q, 2H, ^{3}J = 5.3 Hz); 4.11 (m, 2H); 5.97 (br. s, 1H); 7.20 (d, 1H, ^{3}J = 8.1 Hz); 7.67 (dd, 1H, ^{3}J = 7.3, ^{3}J = 8.4 Hz); 8.37 (dd, 1H, ^{3}J = 8.4 Hz, ^{4}J = 1.1 Hz); 8.50 (d, 1H, ^{3}J = 8.0 Hz). ^{13}C NMR ($CDCl_3$), δ [ppm]: 178.4, 170.1, 164.5, 164.0, 132.5, 131.1, 130.1, 126.1, 125.7, 114.9, 56.7, 53.0, 41.8, 36.0, 29.7, 23.4, 21.4, 11.5. M.p. 217–219 °C. ESI-MS calcd for MH^+: 409.2234, found 409.2250.

Compound **2.36** (5,5'-(heptane-4,4-diyl)bis(*N*-(2-(4-(1,3-dioxo-2-propyl-2,3-dihydro-1*H*-benzo[de]isoquinolin-6-yl)piperazin-1-yl)ethyl)-1*H*-pyrrole-2-carboxamide))

The dipyrrolylmethane diacid **2.30** (0.0411 g, 0.13 mmol) was dissolved in 10 mL of dry DCM, the solution was cooled to 0 °C. EDC·HCl (0.060 g, 0.31 mmol), HOBt (0.042 g, 0.31 mmol) and *N*,*N*-diisopropylethylamine (0.101 g, 0.78 mmol) were added to this solution and stirred for 1 h with cooling. After that, solution of compound **2.44** in 10 mL of dry DCM was added. The reaction mixture was stirred overnight. As a result, yellow precipitate was obtained and filtered. Purification was made by dissolving the product in pure acetic acid, neutralizing with $NaHCO_3$ and following extraction with the help of EtOAc. After removing the solvent, yellow powder was obtained (almost insoluble in organic solvents), yield 46%. ^{1}H NMR ($CDCl_3$ + acetic acid-d_4), δ [ppm]: 0.80 (t, 6H, ^{3}J = 7.2 Hz); 0.91 (t, 6H, ^{3}J = 7.4 Hz); 1.03 (m, 4H); 1.67 (m, 4H); 1.98 (m, 4H); 3.37 (t, 4H, ^{3}J = 5.4 Hz); 3.44 (s, 8H); 3.56 (br. s, 8H); 3.76 (t, 4H, ^{3}J = 5.4 Hz); 4.05 (m, 4H); 5.99 (d, 2H, ^{3}J = 3.9 Hz); 6.65 (d, 2H, ^{3}J = 3.9 Hz); 7.22 (d, 2H, ^{3}J = 8.0 Hz); 7.64 (dd, 2H, ^{3}J = 8.4, ^{3}J = 7.4 Hz); 8.25 (dd, 2H, ^{3}J = 8.4 Hz, ^{4}J = 0.9 Hz); 8.46 (d, 2H, ^{3}J = 8.0 Hz); 8.52 (dd, 2H, ^{3}J = 7.2 Hz, ^{4}J = 0.9 Hz); 9.86 (br. s, 2H).

Compound **2.37** (1,1',1''-(nitrilotris(ethane-2,1-diyl))tris(3-(2-(4-(1,3-dioxo-2-propyl-2,3-dihydro-1*H*-benzo[de]isoquinolin-6-yl)piperazin-1-yl)ethyl)thiourea))

Compound **2.44** (0.300 g, 0.688 mmol) was dissolved in 30 mL of DCM, tris(2-isothiocyanatoethyl)amine (0.062 g, 0.228 mmol) and *N*,*N*-diisopropylethylamine (0.177 g, 1.37 mmol) were added. The mixture was stirred overnight at r. t. After that, the solution was washed with water (2 x 10 mL), dried under Na_2SO_4, and the solvent was evaporated. The product was purified with the help of gradient column chromatography ($CHCl_3$–MeOH from 97:3 to 93:7). Yellow powder, yield 95%. ^{1}H NMR (DMSO-d_6), δ [ppm]: 0.87 (t, 9H, ^{3}J = 7.4 Hz); 1.58 (m, 6H); 2.55 (m, 6H); 2.66 (m, 18H); 3.16 (br. s, 12H); 3.53 (br. d, 12H); 3.93 (t, 6H, ^{3}J = 7.4 Hz); 7.22 (d, 3H, ^{3}J = 8.1 Hz); 7.63 (br. s, 6H); 7.70 (t, 3H, ^{3}J = 7.9 Hz); 8.29 (d, 3H, ^{3}J = 8.1 Hz); 8.30 (d, 3H, ^{3}J = 8.2 Hz); 8.36 (d, 3H, ^{3}J = 7.1 Hz). ^{13}C NMR ($CDCl_3$), δ [ppm]: 177.3, 164.3,

163.9, 132.2, 131.2, 129.8, 129.7, 126.0, 125.9, 123.3, 114.9, 53.3, 52.9, 41.8, 21.4, 11.5. M.p. 121–123 °C. ESI-MS calcd for $(M+3H)^{3+}$: 457.8870, found 457.8887.

Compound **2.38** (N^2,N^6-bis(2-(4-(1,3-dioxo-2-propyl-2,3-dihydro-1*H*-benzo[de]isoquinolin-6-yl)piperazin-1-yl)ethyl)pyridine-2,6-dicarboxamide)

Compound **2.44** (0.100 g, 0.228 mmol) was dissolved in 10 mL of dry DCM, and *N*,*N*-diisopropylethylamine (0.088 g, 0.684 mmol) was added. The solution was cooled to 0 °C, and 2,6-pyridinedicarbonyl dichloride (0.023 g, 0.114 mmol) in 5 mL of dry DCM was added dropwise over 1 h. The mixture was stirred overnight at r. t. After that, the mixture was washed with water (2 x 15 mL), organic layer was dried under Na_2SO_4, and the solvent was evaporated. The product was purified with the help of gradient column chromatography (from pure $CHCl_3$ to $CHCl_3$–MeOH 100:5). Yellow powder, yield 93%. ^{1}H NMR ($CDCl_3$), δ [ppm]: 0.96 (t, 6H, ^3J = 7.4 Hz); 1.77–1.56 (m, 4H); 2.82 (br. s, 4H); 2.87 (br. s, 8H); 3.27 (br. s, 8H); 3.73 (m, 4H); 4.10–4.03 (m, 4H); 7.09 (d, 2H, ^3J = 8.1 Hz); 7.64 (dd, 2H, ^3J = 8.4 Hz, ^3J = 7.4 Hz); 8.03 (t, 1H, ^3J = 7.8 Hz); 8.27 (dd, 2H, ^3J = 8.5 Hz, ^4J = 1.0 Hz); 8.34 (d, 4H, ^3J = 8.0 Hz); 8.53 (dd, ^3J = 7.3 Hz, ^4J = 1.0 Hz); 8.57 (br. s, 2H). ^{13}C NMR ($CDCl_3$), δ [ppm]: 164.2, 163.8, 163.7, 155.0, 148.7, 139.0, 132.0, 131.1, 129.7, 129.7, 125.90, 125.85, 125.0, 123.3, 117.1, 114.7, 57.6, 53.2, 52.8, 41.8, 36.2, 29.7, 21.3, 11.5. M.p. 252–254 °C with decomposition. ESI-MS calcd for MH^+: 864.4192, found 864.4213.

Compound **2.39** (N^1,N^3-bis(2-(4-(1,3-dioxo-2-propyl-2,3-dihydro-1*H*-benzo[de]isoquinolin-6-yl)piperazin-1-yl)ethyl)isophthalamide)

Compound **2.44** (0.150 g, 0.342 mmol) was dissolved in 10 mL of dry DCM, and *N*,*N*-diisopropylethylamine (0.133 g, 1.03 mmol) was added. The solution was cooled to 0 °C, and isophatloyl chloride (0.034 g, 0.171 mmol) in 15 mL of dry DCM was added dropwise over 1 h. The mixture was stirred overnight at r. t. After that, the mixture was washed with water (2 x 15 mL), organic layer was dried under Na_2SO_4, and the solvent was evaporated. The product was purified with the help of gradient column chromatography ($CHCl_3$–MeOH from to 100:2 100:4). Yellow powder, yield 85%. ^{1}H NMR ($CDCl_3$), δ [ppm]: 0.98 (t, 6H, ^3J = 7.4 Hz); 1.73 (m, 4H); 2.76 (t, 4H, ^3J = 5.9 Hz); 2.83 (br. s, 8H); 3.29 (br. s, 8H); 3.64 (m, 4H); 4.16–4.04 (m, 4H); 6.88 (t, 2H, ^3J = 4.5 Hz); 7.19 (d, 2H, ^3J = 8.1 Hz); 7.53 (t, 1H, ^3J = 7.7 Hz); 7.67 (dd, 2H ^3J = 8.4 Hz, ^3J = 7.4 Hz); 7.92 (dd, 2H, ^3J = 7.7 Hz, ^4J = 1.7 Hz); 8.28 (s, 1H); 8.37 (dd, 2H, ^3J = 8.4 Hz, ^4J = 1.1 Hz); 8.47 (d, 2H, ^3J = 8.0 Hz); 8.55 (dd, 2H, ^3J = 7.3 Hz, ^4J = 1.0 Hz). ^{13}C NMR ($CDCl_3$), δ [ppm]: 166.5, 164.4, 164.0, 155.6, 134.9, 132.4, 131.1, 130.1, 129.8, 129.7, 129.0, 126.1, 125.7,

125.7, 123.3, 117.0, 115.0, 56.5, 53.0, 41.8, 36.5, 21.4, 11.5. M.p. 122–124 °C. ESI-MS calcd for MH^+: 863.4239, found 863.4262.

Compound **2.49** (6-(4-(2-(methylamino)ethyl)piperazin-1-yl)-2-propyl-1*H*-benzo[de]isoquinoline-1,3(2*H*)-dione)

N-propyl-4-piperazine-1,8-naphthalimide **2.42** (0.400 g, 1.24 mmol) was dissolved in 60 mL of dimethylformamide, 2-bromo-*N*-methylethanamine hydrobromide **2.47** (2.166 g, 9.89 mmol), sodium carbonate (1.026 g, 7.42 mmol), sodium iodide (0.742g, 4.95 mmol) were added. The mixture was stirred at 110 °C ca. 16 h. Reaction was controlled with the help of TLC ($CHCl_3$–MeOH–NH_3(aq) 100:5:5, Rf of the product 0.2). After that, the solvent was evaporated, and the product was obtained with the help of gradient column chromatography (from $CHCl_3$–MeOH 100:2 to $CHCl_3$–MeOH–NH_3(aq) 100:2:1.5). Orange solid, yield 31%. ^{1}H NMR ($CDCl_3$), δ [ppm]: 0.98 (t, 3H, ^3J = 7.4 Hz); 1.73 (m, 2H); 2.46 (s, 3H); 2.63 (t, 2H, ^3J = 5.9 Hz); 2.73 (t, 2H, ^3J = 6.1 Hz); 2.76 (br. s, 4H); 3.27 (br. s, 4H); 4.11 (m, 2H); 7.18 (d, 1H, ^3J = 8.1 Hz); 7.65 (dd, 1H, ^3J = 7.4 Hz, ^3J = 8.3 Hz); 8.38 (dd, 1H, ^3J = 8.4 Hz, ^4J = 0.9 Hz); 8.48 (d, 2H, ^3J = 8.0 Hz); 8.55 (dd, 1H, ^3J = 7.3 Hz, ^4J = 0.8 Hz). ^{13}C NMR ($CDCl_3$), δ [ppm]: 164.5, 164.0, 155.9, 132.5, 131.0, 130.2, 129.8, 126.1, 125.6, 123.2, 116.7, 114.8, 57.8, 53.3, 53.0, 48.6, 41.7, 36.5, 29.7, 21.39, 11.5. M.p. 93–95 °C. ESI-MS calcd for MH+: 381.2285, found 381.2312.

Compound **2.50** (N^2,N^6-bis(2-(4-(1,3-dioxo-2-propyl-2,3-dihydro-1*H*-benzo[de]isoquinolin-6-yl)piperazin-1-yl)ethyl)-N^2,N^6-dimethylpyridine-2,6-dicarboxamide)

Compound **2.49** (0.145 g, 0.38 mmol) was dissolved in 10 mL of dry DCM, and *N*,*N*-diisopropylethylamine (0.049 g, 0.38 mmol) was added. The solution was cooled to 0 °C, and 2,6-pyridinedicarbonyl dichloride (0.039 g, 0.19 mmol) in 10 mL of dry DCM was added dropwise over 1 h. The mixture was stirred overnight at r. t. After that, the mixture was washed with water (2 x 15 mL), organic layer was dried under Na_2SO_4, and the solvent was evaporated. The product was purified with the help of column chromatography ($CHCl_3$–MeOH 100:1). Yellow powder, yield 61%. ^{1}H NMR (DMSO-d_6), δ [ppm]: 0.84–0.91 (m, 6H); 1.51–1.66 (m, 4H); 2.56 (br. s, 4H); 2.69 (br. s, 8H); 2.99, 3.00, 3.06 (s, 6H); 3.09, 3.20 (br. s, 8H); 3.49 (m, 2H); 3.66 (t, 2H, ^3J = 6.2); 3.87–3.97 (m, 4H); 7.16–7.28 (m, 2H); 7.61–7.77 (m, 4H); 8.04–8.10 (m, 1H); 8.19–8.42 (m, 6H). ^{13}C NMR (DMSO-d_6), δ [ppm]: 168.3, 168.2, 167.9, 163.9, 163.8, 163.4, 163.3, 155.8, 153.7, 153.5, 139.0, 132.5, 130.9, 130.7, 129.4, 126.3, 126.2, 125.5, 125.4, 124.3, 124.2, 123.7, 122.9, 122.82, 122.76, 115.9, 115.8, 115.3, 115.2, 56.2, 56.0, 55.2, 55.0,

53.3, 53.2, 52.9, 48.0, 47.7, 44.7, 44.5, 41.4, 37.5, 37.3, 33.8, 33.5, 21.3, 11.80. M.p. 117–119 °C. ESI-MS calcd for MH^+: 892.4505, found 892.4513.

Anion binding studies (NMR)

NMR titration of **2.38** with sulfate was performed as following. 0.6 mg of receptor **2.38** were dissolved in 420 mkL of THF-d_8. To an NMR tube were added: the receptor solution, 280 mkL of 50 mM buffer prepared from AcOD/D_2O–NaOH pH 4.1. Thus, the resulted solution in the NMR tube contained 40% vol. of the D_2O-based buffer, 60% vol. of THF-d_8, and 1 mM of receptor **2.38**. For the NMR titration 1.4 M solution of tetramethylammonium sulfate was prepared in the same D_2O-based acetate buffer (1 mkL of the solution corresponding to 2 equiv of the receptor in NMR tube). To the prepared receptor solution small aliquots of the salt solutions were added, total added volume 10 mkL (20 equiv). After addition of every aliquot ^1H NMR spectrum was recorded.

For the ROESY experiment without sulfate the sample was prepared as for the titration. For the ROESY experiment with sulfate the sample was prepared as following: 1.8 mg of receptor **2.38** were dissolved in 690 mkL of THF-d_8, 175 mkL of 50 mM buffer prepared from AcOD/D_2O–NaOH pH 3.6 were added. Tetrabutylammonium hydrogen sulfate (61.1 mg) was dissolved in 150 mkL of the same buffer. 35 MkL of the sulfate solution were added to the probe in NMR tube. Thus, the resulted concentrations in the NMR tube were: $2.3 \cdot 10^{-3}$ M for receptor **2.38**, 0.047 M (20 equiv) for $TBAHSO_4$. The spectrum was recorded at 45 °C in order to avoid precipitation.

Anion binding studies (UV-vis and fluorescence)

The stock solutions of compounds ($2 \cdot 10^{-4}$ M or $2.5 \cdot 10^{-4}$ M) in tetrahydrofuran were prepared in 50 mL volumetric flasks. For an experiment THF solution was diluted with the corresponding buffer (for titrations) or with specially prepared solutions containing certain amount of acetate, phosphate, and sulfate (for pH studies) in order to obtain 10^{-4} M concentration (for fluorescence) or $5 \cdot 10^{-5}$ M concentration (for UV-vis, stock solution was first diluted with THF, then with the buffer). The solutions of sodium salts (0.002–2 M) were prepared in the same buffer. The receptor solution in a 10 mm cuvette (2 mL) was then titrated with the salt solution and each time the fluorescence or UV-vis spectrum was recorded. Fluorescence parameters: excitation 350 nm (**2.38**, **2.39**, **2.50**); 400 nm (**2.37**); 380 nm (**2.40**); emission 440–620 nm. The resulting data was imported in HypSpec program[17] and fitted to obtain stability constants.

For the competitive binding experiment the diluted solutions of receptors were prepared as described; 30 equiv of sodium sulfate solution were added first to the receptor solution, and the fluorescence spectrum was measured. After that, 100 equiv of different sodium salts were added to the solution containing the receptor and sulfate (for the each competing anion a new portion of the solution was needed), and changes in fluorescence response were recorded.

Potentiometric titrations

The solutions of **2.38** and its sulfate complex were prepared in the mixture of THF and 0.1 M NaCl with $1 \cdot 10^{-4}$ M concentration of the compound. Before titrations, **2.38** was converted into corresponding hydrochloride by adding 10 equiv of HCl. Standard 0.1 M solution of NaOH was used for titrations. The reaction vessel was kept at constant temperature 23 °C.

2.4. Summary of chapter 2

In this chapter, a novel approach for the design of fluorescent sulfate receptors has been described. The receptors contain one or more naphthalimide dyes, amino groups that can be protonated, and anion binding fragments possessing multiple hydrogen bonding sites. It has been shown that both aromatic and aliphatic amines can be used for the design of fluorescent receptors. Fluorescence enhancement observed upon an addition of sulfate anion is attributed to hindering of the photoinduced electron transfer by the protonation of the amine groups. Shift in pK_a of the receptors caused by sulfate coordination has been confirmed by fluorescence, Uv-vis, and potentiometry. Furthermore, it has been demonstrated that hydrogen bonding plays a significant role in the recognition process even in a competitive aqueous medium. For one of the receptors, DFT calculations have been performed, and the calculated structure have been unambiguously confirmed by ROESY NMR. All receptors have high affinities towards sulfate with binding constants > 10^3 M^{-1} and a good selectivity over environmentally important monoanions. A significant fluorescence enhancement reaching 5-fold allows us to consider this type of sulfate sensors as very promising. In future, the receptors can be additionally modified in order to increase water solubility, and, therefore, to facilitate practical applications.

3. Understanding stacking interactions between an aromatic ring and nucleobases in aqueous solution: experimental and theoretical study

E. A. Kataev, T. A. Shumilova, B. Fiedler, T. Anacker, and J. Friedrich, *J. Org. Chem*. **2016**, *81*, 6505–6514. Understanding stacking interactions between an aromatic ring and nucleobases in aqueous solution: experimental and theoretical study.

Synthesis and experimental studies have been performed by T. Shumilova; the theoretical studies have been accomplished by B. Fiedler, T. Anacker, and J. Friedrich.

3.1. State of the art

3.1.1. Importance

Non-covalent interactions between nucleobases and aromatic compounds, for example, amino acids are essential to life. They play an important role in stabilization of natural DNA-protein complexes,[143] which participate in processing and replication of genetic information, as well as protein synthesis.[144] Recent studies show that non-covalent interactions between halogenated aryl moieties dramatically increase the efficiency of inhibitors as compared to non-halogenated analogues.[145] Similar effects were observed for the interaction of halogenated dyes intercalated in DNA.[146] Therefore, experimental studies of non-covalent interactions between nucleobases and aromatic compounds should shed light on the origin of these interactions and lead to new developments in rational drug design, control of gene expression, and artificial receptors or sensors for nucleotides and nucleic acids.[147] Selective recognition and sensing of single nucleotides like nucleoside mono- or triphosphate (NMPs and NTPs) can benefit different fields of biochemistry and medicine, e.g. single molecular imaging, analysis of enzyme kinetics and cellular transport.

3.1.2. Arene–arene interactions

Experimental and theoretical study of arene–arene interactions has attracted considerable attention in recent years.[148] Traditionally, there are two geometries for the simplest system of benzene dimers: parallel-displaced, and T-shaped edge-to-face, whereas an eclipsed face-to-face structure is not energetically favored. The Hunter–Sanders electrostatic hypothesis postulated in

1990s explained it and offered simple "rules" for understanding and prediction of such interactions.[149,150] The authors noted that π-electron density on most aromatic rings creates a quadrupole moment with partial negative charge allocated above and below the ring surface, and a partial positive charge around the periphery. Two such quadrupoles closely positioned to each other should favor perpendicular edge-to-face interactions or off-centered parallel stacking, and not face-centered parallel stacking, which may seem like a more obvious choice at the first glance. Moreover, this hypothesis suggested that when one of the rings contain a substituent, this substituent influences π-electron distribution, and therefore, the strength of the π–π interaction between the rings. Therefore, electron-withdrawing groups should enhance this interactions, whereas electron-donating group should reduce them. Experimental observations often supported these results.

However, modern computational results performed by Wheeler and others demonstrated that the presence of substituents increases the strength of π–π interactions independently of their properties.[151–153] Instead of the traditional hypothesis, the researchers proposed that a substituent itself interacts with the unsubstituted aromatic ring by means of electrostatic dipole — quadrupole — and dispersive interactions. Theoretical calculations performed by other groups revealed that the Wheeler–Houk hypothesis for arene–arene-X interactions is more accurate than the Hunter–Sanders hypothesis.[154] Some experimental studies, involving studies with molecular balances, also supports the Wheeler's calculations, i.e. direct interactions of substituents with the aromatic ring.[155,156] However, Dietrich et al. has recently demonstrated that intermolecular distance between the X-substituent belonging to the one aromatic ring and another aromatic ring results in a strongly different substituent effect. [157] Namely, when the partial overlap between X and the second ring is present, π–π stacking interactions are stabilized independent on the electronic nature of X (Fig. 3.1). This result confirms Wheeler–Houk hypothesis. On the other hand, when the substituent and the second ring are shifted further from each other, Hunter–Sanders model is realized.

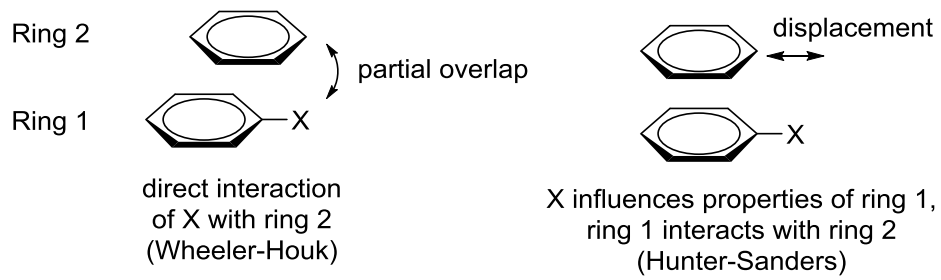

Figure 3.1: Realization of Wheeler-Houk and Huter-Sanders hypothesis

3.1.3. Nucleobases–arene interactions in recognition of nucleotides

Theoretical calculations of direct interactions nucleobase–arene have been performed by different groups, but they show relatively high values as compared with the experiment.[154,158,159] Experimental assessment of these interactions in water is a difficult task because the interactions are relatively weak, geometry of the complex in solution is difficult to determine, and also because there is a challenge in distinguishing between hydrophobic and dispersion components of the interaction. However, several research groups obtained some insights towards solving these problems. For example, there are some reports discussing interactions of positively charged dyes with nucleobases in water or a buffer solution.[160–162] These studies usually describe complexes in the excited state. Thus, Kubota and coworkers investigated fluorescence changes induced by the addition of different acridine dyes to nucleotides in a phosphate buffer at pH 7 (Fig. 3.2).[160] The authors observed static and dynamic quenching of dyes in the presence of nucleotides and the determined binding constants were in the order of 100 M^{-1}. 10-Methylacridine binds AMP with K = 40 M^{-1} and selectivity AMP = GMP > TMP > CMP. In another study, Seidel investigated quenching of a series of coumarine dyes by nucleotides.[162] He performed a detailed analysis of redox properties of nucleobases and dyes, which allowed him to assess the direction of PET (photoinduced electron transfer). Leonard used a different approach to assess stacking interactions between indole and nucleobases.[161] He connected both aromatic compounds with a linker consisting of three and four carbon atoms and gathered the information about the interactions with the help of NMR and UV-vis spectroscopy.

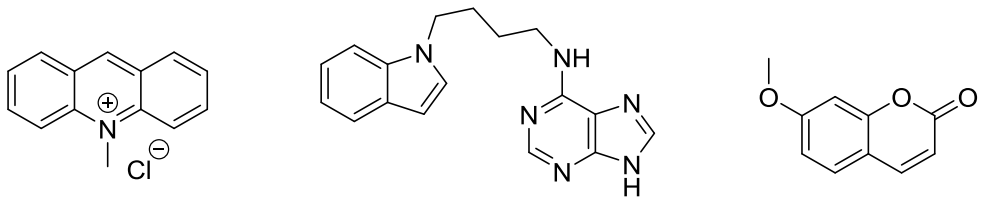

3.1 **3.2** **3.3**

Figure 3.2: Examples of dyes used by Kubota (**3.1**), Leonard (**3.2**) and Seidel (**3.3**) to study their interaction with nucleobases.

Another big group of studies dealing with complexes in the ground state was recently reviewed by Yoon.[163] A huge amount of receptors for nucleobases and nucleotides has been developed up to nowadays; however, the mechanism of particular selectivity was determined only in several cases.[8,164] For example, Lehn and co-workers synthesized macrocyclic bis-intercaland **3.4** and studied its binding properties with different nucleosides and nucleotides in a

buffer at pH 6 (Fig. 3.3).[165] They discovered that the binding strength increased with the size and charge of the substrate, and a slight preference for A and G nucleosides and nucleotide monophosphates over C- and U-containing guests was observed. The authors concluded that both stacking and electrostatic effects are present; therefore, they decided to increase the area of the aromatic surface. As a result, acridine-containing macrocycle **3.5** was obtained.[166] This compound demonstrated remarkable properties in nucleoside binding selectivity, namely, a strong preference towards purines A and G was detected. The selectivity was explained by a greater contact with the acridine complexing units, as purines have larger aromatic surface compared to pyrimidines.

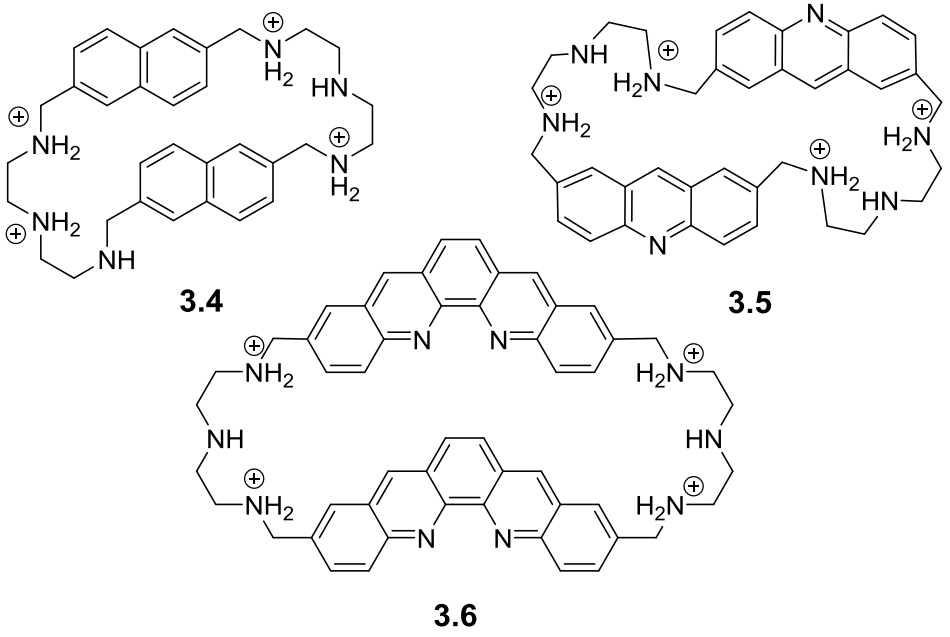

Figure 3.3: Macrocycles studied by Lehn and co-workers.

Similarly to the previous study, the affinity was enhanced approx. by a factor 100 from nucleosides to nucleotides, and then by a factor of 10 for each additional phosphate group. These results indicates that electrostatic forces play the most important role in stability of these complexes. Interestingly, the increase of substrate's charge didn't result in a decrease of the purines/pyrimidines selectivity. On the contrary, the ratio between A and U substrates was significantly larger for tri- and dinucleotides (*K*(ATP) / *K*(UTP) = 780, *K*(ADP) / *K*(UDP) = 1100) than for the corresponding mononucleotides (*K*(AMP) / *K*(UMP) = 190). In order to further improve binding properties of the receptor, the authors increased the aromatic surface one more time by synthesizing quinacridine macrocycle **3.6**.[167] This compound was found to be selective for guanosine derivatives as compared to other nucleobases, while its predecessor **3.5**

demonstrated a slight preference for adenosine. Another interesting result was observed during the analysis of the stoichiometry of binding. Namely, nucleotide monophosphates formed 1:2 (host : guest) complexes, but for di- and trinucleotides only 1:1 associates were present. This result was attributed to a good complementarity between the host and the guest molecules compatible with anchorage of one nucleotide monophosphate on each cationic bridge.

From a significant number of publications on this topic it is worth to outline those receptors that can discriminate between different nucleotides; selected examples are shown in Fig. 3.4. The major problem that arises after the analysis of selectivities of the probes in Fig. 3.4 is the difficulty to draw any structure–selectivity patterns that can be used for further improvements of receptors design. Sometimes explanations of the authors or the observed receptor behaviors contradict each other. For example, Yoon and coworkers[168] ascribed the selectivity of their receptor for GTP over ATP to different H–π interactions, while Lehn[167] explained this fact with different intercalating strength between an aromatic ring and a nucleobase. Moreover, only in a few publications the mechanism of a selective fluorescence response was provided and supported by experimental data.

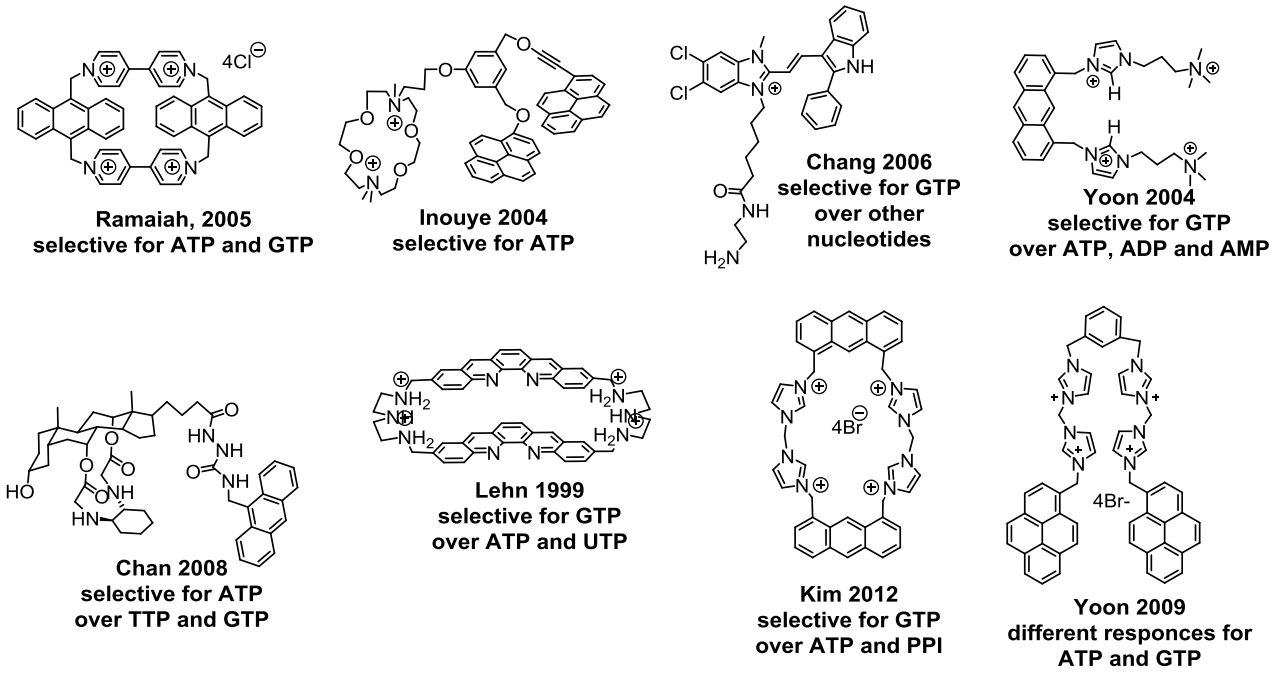

Figure 3.4: Selected receptors that can discriminate between different nucleotides: Ramaiah,[169,170] Inouye,[171] Chang,[172] Yoon,[168] Chan,[173] Lehn,[167] Kim,[174] Yoon.[175]

Recognition of nucleotides using hydrogen bonds has a great advantage, as it might help to achieve higher selectivity towards selected nucleotides. However, this task is very challenging because water is a highly competitive solvent. There are a limited number of publications, which

deal with recognition through hydrogen bonds in water. For example, Lhomme in 1987 showed that hydrogen bonding between adenine and uracil is possible in water only if additional stacking interactions are present (Fig. 3.5).[176] The same evidence was obtained by Rebek using Kemp's acid as a binding site for nucleotides.[177,178] It is worth mentioning that these authors were the firsts, who examined an effect of the structure of an aromatic ring on its stacking properties with adenine in water. They discovered that the extension of the hydrophobic surface from phenyl to naphthyl corresponds to an increase in free binding energy of −1.5 kcal/mol. Additional electrostatic interactions allowed the authors to bind cAMP with affinity K = 600 M^{-1}.[179] Zimmerman has shown that a combination of an intercalating dye with a hydrogen bonding motif leads to a tight and selective binding of the receptor to CUG repeats in RNA. The molecule inhibits protein–RNA interaction and helps to cure myotonic dystrophy type 1.[180] One more interesting work has been recently published by Fujita and co-workers.[181] Normally, hydrogen bonds between nucleobases G and C have very low interactions energy, so they are impossible in water. However, the authors have shown that these two nucleosides can interact in water in the presence of a special cage compound. The structure of the supramolecular complex was obtained from the X-ray single crystal analysis. The cage provided a hydrophobic cavity and stabilized Watson–Crick base paring by stacking interactions.

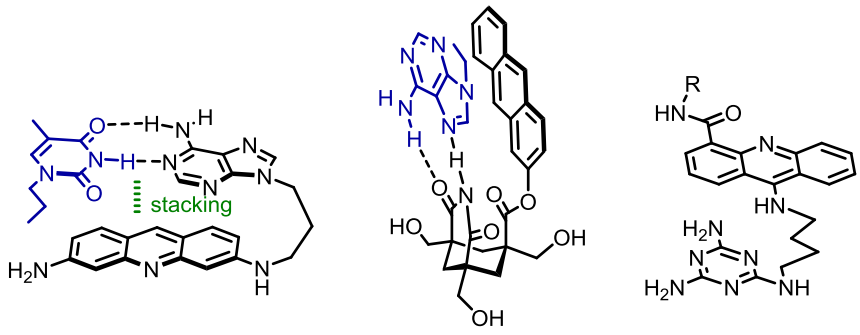

3.7 **3.8** **3.9**

Figure 3.5: Selected receptors synthesized by Lhomme (**3.7**), Rebek (**3.8**) and Zimmerman (**3.9**), which bind nucleobases and nucleotides through hydrogen bonds and π–π stacking interactions.

In summary, there are two main problems regarding quantification of stacking interactions between aromatic compounds and nucleobases. First, binding affinities have small values so that it is difficult to measure them with standard analytical methods. Second, measurements in aqueous solution are usually complicated due to the low solubility of organic compounds. In the following work, we address these challenges by extracting stacking free energies from thermodynamic quantification of nucleotide binding to di(2-picolyl)amine-Zn(II) complexes.

The overall stability constants for the complexes are high and allow one to measure binding affinities with high accuracy.

3.2. Results and discussion

3.2.1. Design of model systems

As discussed above, recognition and sensing of nucleotides is a rapidly growing field. There are a number of selective receptors and fluorescent probes developed to date, whose structures are based on positively charged aromatic rings or metal complexes bearing an aromatic ring. Considering the recognition in an aqueous buffered solution, the affinity of single-charged aromatic systems for nucleotides are usually less than 100 M^{-1}.[182] Within the experimental error the affinities for closely structured nucleotides, e.g., for ATP and GTP, are the same. Thus, it is difficult to elucidate the effect of the structure of a nucleobase on the binding strength. On the other hand, dyes with Zn(II) complexes show much higher affinities (ca. 10^5 M^{-1}) for nucleotides due to strong electrostatic interactions between the Zn(II) site and the phosphate residue and, therefore, are more suitable to detect small differences between nucleobases.[183,184]

There are two general designs of Zn(II) complexes used for recognition and sensing of nucleotides. The first design consists of a rigid fluorescent scaffold with one or two Zn(II) sites. The selectivity of complexes for nucleotides (bearing different nucleobases) is usually low because electrostatic interactions dictate the overall affinity.[185,186] The second design consists of a Zn(II) site and a dye that is connected through a flexible linker. The dye is assumed to form π–π interactions with a nucleobase.[187] Hence, it was often expected that stacking interactions between the dye and a nucleobase introduce a selectivity for a certain nucleotide into the complex. Independently of this, it was shown that such complexes allow one to differentiate between nucleotides by using fluorescence spectroscopy, because different nucleobases interact with an excited dye with different binding strengths. For example, ATP often induces an increase in fluorescence of Zn(II) complex, while addition of GTP leads to quenching of fluorescence.[163]

For our studies we used the second design and synthesized ligands LAntr, LH, LQAntr and LQH (Fig. 3.6) according to the literature known procedures.[188–191] The Zn(II) complexes for these ligands are also known, but they have never been studied in complexation with nucleotides. In principle, any Zn(II) complex bearing free coordination sites for binding an anionic species can be a potential receptor for nucleotides. In our design, the Zn(II) site is responsible for electrostatic interactions with phosphate, while the anthracene dye can form π–π interactions

with a nucleobase. This concept — a combination of both types of interactions — rests on our previous investigation of Cu(II) complex **3.10** (Fig. 3.6), which demonstrated selectivity for ATP (adenosine triphosphate) over ADP (adenosine diphosphate) and AMP (adenosine monophosphate).[192] Quantum chemical calculations and spectroscopic measurements provided an evidence of high complementarity in complex **3.10**, i.e., adenine forms π–π interactions with anthracene. The proximity of two aromatic systems were impossible in cases of shorter nucleotides such as ADP or AMP.

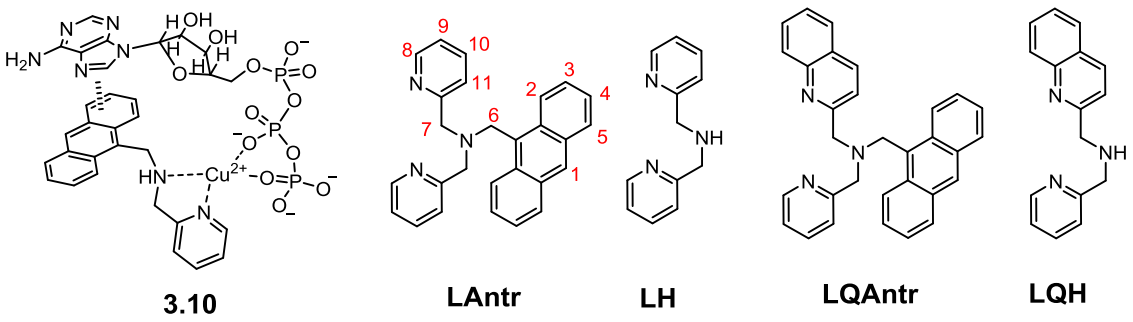

Figure 3.6: Complex with ATP (**3.10**) studied in the previous work. Structures of ligands used in this work to quantify stacking interactions between anthracene and nucleobases.

In preliminary studies, we investigated the interaction of free ligand LAntr with nucleotides in a 10 mM TRIS buffer (pH 7.4, 100 mM NaCl). The ligand has pK_a value of 5.25 and thus, only 0.4% of the ligand are singly protonated at pH 7.4. The ligand binds NTPs, but with relatively low affinities (less than 500 M^{-1}). The observed increase in fluorescence of the ligand during the titrations with ATP and CTP (Fig. 3.7a) can be explained by the fact that the complexation favors protonation of the tertiary amine. This protonation hinders a photoinduced electron transfer (PET) between the dye and the amine leading to a fluorescence increase.[189]

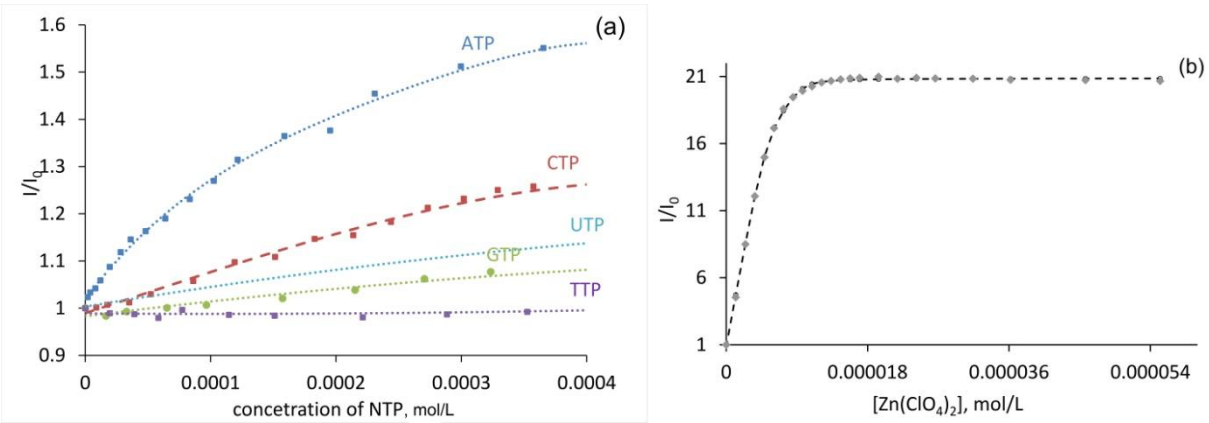

Figure 3.7:. (a) Changes in fluorescence intensity of the ligand (10^{-5} M) at 415 nm induced by addition of five nucleoside triphosphates. (b) Fluorescence changes induced by addition of zinc(II)

perchlorate to ligand LAntr (10^{-5} M). Conditions: 10 mM TRIS buffer (pH 7.4, 4% vol. MeOH, 0.1 M NaCl). Excitation at 370 nm.

Formation of complex LAntr·Zn(II) from the ligand and zinc(II) perchlorate accompanies with strong fluorescence increase (Fig. 3.7b). The stability constant of LAntr·Zn(II) in a 10 mM TRIS buffer is log K_{11} = 8.2. However, according to fluorescence titrations complex $LAntr_2$·Zn(II) is also formed with stability constant log K_{21} = 14.3. To ensure the formation of a 1:1 complex, we performed all titrations with nucleoside triphosphates in the presence of 10 equiv of Zn(II).

The Zn(II) complex shows a different profile of fluorescence changes in the presence of nucleotides compared to one of the free ligand. Adenosine and cytosine triphosphates increase the fluorescence of the complex further, while thymidine, guanosine and uridine triphosphates quench the fluorescence of the ligand (Fig. 3.8). Increasing amounts of a nucleotide favor the formation of a ternary complex LAntr·Zn·NTP (NTP, nucleoside triphosphate), whose fluorescence has a structure characteristic for anthracene (Fig. 3.8). According to De Silva[193] and Hamachi[186] coordination of an anion to a Zn(II) site suppresses the PET quenching of the photoexcited anthracene by the cationic pyridine leading to an increase of fluorescence. Such an increase we observed for ATP, CTP and pyrophosphate. On the contrary, UTP, TTP and GTP quench the fluorescence of the complex due to a different PET process, from nucleobases to anthracene, as revealed previously by Seidel and co-workers in dye–nucleobase complexes.[162]

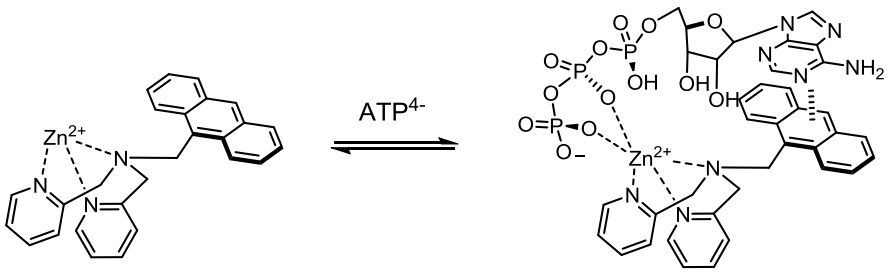

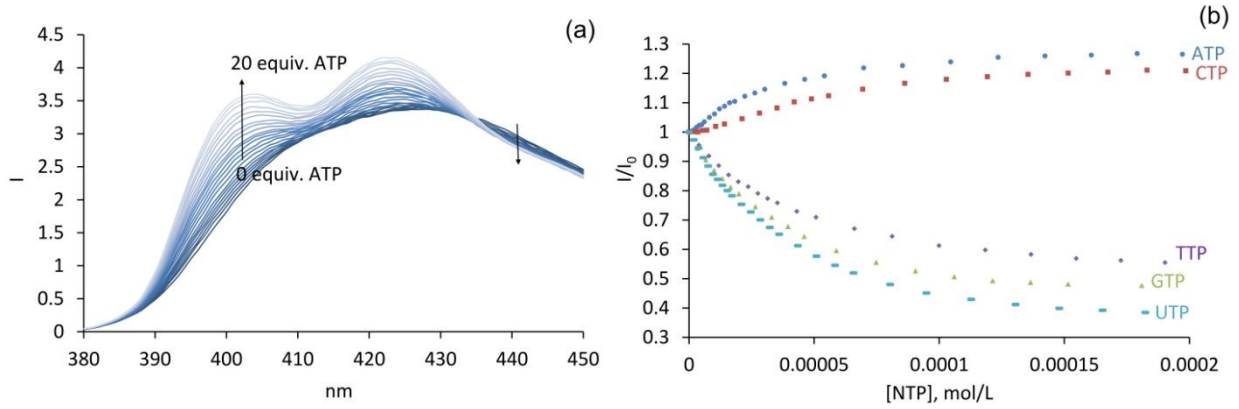

Figure 3.8: Coordination of ATP to complex LAntr·Zn(II) and (a) the observed changes in fluorescence during the titration experiment (excitation at 375 nm). (b) Fluorescence changes at 423 nm upon addition of five nucleoside triphosphates to complex LAntr·Zn(II). Conditions: 10 mM TRIS buffer (pH 7.4, 4% vol. MeOH 0.1 M NaCl), 10^{-5} M LAntr, 10^{-4} M zinc(II) perchlorate.

An evidence of stacking between anthracene and nucleobases was obtained from UV−vis titration of LAntr·Zn(II) complex with nucleotides. Addition of nucleotides induced a red shift of the absorption spectra, while addition of a pyrophosphate anions induced a blue shift (Fig. 3.9). Changes in both UV-vis and fluorescence induced by the interaction of the complex with nucleoside triphosphates are similar to those observed for the anthracene-containing DNA intercalators explored by Kumar.[194,195] Bathochromic shifts are considered as an evidence of stacking interactions and were reported for pure organic receptors for nucleotides,[168,182] as well as for metal complexes intercalating with DNA[196] and coordinating nucleotides.[197]

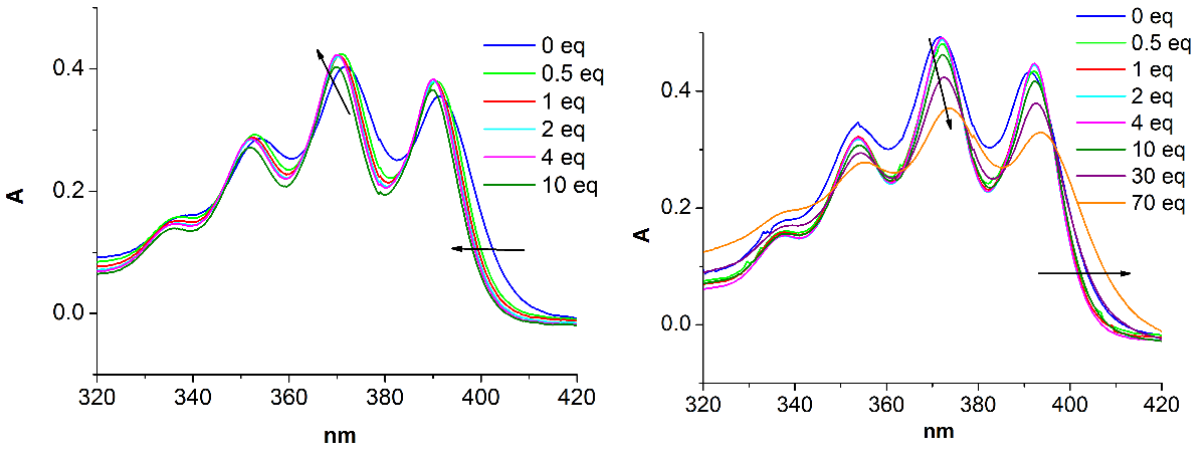

Figure 3.9: Absorption spectra of complex LAntr·Zn(II) at 10^{-4} M concentration in a 10 mM TRIS buffer (pH 7.4, 4% vol. MeOH, 0.1 M NaCl) with increasing amounts of (a) pyrophosphate and (b) ATP.

Interaction of two aromatic rings in the solution was additionally studied by $^{1}H-^{1}H$ ROESY measurements. As can be inferred from Fig. 3.10, proton H8a (adenine) interacts with protons

H3/H4 (anthracene) and H2'/H1' (sugar), while proton H2a (adenine) interacts only with protons H3/H4 (anthracene). These interactions are in a good agreement with the DFT optimized structures of ternary complexes (see below).

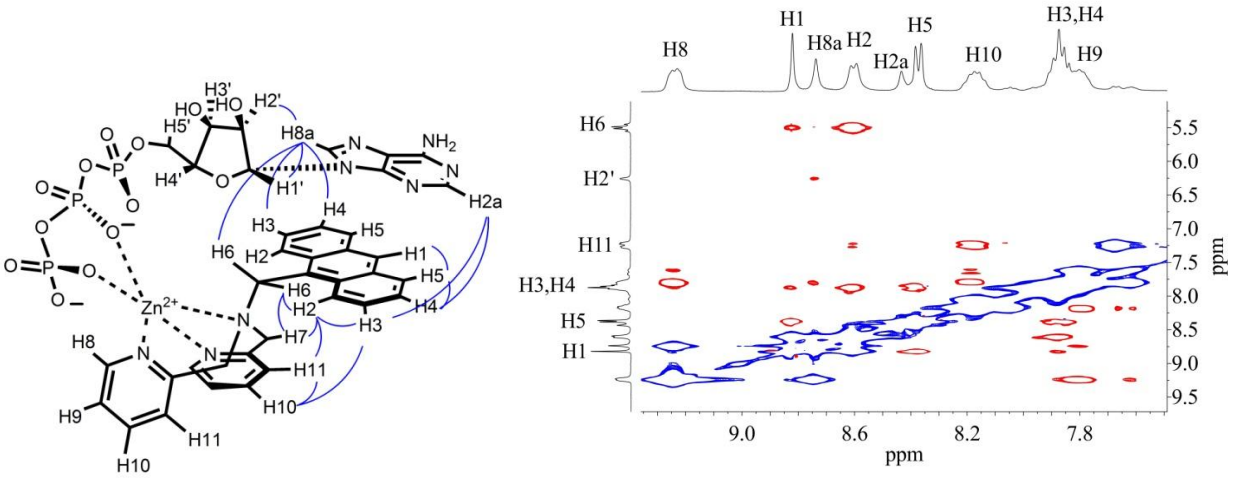

Figure 3.10: ^{1}H–^{1}H ROESY spectrum of complex LAntr·Zn(II) in the presence of 1 equiv of ATP. Lines between protons in the structure of the complex demonstrate correlations, as inferred from the spectrum. Conditions: concentration of the complex 8 mM, the pH of the solution was adjusted to pH 7.4 with NaOH, 3:2 CD_3CN:D_2O 298 K, 400MHz.

3.2.2. Experimental quantification of stacking interactions

For the assessment of stability constants of complexes, potentiometric pH-titrations were performed. These titrations have several advantages (a) they are precise and the error can be easily derived from several repeating experiments; (b) chromophores in the structure of the ligand are not required in contrast to fluorescence or UV−vis titrations. We used the double mutant cycle depicted in Fig. 3.11 for the calculation of stacking free energies between anthracene and nucleobases. The stabilities of complexes I−IV were obtained from potentiometric titrations. The R group corresponds to a substituent, which shows negligible propensity to interact with nucleobases. The stacking free energy between, e.g., adenine and anthracene can be calculated as $\Delta G_{st} = \Delta G_{I,III} - \Delta G_{II,IV} = \Delta G_{III,IV} - \Delta G_{I,II}$. Sigel assessed some contributions of stacking interaction between nucleobases and phenanthroline-, bipyridine-[198], and amino acid-based[199,200] metal complexes[201] by using a simpler scheme. His method is based on the calculation of only one mutation: $\Delta G_{I,II}$. Similar approach was used by Rebek and co-workers.[178] In this work, we assessed mutations $\Delta G_{I,III}$ and $\Delta G_{II,IV}$ for the calculation of interaction free energies. We used 2,2′-dipicolylamine as a ligand of comparison that does not bear any aromatic ring. In principle, *N*-ethyl-2,2′-dipicolylamine can also be used in the double

mutant cycle. However, as appeared from potentiometric measurements, 2,2′-dipicolylamine and *N*-ethyl-2,2′-dipicolylamine yielded almost similar $\Delta G_{I,III}$ values. For instance, according to the potentiometric titrations, $\Delta G_{I,III}$ values (= $\Delta G_I - \Delta G_{III}$) for 2,2′-dipicolylamine are 0.21 ± 0.05 kcal/mol (ATP) and 0.69 ± 0.06 kcal/mol (UTP), while for *N*-ethyl-2,2′-dipicolylamine the values are 0.23 ± 0.05 kcal/mol (ATP) and 0.74 ± 0.06 kcal/ mol (UTP), respectively. Thus, for further measurements we used 2,2′-dipicolylamine (LH).

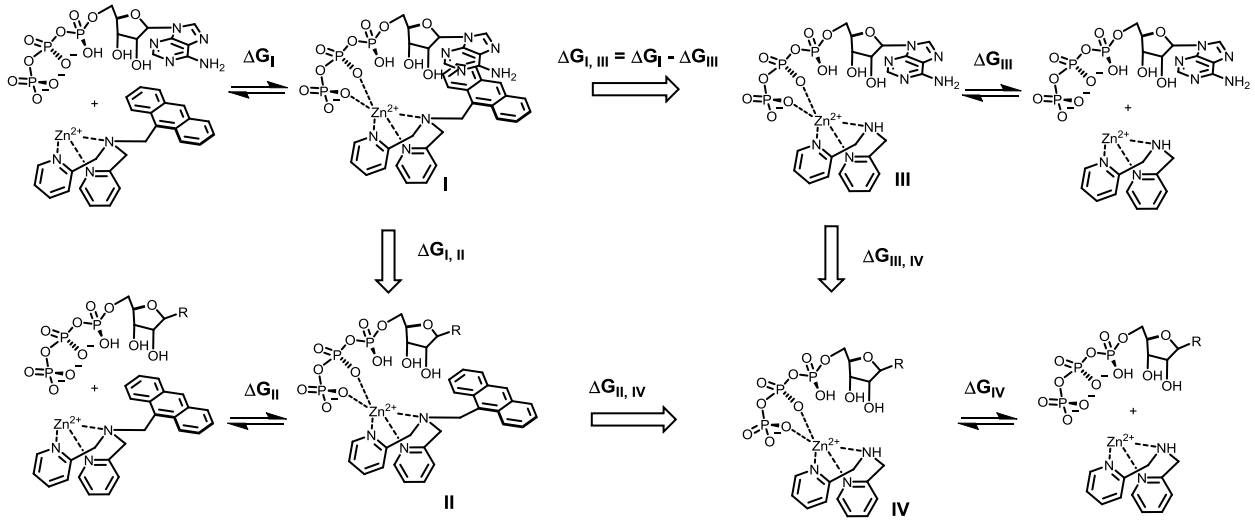

Figure 3.10: Double mutant cycle constructed for the calculation of the stacking free energy between adenine and anthracene and the corresponding equilibriums assessed in this work.

Potentiometric titrations were carried out with ligands LH and LAntr in water containing 2.4% methanol and 0.1 M NaCl for the constant ionic strength. Since our solvent system contains small amount of methanol for a better solubility of ligands, we determined pK_a values for all compounds in question (Table 3.1). The ligands were titrated in the presence of zinc(II) perchlorate and nucleoside triphosphates. The pKa values and stability constants of the complexes were calculated with the help of the Hyperquad program.[17] Stability constants β and K are defined from eq 1 and 2, respectively. The stability constant K in eq 2 can be also described as an affinity of the Zn(II) complex for ATP. For simplicity the charges on zinc and nucleoside triphosphates (NTP) are omitted.

$$LH + Zn + ATP \leftrightarrow LH{\cdot}Zn{\cdot}ATP \qquad \beta_{LHZnNTP} \frac{[LH{\cdot}Zn{\cdot}ATP]}{[LH][Zn][ATP]} \qquad (1)$$

$$LH{\cdot}Zn + ATP \leftrightarrow LH{\cdot}Zn{\cdot}ATP \qquad K^{LH{\cdot}Zn}_{LH{\cdot}Zn{\cdot}ATP} = \frac{[LH{\cdot}Zn{\cdot}ATP]}{[LH{\cdot}Zn\,][ATP]} \qquad (2)$$

Equilibrium	log β (LH)	log β (LAntr)
$L + H^+ \leftrightarrow LH^+$	7.43 ± 0.04	5.29 ± 0.04

$L+ 2H^+ \leftrightarrow [LH_2]^{2+}$	10.33 ± 0.16	9.58 ± 0.16
$L+ 3H^+ \leftrightarrow [LH_3]^{3+}$	14.57 ± 0.30	12.86 ± 0.30
$L+ Zn^{2+} \leftrightarrow [LZn]^{2+}$	7.51 ± 0.01	4.91 ± 0.01
$L + Zn^{2+} + ATP^{4-} \leftrightarrow [LZnATP]^{2-}$	14.72 ± 0.01	12.30 ± 0.01
$L + Zn^{2+} + CTP^{4-} \leftrightarrow [LZnCTP]^{2-}$	12.20 ± 0.04	10.02 ± 0.04
$L + Zn^{2+} + GTP^{4-} \leftrightarrow [LZnGTP]^{2-}$	12.66 ± 0.05	11.33 ± 0.05
$L + Zn^{2+} + UTP^{4-} \leftrightarrow [LZnUTP]^{2-}$	13.43 ± 0.07	11.33 ± 0.07

Table 3.1: Stability constants for protonation of ligands LH and LAntr and complex formation with nucleotides as determined from potentiometric titrations.

The results of potentiometric titrations are shown in Table 3.2. The data is shown only for four nucleobases, except thymine, for which we were not able to obtain reproducible results. Interestingly, the affinities of LAntr·Zn(II) for nucleoside triphosphates (defined as $logK^{\mathrm{LAntr{\cdot}Zn}}_{\mathrm{LAntr{\cdot}Zn{\cdot}NTP}}$) do not correlate with $\Delta G_{\mathrm{I,III}}$. However, these affinities were often compared in the literature to speculate which nucleobase has the strongest stacking interaction with an aromatic ring in the complex. The correct answer give $\Delta G_{\mathrm{I,III}}$ values calculated as a difference between the free energies of the complex formations with and without the anthracene ring. Since the triphosphate with R = H (Fig. 3.11) is scarcely accessible in sufficient quantities and purity, we suggested to calculate $\Delta G_{\mathrm{II,IV}}$ from stabilities of complexes with the pyrophosphate anion (PPi). $\Delta G_{\mathrm{II,IV}}$ is a constant value for all nucleobases and with this approximation the full double mutant cycle was calculated.

NTP	$lgK^{\mathrm{LAntr{\cdot}Zn}}_{\mathrm{LAntr{\cdot}Zn{\cdot}NTP}}$	$lgK^{\mathrm{LH{\cdot}Zn}}_{\mathrm{LH{\cdot}Zn{\cdot}NTP}}$	Stacking free energies ΔG_{st} between anthracene and a nucleobase, kcal/mol
A	7.39 ± 0.02	7.20 ± 0.03	0.21 ± 0.06
C	5.11 ± 0.02	4.68 ± 0.02	0.53 ± 0.06
G	6.13 ± 0.04	4.86 ± 0.07	1.68 ± 0.13
U	6.43 ± 0.02	5.92 ± 0.02	0.64 ± 0.05

Table 3.2: Affinities (log *K*) of Zn(II) complexes for NTPs and ΔG_{st} as determined by potentiometric pH titration at 23 °C, 2.4% vol. MeOH and *I* = 0.1M (NaCl). Affinities are calculated as follows: e.g.

$$\boldsymbol{lgK^{\mathrm{LH{\cdot}Zn}}_{\mathrm{LH{\cdot}Zn{\cdot}NTP}} = lg\beta_{\mathrm{LHZnNTP}} - lg\beta_{\mathrm{LHZn}}}$$

As determined by potentiometric pH titrations, the affinities of complexes LAntr· Zn(II) and LH·Zn(II) for PPi are $K^{\mathrm{LAntr{\cdot}Zn}}_{\mathrm{LAntr{\cdot}Zn{\cdot}PPi}}$ = 7.97 ± 0.02 and $K^{\mathrm{LH{\cdot}Zn}}_{\mathrm{LH{\cdot}Zn{\cdot}PPi}}$ = 7.93 ± 0.02, respectively. The difference between these values (which is $\Delta G_{\mathrm{II,IV}}$) is 0.04 logarithm units or 0.05 kcal/mol. This

value is even smaller than the experimental error. Therefore, in a rough approximation, $\Delta G_{I,III}$ is equal to the ΔG_{st} considering pyrophosphate as a reference.

Fluorescence spectroscopy was the second method for determination of association constants because of its high sensitivity. For this purpose ligands LQAntr and LQH were synthesized. Both ligands bear a quinoline dye, which may allow one to compare stability constants of complexes with and without anthracene. Fluorescence titrations were carried out in 10 mM TRIS buffer (pH 7.4, 0.1 M NaCl) and zinc(II) perchlorate. Affinity constants were calculated by fitting the experimental data with the HypSpec program. Analysis of stacking free energies obtained from fluorescence titrations (Table 3.3) reveals that (a) the values are smaller in comparison with those obtained from potentiometric measurements; (b) experimental errors are relatively high; and (c) the selectivity trend in interaction free energies calculated as $\Delta G_{I,III}$ agrees with that determined from potentiometric titrations. Small differences in stability constants for complexes with LQAntr and LQH may be explained by the fact that nucleobases may form relatively strong stacking interactions with both quinoline and anthracene. The presence of both interactions substantially level the effect of anthracene present in ligand LQAntr.

NTP	$logK^{\mathrm{LQAntr{\cdot}Zn}}_{\mathrm{LQAntr{\cdot}Zn{\cdot}NTP}}$	$logK^{\mathrm{LQH{\cdot}Zn}}_{\mathrm{LQH{\cdot}Zn{\cdot}NTP}}$	$\Delta G_{I,\,III}$, kcal/mol
A	[a]	[a]	–
C	5.40 ± 0.05	5.29 ± 0.02	0.14 ± 0.09
G	5.95 ± 0.04	5.10 ± 0.05	0.85 ± 0.12
T	5.18 ± 0.05	5.07± 0.06	0.20 ± 0.15
U	5.04 ± 0.05	4.89 ± 0.06	0.14 ± 0.15

Table 3.3: Affinities (log *K*) of Zn(II) complexes for NTPs and $\Delta G_{I,III}$ values as determined by fluorescence titrations at 23 °C in a 10 mM TRIS buffer (4% vol. MeOH, pH 7.4, 0.1 M NaCl). Excitation wavelength 370 nm, emission region 380–460 nm. a) small changes of fluorescence were observed.

Because the experimental values of stacking interactions are different in Table 3.2 and Table 3.3, we tested a different, third approach to calculate the contribution of stacking interactions to overall binding free energies. The strongest changes and precise stability constants were observed from fluorescence titrations of LAntr·Zn(II) complexes with nucleotides (Fig. 3.8). In the previous work, we showed that nucleoside monophosphates do not form stacking interactions with anthracene because they are too short in comparison with nucleoside triphosphates.[192] Thus, the difference in affinities of the complexes for NTPs (nucleoside triphosphates) and NMPs (nucleoside monophosphates) can give stacking free energies for nucleobases, when corrected to electrostatic interactions. It is reasonable to assume that the mutation from structure

I to III (Fig. 3.12) results in a loss of one negative charge. According to the potentiometric titrations, pyrophosphate and phosphate are present in monoprotonated forms at pH 7.4. The contribution of this charge loss can be calculated by the mutation from structure II to IV (Fig. 3.12). The resulting double mutant cycle shown in Fig. 3.12 was used to calculate ΔG_{st} values (Table 3.4). The affinities of the complex for the pyrophosphate anion and the phosphate anion are $logK^{\mathrm{LAntr{\cdot}Zn}}_{\mathrm{LAntr{\cdot}Zn{\cdot}PPi}}$ = 5.00 ± 0.05 and $logK^{\mathrm{LAntr{\cdot}Zn}}_{\mathrm{LAntr{\cdot}Zn{\cdot}Pi}}$ = 4.80 ± 0.05, respectively. It appeared that ΔG_{st} values have excellent agreement with the results obtained by potentiometric titrations.

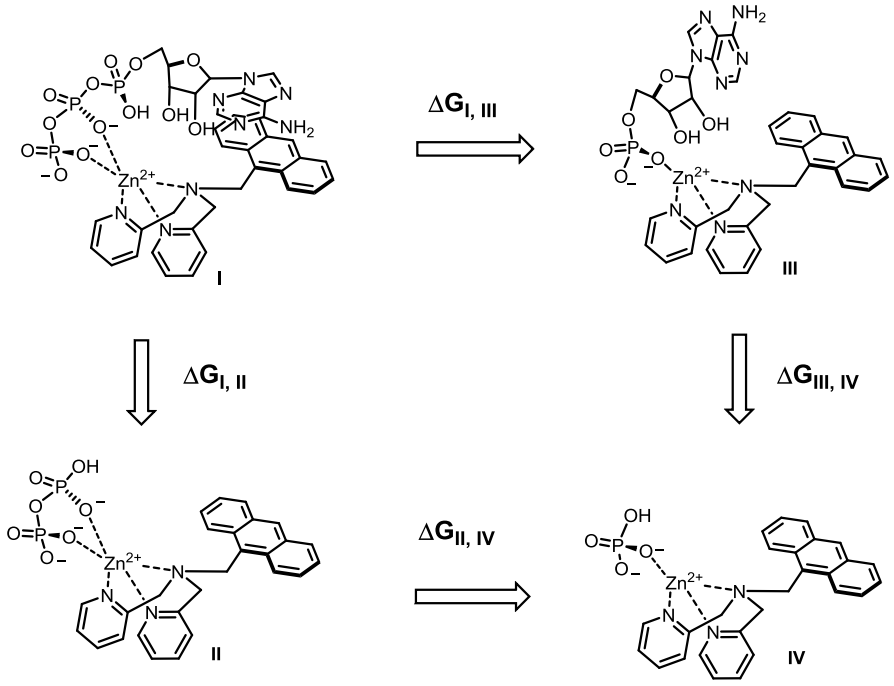

Figure 3.12: Double mutant cycle constructed for the assessment of the binding free energy between adenine and anthracene. Mutations take into account contribution of electrostatic interactions.

NTP	$logβ^{LAntrZn}_{LAntrZnNTP}$	$logβ^{LAntrZn}_{LAntrZnNMP}$	Stacking free energies between anthracene and a nucleobase ΔG_{st}, kcal/mol
A	4.67 ± 0.01	4.22± 0.03	0.34 ± 0.05
C	4.28 ± 0.01	3.70± 0.03	0.52 ± 0.05
G	4.53 ± 0.01	3.40 ± 0.04	1.27 ± 0.07
T	4.44 ± 0.01	3.54± 0.02	0.94 ± 0.05
U	4.45 ± 0.01	3.63± 0.02	0.84 ± 0.05

Table 3.4: Affinities (log *K*) of LAntr·Zn(II) Complex for NTPs and NMPs and Δ*G*st values as determined from fluorescence titrations at 23 °C in a 10 mM TRIS buffer (4% vol. MeOH pH 7.4, 0.1 M NaCl). Excitation wavelength 370 nm, emission region 380−460 nm. $\Delta G_{st} = \Delta G_{I,III} - \Delta G_{II,IV}$.

3.2.3. Computational analysis of stacking interactions

A parallel approach to assess stacking energies between anthracene and nucleobases was undertaken by using quantum chemical calculations. The computational analysis was based on the same double mutant cycle used in potentiometric titrations (Fig. 3.11), but with protonated complexes to avoid charged structures. The obtained energies (E) are formally equivalent to free energies at 0 K, as they contain neither temperature nor entropic contributions. Since the term "stacking free energies" suggests to feature such contributions, especially as we compare computational and experimental results at 298 K, we will further use only the term “stacking energies” to avoid confusion. A comparison of the calculated stacking energies (ΔE_{st}) and the experimental values will allow us to reveal the origin of stacking interactions. The structure of ternary complex LAntr·Zn·ATP (Fig. 3.10), constructed from $^{1}H–^{1}H$ ROESY measurements, was the starting point for the geometry optimization. There are two possible orientations of the adenine ring over the anthracene ring. These two conformation were generated by rotating the nucleobase ring by 180° over the sugar–nucleobase bond. The corresponding structures were optimized and the resulting geometries are shown in Fig. 3.13. Configuration 1 (conf. 1) always represents the most stable configuration and the energetic differences between both configurations (conf. 2 relative to conf. 1) are shown in Table 3.5. To eliminate the errors in calculations of stacking energies, the conformations of the nucleobase in complexes I and III were kept the same (Fig. 3.11).

Nucleobase	ΔE_{st}, conf. 1	ΔE_{st}, conf. 2	$E_{I,conf.2} - E_{I,conf.1}$
A	1.3	5.4	2.6
C	0.6	−2.6	6.1
G	7.1	−0.9	2.5
T	4.6	1.5	5.7
U	4.0	1.3	4.4

Table 3.5: Calculated stacking energies $\Delta E_{st} = \Delta E_{I} - \Delta E_{III} - (\Delta E_{II} - \Delta E_{IV})$ for nucleobases by using a double mutant cycle shown in Fig. 3.10. The energies were calculated for two configurations conf. 1 ($E_{conf.1}$) and conf. 2 ($E_{conf.2}$); Conf. 1 always corresponds to the configuration of LAntr·Zn·NTP with the energetically preferred minimum. All calculated energies are in kcal/mol and contain zero-point vibrational energies (ZPEs).

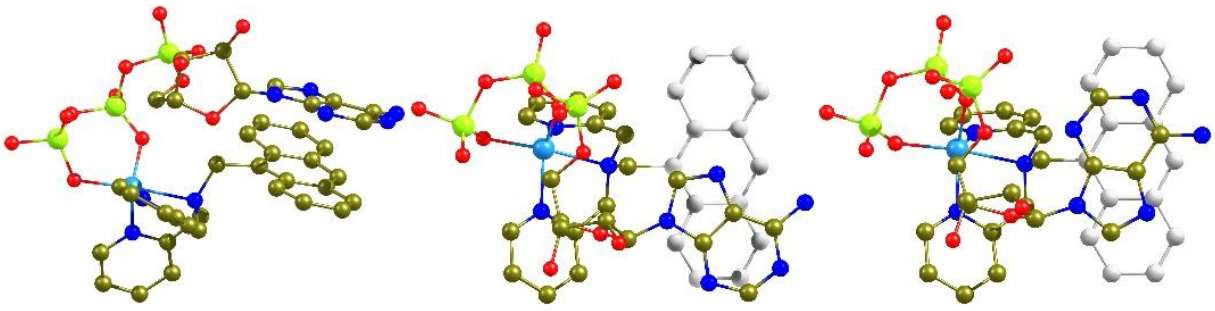

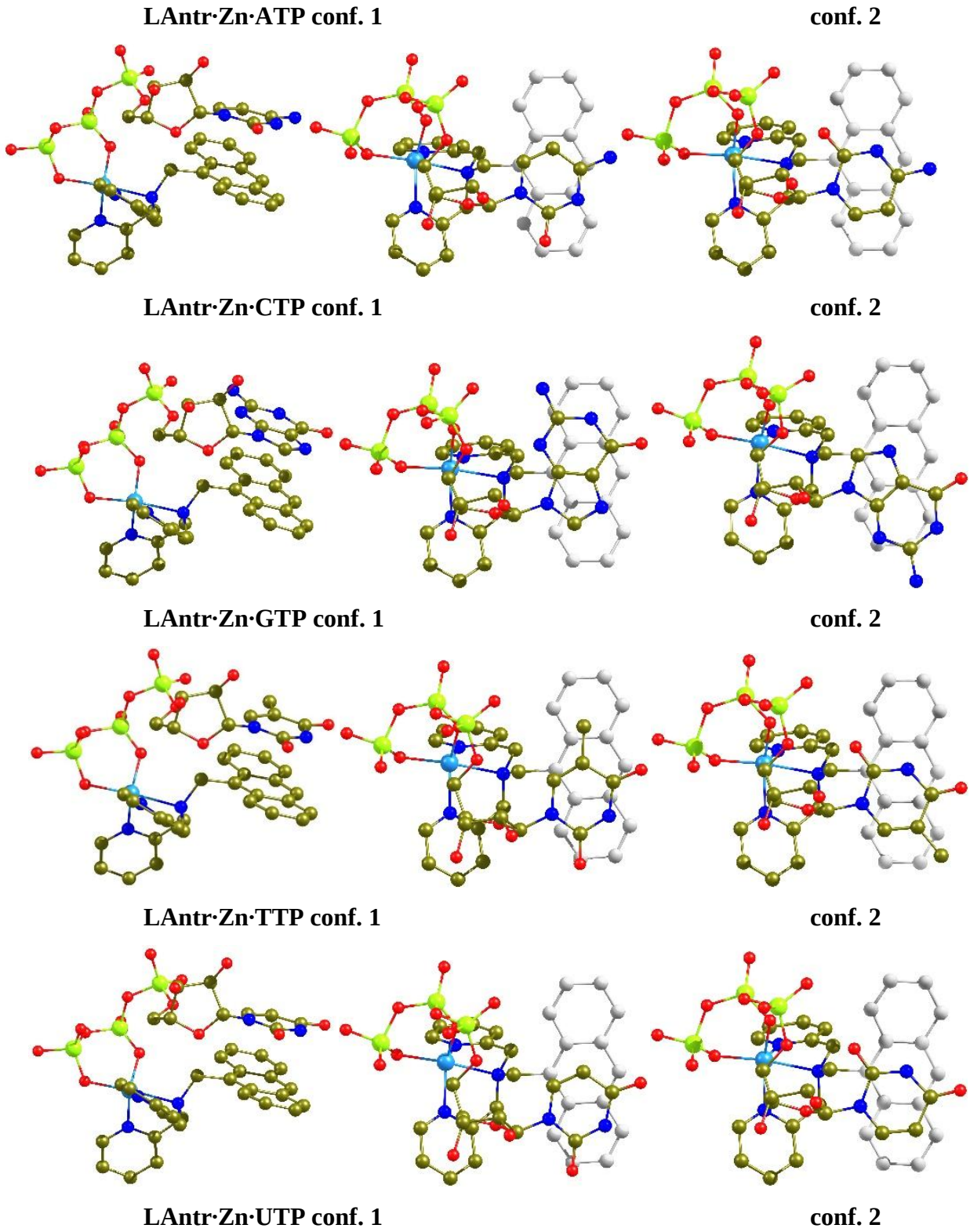

Figure 3.13: Side- and top-views of ternary complexes with five nucleotides. For top-view figures of configurations 1 and 2 the anthracene ring is shown in gray color for best view of the rings.

As can be inferred from the side-views of the complexes, Zn(II) cation coordinates two oxygen atoms from first two phosphate residues, i.e., similar to the coordination of pyrophosphate. Sigel and co-workers observed this coordination mode in a number of different complexes with nucleotides.19 The average distance between nucleobases and the anthracene ring is 3.3 Å. interestingly, adenine prefers conformation 1, while guanine forms more stable complex in conformation 2. A close analysis of structure "LAntr·Zn·GTP conf. 1" reveals that the amino group of guanine forms a hydrogen bond (N···O is 2.8 Å) with the oxygen of the phosphate residue. This hydrogen bond is not possible in case of adenine.

The affinities of Zn(II) complexes for nucleotides were calculated similar to the method used in experimental assessments. Analysis of Table 3.5 reveals a general trend of strong interactions between anthracene and guanine. Interestingly, the calculated values of stacking energies are higher than those obtained experimentally. The calculated values are in the range of 0.6−7 kcal/mol, while the experimental values are in the range of 0.1−1.3 kcal/mol. There are several reasons that can cause this deviation. First, experimental measurements were carried out in a buffered solution with a constant ionic strength. Second, additional approximations are the average description of solvation by the COSMO model, as well as the use of neutral instead of charged complexes in calculations. Third, the errors of the quantum chemical methods might not be negligible, especially when considering the small relative energies.[202] However, our calculations are able to indicate trends in binding energy and they are in a good agreement with the experimental data in terms of selectivity of non-covalent interactions between nucleobases and the anthracene ring. Taking into consideration complexes LAntr·Zn·NTP with the energetically preferred minimum, the following selectivity trend can be ruled out: G > T > U > A > C.

3.2.4. Comparison of the measured and computed data

In literature, the selectivity of a receptor for a certain nucleobase is often ruled out from the selectivity for a certain nucleotide.[165,167,173,203,204] This can be in principle correct, when we do not take into account the processes, which are individual for each nucleotide, such as conformational changes and solvation/desolvation upon binding. For example, in theoretical calculations, where we do not consider reaction entropy, the selectivity of LAntr·Zn(II) complex for guanine, thymine and uracil can be directly derived from energies of the complexes with nucleotides. In particular, in the theoretical calculations the binding selectivity of complex

LAntr·Zn(II) for nucleotides is GTP > TTP > UTP > ATP > CTP. This relationship correlates to the ΔG_{st} pattern: G > T > U > C > A (Table 3.5). On the contrary, according to the experiment, the affinity of LAntr·Zn(II) for ATP is slightly higher than the affinity for GTP (ATP > GTP). Hence, there is no correlation between affinities of the complex for nucleotides and the experimentally determined ΔG_{st} values (G > A). These facts underline the importance of calculating stacking free energies by using the double mutant cycle. It is conceivable to suggest that the easier to desolvate a nucleobase, the stronger is the stabilization of a stack. However, guanine as a highly solvated nucleobase has the highest stacking free energy. The selectivity pattern for the nucleobase binding determined in our studies does not correlate with solvation energies of nucleobases.[205] This fact indicates that the contribution of hydrophobic interactions between anthracene and nucleobases into the overall binding energy is relatively low in comparison with the stacking interactions, which determine the observed selectivity pattern. A support for this conclusion can be found in literature.[206,207] For instance, Inoue and co-workers analyzed binding parameters of thymidine and uridine derivatives to cyclodextrins and positively charged hosts in an aqueous solution.[208] The entropically driven interaction of nucleobases with cyclodextrins in a buffered aqueous solution was much lower than the interaction of nucleobases with the hosts able to form stacking interactions.

The experimental values for stacking free energies between aromatic compounds and nucleobases have relatively low values, in the range of 1 kcal/mol, but they perfectly agree with the experimental results obtained previously by Rebek[178] and Sigel.[209] Interestingly, the measured and calculated stacking free energies have still excellent agreement in selectivity pattern (G, T, U > C, A). This fact supports the proposed structures of the complexes and reliability of the experimental methods.

In the recent literature more attention has been paid to understanding the selectivity of nucleobase recognition by stacking with aromatic compounds. For example, Garcia-Espana reported on polyammonium receptors bearing anthracene.[197] DFT calculations of stacking free energies between anthracene and nucleobases in a gas phase resulted in a pattern, which agrees with our results: GTP > UTP > ATP. The preference of anthracene-based Zn(II) complexes to bind guanine, thymine and uracil nucleotides were reported by Fabbrizzi and co-workers. The authors attached two anthracene arms to 2,4,6-triamino-1,3,5-trimethoxycyclohexane and investigated its Zn(II) complex as a receptor for nucleotides. While addition of AMP and CMP induced very small changes in fluorescence, GMP, TMP and UMP induced strong quenching.

Apparent binding affinities of the Zn(II) complex for nucleotides decreased in the order: TMP > GMP > UMP.[210] Grimme and co-workers carried out theoretical investigations of interaction of free nucleobases with graphenes and obtained stacking free energies[159]. The reported sequence for the interaction energies between nucleobases and, e.g., graphene $C_{96}H_{24}$ (G > A > T > C > U) is different from that obtained in this work. This difference presumably indicates that the structure of a stacking component also has an influence on the selectivity of nucleobase binding.

3.2.5. Interaction with tetranucleotides

Understanding the relationship between the structure of an aromatic ring and its binding affinity/selectivity toward a certain nucleobase can be useful for the design of new DNA binders.[211–215] Thus, we were interested to understand whether the binding selectivities and fluorescence response observed for nucleotides can be translated to the binding of DNA oligonucleotides. To answer this question we examined the interaction of complex LAntr· Zn(II) with DNA oligonucleotides A4 (5′-AAAA-3′), C4, T4 and G4, each of them carrying three phosphate residues and three negative charges. Addition of oligonucleotides to complex LAntr·Zn(II) resulted in quenching of fluorescence and the quenching pattern was similar to that observed for nucleoside monophosphate (NMPs) (Fig. 3.14). The curves were fitted to a 1:1 interaction model, which was extracted from the Job's plot analysis. Interestingly, the stability constants between the complex and tetranucleotides were in most cases lower than those for nucleoside triphosphate (Table 3.6).

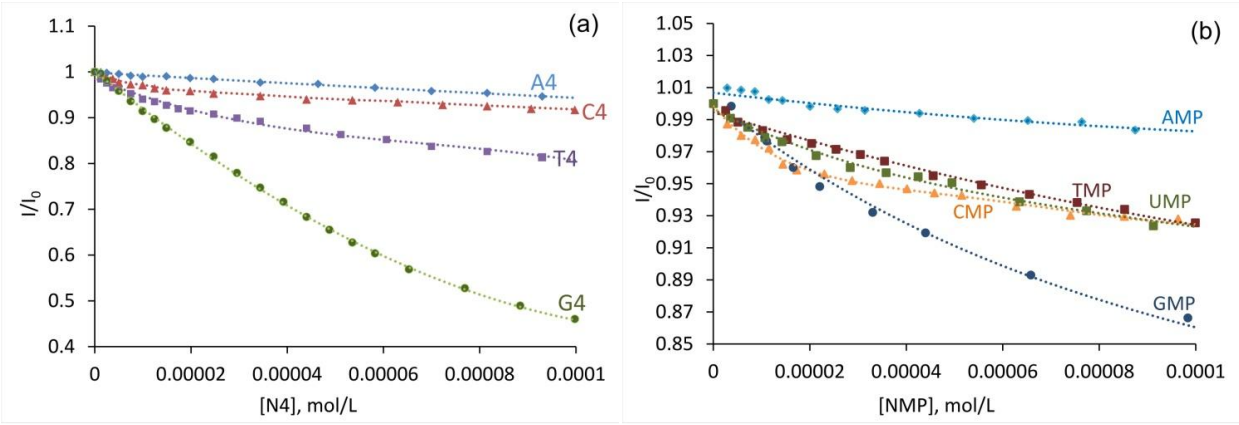

Figure 3.14: (a) Coordination of DNA oligonucleotides and (b) nucleoside monophosphates to complex LAntr·Zn(II) and the observed changes in fluorescence intensity at 423 nm during titrations. Conditions: 10 mM TRIS buffer (pH 7.4, 4% vol. MeOH, 0.1 M NaCl) at 10^{-5} M concentration of the ligand in the presence of 10^{-4} M zinc(II) perchlorate.

Tetranucleotide N4	$log\beta_{LAntr\cdot Zn\cdot N4}^{LAntr\cdot Zn}$
A4	3.10 ± 0.05
C4	4.60 ± 0.01
G4	3.97 ± 0.01
T4	4.29 ± 0.01

Table 3.6: Affinities (log *K*) of LAntr·Zn(II) complex for oligonucleotides.

The major difference in binding of oligonucleotides and nucleoside monophosphate was the fact that LAntr·Zn(II) has a selectivity for C4 and T4 oligonucleotides, while it binds nucleoside monophosphate with the preference for CMP and AMP. Additionally, G4 quenches the fluorescence of the complex much strongly than GMP does. This observation can be explained in terms of more guanines in the binding molecule and they all participate in the interaction with anthracene. Similar behavior was observed by Fox for pyrenyl-*N*-alkylbutanoamide end-labeled oligonucleotides.[216] The results of the fluorescence titrations show that although the quenching pattern for tetranucleotides and nucleoside monophosphate have similarities, the interaction mode of LAntr·Zn(II) with tetranucleotides is likely more complex. To obtain more information about these interactions in solution the complexes with more sensitive dyes are required, e.g., the dyes, which efficiently report on stacking interaction with a nucleobase.

3.2.6. Conclusions

Stacking interactions between aromatic compounds and nucleobases are essential in recognition of nucleotides and nucleic acids. In this work, we designed and studied different approaches to assess stacking free energies between anthracene and nucleobases. We used Zn(II) complexes with dipicolyl- amine-based ligands to bind nucleoside triphosphates. The receptors bearing the anthracene dye bind nucleotides by a combination of electrostatic and stacking interactions. For the first time, stacking free energies between five nucleobases and anthracene were experimentally determined. The anthracene ring prefers to bind nucleobases in the following order G (1.3 kcal/mol) > T (0.9 kcal/mol) > U (0.8 kcal/mol) > C (0.5 kcal/mol) > A (0.3 kcal/mol). The double mutant cycle based on the comparison of binding free energies of complexes with nucleoside monophosphate and triphosphates appeared to be the best in terms of accuracy and simplicity. The values obtained by this methods perfectly correlate to the values obtained by potentiometric titrations. Analysis of the experimental data and quantum chemical calculations suggest that stacking interactions dominate over hydrophobic effects in aqueous solution. These forces presumably determine the selectivity of aromatic compounds for

nucleotides in aqueous solution. Fluorescence studies of DNA tetranucleotides revealed that their behavior resembles the behavior of nucleoside monophosphates rather than triphosphates. The methods reported here may set the stage for the evaluation of highly selective aromatic dyes for stacking with nucleobases, as well as new fluorescent probes for nucleotides and nucleic acids.

3.3. Experimental section

3.3.1. Instruments and materials

DNA oligonucleotides were purchased from Metabion International AG. For the details about instruments see 2.2.4.

3.3.2. UV-vis and fluorescence titrations

The general procedure for the UV-vis and fluorescence binding studies involved preparation of a stock solution with the host (ca. 10^{-5} M) and a stock solution with the guest (ca. 10^{-3} M). The guest is usually dissolved in the stock solution of the host. A typical titration experiments involves sequential additions of the titrant (guest) to a 1.6 mL sample of the host stock solution in the spectrometric cell and monitoring the changes in the spectral features. For the 1:1 binding stoichiometry one requires ca. 10 additions before 1 equiv of the guest and ca. 10 points after 1 equiv. The total number of data points in both UV-vis and fluorescence experiments were between 20 and 40, depending on the stoichiometry of complexation and binding affinity. The data points were then collated and combined to produce plots that, in turn, were processed by HypSpec computer program.

3.3.3. Potentiometric titrations

Titrations were carried out using a titrating device at 23 °C. The pH scale was calibrated prior to each experiment with the help of three standard buffers: pH 4.0, 7.0, and 9.0 (Roth). For titrations ca. 20−25 mg of the ligand (10^{-3} M) were dissolved in 1.2 mL of MeOH, 2−5 equiv of 1 M HCl were added and the solution was diluted with 0.1 M NaCl solution until the total volume reached 50 mL. All titrations were carried out using 0.1 M standard NaOH solution. Each titration was repeated at least 3−6 times to minimize the error. To determine the binding constants with zinc(II) salts and nucleotides, 0.5−1 equiv of $Zn(ClO_4)_2$ and 1 equiv of a nucleotide were added. Refinement of the potentiometric data was carried out using the Hyperquad program, which minimizes a least-squares function.

3.3.4. Theoretical calculations

All calculations were performed by means of density functional theory (DFT)[217] with the RI approximation[218,219] as implemented in TURBOMOLE V6.5[220]. For the geometry

optimizations we applied the BP86 functional,[221–224] the def2-SVP basis set,[225,226] Grimme's D3 model for dispersion correction[227,228] as well as the COSMO solvation model with $\varepsilon = \infty$ for water.[229] The stationary points were characterized by analyzing the numerically vibrational frequencies, obtained from the Hessian matrix.[230] In order to get more accurate energies, we performed single-point calculations for the received geometries, using the PW6B95 functional,[231] def2-TZVP basis set,[226,232] the D3 correction and the COSMO model. Furthermore, we always added the zero-point vibrational energy (ZPE), received from the numerical frequency analyses at the BP86/def2-SVP level of theory, to the SCF energies.

4. Summary

The dissertation consists of two parts covering two closely related topics of supramolecular chemistry. The first part is dedicated to the design and synthesis of new sulfate-selective receptors and discussed in Chapter 2. Two generations of receptors have been developed during this work. The first generation, receptor **4.1** bears two aromatic amino groups and an amidopyrrole binding subunit. Naphthalimide dyes are incorporated in the structure of the receptor to ensure the emission properties. Receptor **4.1** represents an example of a rational design of a turn-on fluorescent probe for anions by utilizing a PET process. The receptor has been synthesized and its anion binding properties in aqueous solution have been studied. It has been found that the intrinsic selectivity of the amidopyrrole binding motif for phosphate present in DMSO completely disappears in 10% DMSO aqueous buffer at pH 3.6, at which the receptor is protonated. The electrostatic interactions between the receptor and an anion dominate, which results in selectivity for sulfate over phosphate. The preorganized conformation of **4.1** for anion binding has been confirmed by ROESY experiments. It has been found that the ability of sulfate anion to facilitate protonation of the amino group leads to a suppression of the photoinduced electron transfer on the dye, resulting in a selective turn-on fluorescent response. The receptor has been shown to possess high selectivity for sulfate in a 50 mM acetate buffer at pH 3.6 (containing 10 vol.% DMSO). This has been proved by measuring binding affinities for a series of various anions and by the competition experiments.

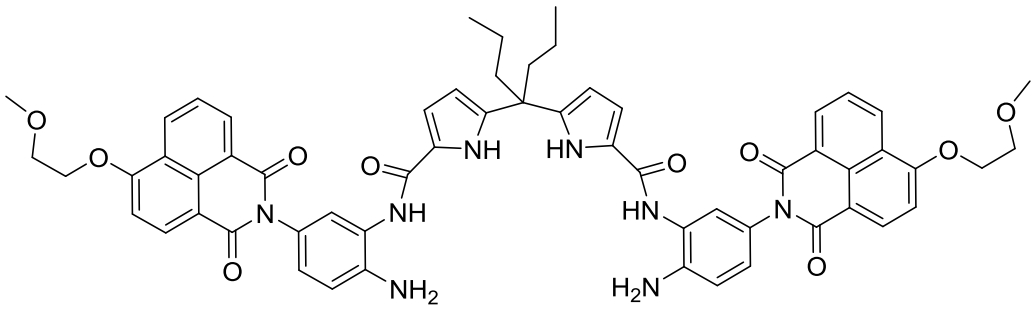

4.1

Figure 4.1: Structure of receptor **4.1**.

To improve binding and sensing properties of the receptor for sulfate, the second generation — three new compounds **4.2**–**4.4** — has been designed and synthesized. These receptors contain two or three naphthalimide dyes, piperazine amino groups that can be protonated, and anion binding fragments with multiple hydrogen bonding sites. The partial protonation of the receptors

upon addition of sulfate, i.e. the pK_a shift of the complexed receptors compared to the unbound ones, has been independently confirmed by fluorescence and UV-vis spectroscopy, and potentiometry. All receptors have shown high affinities towards sulfate with binding constants exceeding $10^3\,M^{-1}$ and good selectivity over environmentally important monoanions in a 1:1 THF–water mixture. A fluorescence enhancement up to a 5-fold for receptor **4.2** has been observed. DFT calculations have been performed to understand structure of the host–sulfate complex. Furthermore, two reference compounds **4.5** and **4.6** have been synthesized. Compound **4.5** possessing only one fragment of the naphthalimide–piperazine dye has not showed a pK_a shift and fluorescence enhancement upon addition of sulfate. From these results, it has been concluded that at least two charges are necessary for efficient binding of sulfate. Reference compound **4.6** — a methylated analogue of receptor **4.2** — has been designed in order to elucidate the role of the hydrogen bonds between NH-amide protons and the anion in the host–guest complex. Although compound **4.6** has demonstrated a small pK_a shift and a moderate affinity and selectivity for sulfate, its binding constants for anions are lower as compared to receptor **4.2**. From the combined data, we have inferred that hydrogen bonding plays a significant role in sulfate recognition even in a competitive aqueous medium. Nevertheless, the electrostatic component and a suitable geometry seem to be more important in the particular cases of receptors **4.2**–**4.4**.

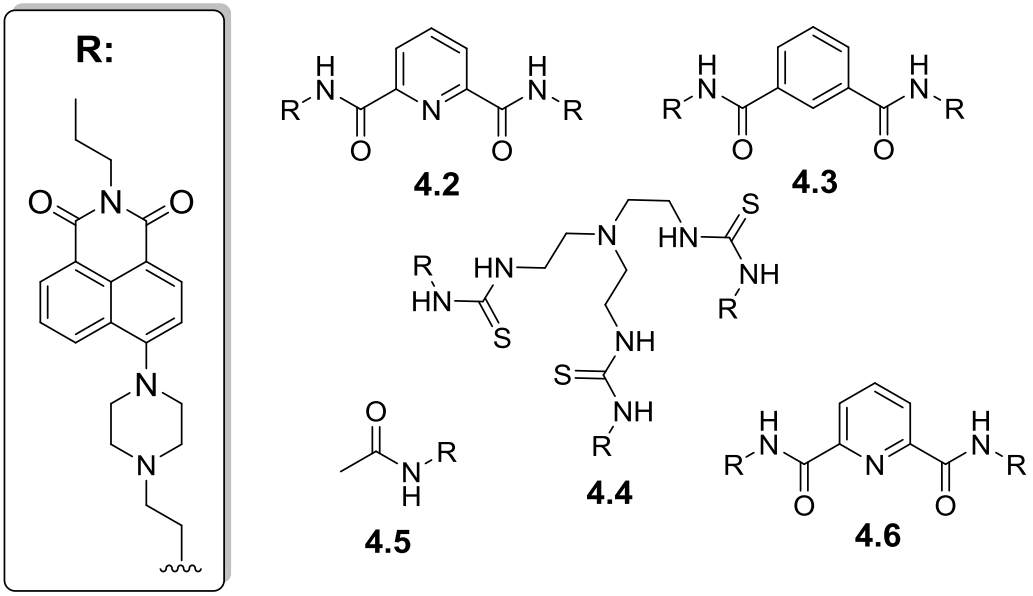

Figure 4.2: Structures of compounds **4.2**–**4.6**.

The second part of the present dissertation (Chapter 3) describes the study concerning stacking interactions between aromatic rings (anthracene, in particular) and natural nucleobases.

Such interactions are crucial in recognition of nucleotides and nucleic acids, but a comprehensive understanding of the strength and selectivity of these interactions in aqueous solution has been elusive. To this end, reference complexes have been designed and analyzed by experiment and theory. For the first time, stacking free energies between five nucleobases and anthracene have been determined experimentally from thermodynamic double mutant cycles. Three different experimental methods have been proposed and evaluated. We have found that the anthracene dye prefers to bind nucleobases in the order (kcal/mol): G (1.3) > T (0.9) > U (0.8) > C (0.5) > A (0.3). The respective trend of interaction free energies extracted from DFT calculations correlates to that obtained experimentally. Analysis of the data suggests that stacking interactions dominate over hydrophobic effects in an aqueous solution and can be predicted with DFT calculations.

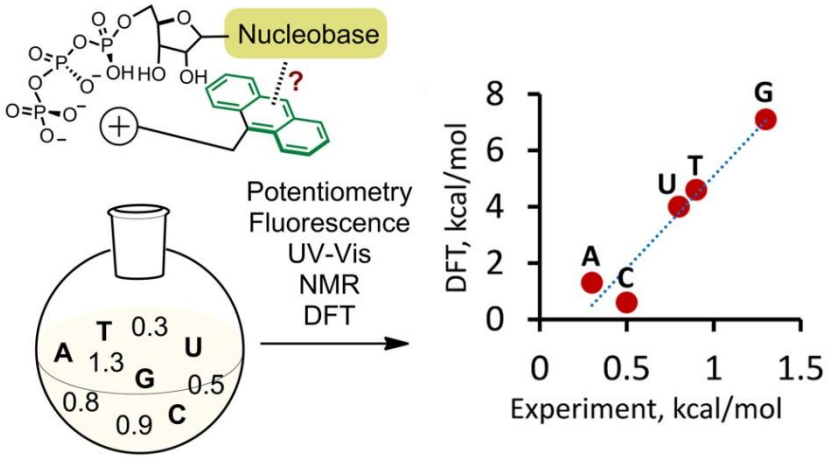

Figure 4.3: Graphical abstract describing the main ideas of Chapter 3 (© 2016 American Chemical Society).

References

[1] https://www.nobelprize.org/nobel_prizes/chemistry/laureates/1987/

[2] J. W. Steed, J. L. Atwood, *Supramolecular Chemistry, 2nd Edition*, Wiley, **2009**.

[3] L. C. Gilday, S. W. Robinson, T. A. Barendt, M. J. Langton, B. R. Mullaney, P. D. Beer, *Chem. Rev.* **2015**, *115*, 7118–7195.

[4] E. B. Veale, T. Gunnlaugsson, *Annu. reports B* **2010**, *106*, 376–406.

[5] M. H. Lee, J. S. Kim, J. L. Sessler, *Chem. Soc. Rev.* **2015**, *44*, 4185–4191.

[6] C. H. Park, H. E. Simmons, *J. Am. Chem. Soc.* **1968**, *90*, 2431–2432.

[7] E. Garcia-Espana, P. Diaz, J. M. Llinares, A. Bianchi, *Coord. Chem. Rev.* **2006**, *250*, 2952–2986.

[8] R. Vilar, *Recognition of Anions*, Springer, **2008**.

[9] D. S. Kim, J. L. Sessler, *Chem. Soc. Rev.* **2015**, *44*, 532–546.

[10] V. Blazek Bregovic, N. Basaric, K. Mlinaric-Majerski, *Coord. Chem. Rev.* **2015**, *295*, 80–124.

[11] P. A. Gale, W. Dehaen, *Anion Recognition in Supramolecular Chemistry*, **2012**.

[12] N. A. Itsikson, Y. Y. Morzherin, A. I. Matern, O. N. Chupakhin, *Russ. Chem. Rev.* **2008**, *77*, 751–764.

[13] J. Cullinane, R. I. Gelb, T. N. Margulis, L. J. Zompa, *J. Am. Chem. Soc.* **1982**, *104*, 3048–3053.

[14] A. Dahan, T. Ashkenazi, V. Kuznetsov, S. Makievski, E. Drug, L. Fadeev, M. Bramson, S. Schokoroy, E. Rozenshine-Kemelmakher, M. Gozin, *J. Org. Chem.* **2007**, *72*, 2289–2296.

[15] J. L. Sessler, E. Katayev, G. D. Pantos, Y. a Ustynyuk, *Chem. Commun.* **2004**, 1276–1277.

[16] O. B. Berryman, F. Hof, M. J. Hynes, D. W. Johnson, *Chem. Commun.* **2006**, *1*, 506–508.

[17] P. Gans, A. Sabatini, A. Vacca, *Talanta* **1996**, *43*, 1739–1753.

[18] Z. Xu, S. Kim, K. H. Lee, J. Yoon, *Tetrahedron Lett.* **2007**, *48*, 3797–3800.

[19] C. A. Schalley, *Analytical Methods in Supramolecular Chemistry*, WILEY-VCH Verlag, **2012**.

[20] F. Ulatowski, K. Dabrowa, T. Bałakier, J. Jurczak, *J. Org. Chem.* **2016**, *81*, 1746–1756.

[21] D. B. Hibbert, P. Thordarson, *Chem. Commun.* **2016**, *52*, 12792–12805.

[22] T. D. Ashton, K. A. Jolliffe, F. M. Pfeffer, *Chem. Soc. Rev.* **2015**, *44*, 4547–95.

[23] J. Wu, B. Kwon, W. Liu, E. V. Anslyn, P. Wang, J. S. Kim, *Chem. Rev.* **2015**, *115*, 7893–7943.

[24] A. P. de Silva, H. Q. N. Gunaratne, T. Gunnlaugsson, A. J. M. Huxley, C. P. McCoy, J. T. Rademacher, T. E. Rice, *Chem. Rev.* **1997**, *97*, 1515–1566.

[25] R. Martinez-Manez, F. Sancenon, *Chem. Rev.* **2003**, *103*, 4419–4476.

[26] J. Wu, W. Liu, J. Ge, H. Zhang, P. Wang, *Chem. Soc. Rev.* **2011**, *40*, 3483–3495.

[27] B. T. Nguyen, E. V. Anslyn, *Coord. Chem. Rev.* **2006**, *250*, 3118–3127.

[28] K. Liu, X. Su, J. Huo, *Mini. Rev. Org. Chem.* **2012**, *9*, 118–124.

[29] M. Bojtar, J. Kozma, Z. Szakacs, D. Hessz, M. Kubinyi, I. Bitter, *Sensors Actuators, B Chem.* **2017**, *248*, 305–310.

[30] N. Singh, D. O. Jang, *Tetrahedron Lett.* **2011**, *52*, 5094–5097.

[31] K. Ghosh, S. S. Ali, A. R. Sarkar, A. Samadder, A. R. Khuda-Bukhsh, I. D. Petsalakis, G. Theodorakopoulos, *Org. Biomol. Chem.* **2013**, *11*, 5666–72.

[32] Z. Zhu, J. Zhou, Z. Li, C. Yang, *Sensors Actuators, B Chem.* **2015**, *208*, 151–158.

[33] H. Khajehsharifi, M. M. Bordbar, *Sensors Actuators, B Chem.* **2015**, *209*, 1015–1022.

[34] P. A. Gale, L. J. Twyman, C. I. Handlin, J. L. Sessler, *Chem. Commun.* **1999**, *2*, 1851–1852.

[35] B. Daly, J. Ling, A. P. de Silva, K. Chulvi, A. Lorente, R. Martinez-Manez, A. M. Costero, W. M. Gong, Y. Lu, J. Y. Wang, *Chem. Soc. Rev.* **2015**, *44*, 4203–4211.

[36] J. S. Kim, D. T. Quang, *Chem. Rev.* **2007**, *107*, 3780–3799.

[37] R. A. Bissell, A. P. De Silva, H. Q. N. Gunaratne, P. L. M. Lynch, C. P. Mccoy, G. E. M. Maguire, K. R. A. S. Sandanayake, *Symp. A Q. J. Mod. Foreign Lit.* **1993**, 45–58.

[38] T. Gunnlaugsson, A. P. Davis, M. Glynn, *Chem. Commun.* **2001**, 2556–2557.

[39] M. E. Huston, E. U. Akkaya, A. W. Czarnik, *J. Am. Chem. Soc.* **1989**, *111*, 8735–8737.

[40] V. Amendola, L. Fabbrizzi, M. Licchelli, A. Taglietti, in *Anion Coord. Chem.*, **2011**, pp. 521–552.

[41] J. Fan, M. Hu, P. Zhan, X. Peng, *Chem. Soc. Rev.* **2013**, *42*, 29–43.

[42] J.-L. Tang, C.-Y. Li, Y.-F. Li, C.-X. Zou, *Chem. Commun. (Camb).* **2014**, *50*, 15411–15414.

[43] D. W. Schindler, *Science (80-.).* **1988**, *239*, 149–157.

[44] W. D. Heizer, R. S. Sandler, E. Seal, S. C. Murray, M. G. Busby, B. G. Schliebe, S. N.

Pusek, *Dig. Dis. Sci.* **1997**, *42*, 1055–1061.

[45] J. C. van den Born, A.-R. S. Frenay, S. J. L. Bakker, A. Pasch, J.-L. Hillebrands, H. J. Lambers Heerspink, H. van Goor, *Nitric Oxide* **2016**, *55–56*, 18–24.

[46] S. H. Wang, E. Raptis, J. Yeh, *J. Chromatogr. A* **2004**, *1039*, 51–58.

[47] *Межгосударственный Стандарт. ГОСТ 31940-2012. Вода Питьевая. Методы Определения Сульфатов.*, **2012**.

[48] *Standard Test Method for Sulfate Ion in Water (D516-02)*, USA, **2002**.

[49] B. Dietrich, M. W. Hosseini, J. M. Lehn, R. B. Sessions, *J. Am. Chem. Soc.* **1981**, *103*, 1282–1283.

[50] M. W. Hosseini, J.-M. Lehn, *Helv. Chim. Acta* **1988**, *71*, 749–756.

[51] G. Wu, R. M. Izatt, M. L. Bruening, W. Jiang, H. Azab, K. E. Krakowiak, J. S. Bradshaw, *J. Incl. Phenom. Macrocycl. Chem.* **1992**, *13*, 121–127.

[52] R. I. Gelb, L. M. Schwartz, L. J. Zompa, *Inorg. Chem.* **1986**, *25*, 1527–1535.

[53] P. Arranz, A. Bencini, A. Bianchi, P. Diaz, E. Garcia-Espana, C. Giorgi, S. V. Luis, M. Querol, B. Valtancoli, *J. Chem. Soc. Perkin Trans. 2* **2001**, *4*, 1765–1770.

[54] P. Mateus, R. Delgado, P. Brandao, S. Carvalho, V. Felix, *Org. Biomol. Chem.* **2009**, *7*, 4661–4673.

[55] P. Mateus, R. Delgado, P. Brandão, V. Félix, *J. Org. Chem.* **2009**, *74*, 8638–8646.

[56] P. Mateus, R. Delgado, V. Andre, M. Teresa Duarte, *Org. Biomol. Chem.* **2015**, *13*, 834–842.

[57] J. W. Pflugrath, F. A. Quiocho, *Nature* **1985**, *314*, 257–260.

[58] B. L. Jacobson, F. A. Quiocho, *J. Mol. Biol.* **1988**, *204*, 783–787.

[59] M. A. Hossain, J. M. Llinares, D. Powell, K. Bowman-James, *Inorg. Chem.* **2001**, *40*, 2936–2937.

[60] S. K. Sahoo, G. D. Kim, H. J. Choi, *J. Photochem. Photobiol. C Photochem. Rev.* **2016**, *27*, 30–53.

[61] A. Pramanik, B. Thompson, T. Hayes, K. Tucker, D. R. Powell, P. V. Bonnesen, E. D. Ellis, K. S. Lee, H. Yu, M. A. Hossain, *Org. Biomol. Chem.* **2011**, *9*, 4444–4447.

[62] Y. Morzherin, D. M. Rudkevich, W. Verboom, D. N. Reinhoudt, *J. Org. Chem.* **1993**, *58*, 7602–7605.

[63] I. Ravikumar, P. Ghosh, P. Dastidar, J. Yang, Y. Liu, C. Jia, C. Janiak, N. Tang, X.-J. Yang, J. A. Shriver, et al., *Chem. Soc. Rev.* **2012**, *41*, 3077–3098.

[64] E. A. Katayev, Y. A. Ustynyuk, J. L. Sessler, *Coord. Chem. Rev.* **2006**, *250*, 3004–3037.

[65] C. Jia, B. Wu, S. Li, Z. Yang, Q. Zhao, J. Liang, Q.-S. Li, X.-J. Yang, *Chem. Commun.* **2010**, *46*, 5376–5378.

[66] P. A. Gale, J. R. Hiscock, C. Z. Jie, M. B. Hursthouse, M. E. Light, *Chem. Sci.* **2010**, *1*, 215–220.

[67] Y. Hao, C. Jia, S. Li, X. Huang, X.-J. Yang, C. Janiak, B. Wu, *Supramol. Chem.* **2012**, *24*, 88–94.

[68] V. J. Dungan, H. T. Ngo, P. G. Young, K. A. Jolliffe, *Chem. Commun.* **2013**, *49*, 264–266.

[69] R. B. P. Elmes, K. K. Y. Yuen, K. A. Jolliffe, *Chem. - A Eur. J.* **2014**, *20*, 7373–7380.

[70] C. Jia, Q.-Q. Wang, R. A. Begum, V. W. Day, K. Bowman-James, *Org. Biomol. Chem.* **2015**, *13*, 6953–6957.

[71] L. Qin, A. Hartley, P. Turner, R. B. P. Elmes, K. A. Jolliffe, *Chem. Sci.* **2016**, *7*, 4563–4572.

[72] S. D. Padghan, R. S. Bhosale, N. V. Ghule, A. L. Puyad, S. V. Bhosale, S. V. Bhosale, *RSC Adv.* **2016**, *6*, 34376–34380.

[73] S. Kubik, R. Goddard, R. Kirchner, D. Nolting, J. Seidel, *Angew. Chemie Int. Ed.* **2001**, *40*, 2648–2651.

[74] S. Kubik, R. Goddard, *Proc. Natl. Acad. Sci.* **2002**, *99*, 5127–5132.

[75] S. Kubik, R. Kirchner, D. Nolting, J. Seidel, *J. Am. Chem. Soc.* **2002**, *124*, 12752–12760.

[76] C. Reyheller, B. P. Hay, S. Kubik, *New J. Chem.* **2007**, *31*, 2095–2102.

[77] F. Sommer, S. Kubik, *Org. Biomol. Chem.* **2014**, *12*, 8851–8860.

[78] C. Reyheller, S. Kubik, *Org. Lett.* **2007**, *9*, 5271–5274.

[79] S. Otto, S. Kubik, *J. Am. Chem. Soc.* **2003**, *125*, 7804–7805.

[80] Z. Rodriguez-Docampo, E. Eugenieva-Ilieva, C. Reyheller, A. M. Belenguer, S. Kubik, S. Otto, *Chem. Commun.* **2011**, *47*, 9798–9800.

[81] M. R. Krause, R. Goddard, S. Kubik, *J. Org. Chem.* **2011**, *76*, 7084–7095.

[82] D. Mungalpara, H. Kelm, A. Valkonen, K. Rissanen, S. Keller, S. Kubik, *Org. Biomol. Chem.* **2017**, *15*, 102–113.

[83] T. Fiehn, R. Goddard, R. Seidel, S. Kubik, *Chem. - A Eur. J.* **2010**, *16*, 7241–7255.

[84] A. Schaly, R. Belda, E. García-España, S. Kubik, *Org. Lett.* **2013**, *15*, 6238–6241.

[85] R. Prohens, G. Martorell, P. Ballester, A. Costa, *Chem. Commun.* **2001**, 1456–1457.

[86] M. N. Piña, B. Soberats, C. Rotger, P. Ballester, P. M. Deyà, A. Costa, *New J. Chem.*

2008, *32*, 1919–1923.

[87] E. Delgado-Pinar, C. Rotger, A. Costa, M. N. Pina, H. R. Jimenez, J. Alarcon, E. Garcia-Espana, *Chem. Commun.* **2012**, *48*, 2609–2611.

[88] H. Zhou, Y. Zhao, G. Gao, S. Li, J. Lan, J. You, *J. Am. Chem. Soc.* **2013**, *135*, 14908–14911.

[89] R. Saini, S. Kumar, *RSC Adv.* **2013**, *3*, 21856–21862.

[90] J. Chang, Y. Lu, S. He, C. Liu, L. Zhao, X. Zeng, *Chem. Commun.* **2013**, *49*, 6259–6261.

[91] S. Samanta, P. Dey, A. Ramesh, G. Das, *Chem. Commun.* **2016**, *52*, 10381–10384.

[92] R. Custelcean, *Chem. Commun.* **2013**, *49*, 2173–2182.

[93] R. Custelcean, A. Bock, B. A. Moyer, *J. Am. Chem. Soc.* **2010**, *132*, 7177–7185.

[94] R. Custelcean, N. J. Williams, C. A. Seipp, *Angew. Chemie Int. Ed.* **2015**, *54*, 10525–10529.

[95] H. J. Kim, S. Bhuniya, R. K. Mahajan, R. Puri, H. Liu, K. C. Ko, J. Y. Lee, J. S. Kim, *Chem. Commun.* **2009**, 7128–7130.

[96] P. Li, Y.-M. Zhang, Q. Lin, J.-Q. Li, T.-B. Wei, *Spectrochim. Acta Part A Mol. Biomol. Spectrosc.* **2012**, *90*, 152–157.

[97] G.-N. Wei, J.-L. Zhang, C. Jia, W.-Z. Fan, L.-R. Lin, *Spectrochim. Acta Part A Mol. Biomol. Spectrosc.* **2014**, *128*, 168–175.

[98] J. Rull-Barrull, M. D'Halluin, E. Le Grognec, F.-X. Felpin, *Chem. Commun.* **2016**, *52*, 2525–2528.

[99] Y. Upadhyay, S. Bothra, R. Kumar, H.-J. Choi, S. K. Sahoo, *Spectrochim. Acta Part A Mol. Biomol. Spectrosc.* **2017**, *180*, 44–50.

[100] Z. Luo, K. Yin, Z. Yu, M. Chen, Y. Li, J. Ren, *Spectrochim. Acta - Part A Mol. Biomol. Spectrosc.* **2016**, *169*, 38–44.

[101] T. Guinovart, P. Blondeau, F. J. Andrade, *Chem. Commun.* **2015**, *51*, 10377–10380.

[102] M. J. Berrocal, A. Cruz, I. H. A. Badr, L. G. Bachas, *Anal. Chem.* **2000**, *72*, 5295–5299.

[103] U. Fegade, S. K. Sahoo, A. Singh, P. Mahulikar, S. Attarde, N. Singh, A. Kuwar, *RSC Adv.* **2014**, *4*, 15288–15292.

[104] S. Chopra, J. Singh, N. Singh, N. Kaur, *Anal. Methods* **2014**, *6*, 9030–9036.

[105] R. Kaur, J. Singh, A. Saini, N. Singh, N. Kaur, *RSC Adv.* **2014**, *4*, 48004–48011.

[106] P. D. Beer, A. R. Graydon, A. O. M. Johnson, D. K. Smith, *Inorg. Chem.* **1997**, *36*, 2112–2118.

[107] P. D. Beer, J. Cadman, J. M. Lloris, R. Martinez-Manez, M. E. Padilla, T. Pardo, D. K. Smith, J. Soto, *J. Chem. Soc. Dalt. Trans.* **1999**, 127–134.

[108] N. H. Evans, C. J. Serpell, P. D. Beer, *Chem. Commun.* **2011**, *47*, 8775–8777.

[109] Y. Al Shihadeh, A. Benito, J. Manuel Lloris, R. Martinez-Manez, J. Soto, M. D. Marcos, *Inorg. Chem. Commun.* **2000**, *3*, 563–565.

[110] D. P. Cormode, S. S. Murray, A. R. Cowley, P. D. Beer, *Dalton Trans.* **2006**, 5135–5140.

[111] I. El Drubi Vega, P. A. Gale, M. B. Hursthouse, M. E. Light, *Org. Biomol. Chem.* **2004**, *2*, 2935–2941.

[112] I. E. D. Vega, S. Camiolo, P. A. Gale, M. B. Hursthouse, M. E. Light, *Chem. Commun.* **2003**, *9*, 1686–1687.

[113] E. A. Kataev, C. Müller, G. V. Kolesnikov, V. N. Khrustalev, *European J. Org. Chem.* **2014**, *2014*, 2747–2753.

[114] P. a. Panchenko, Y. V. Fedorov, O. a. Fedorova, V. P. Perevalov, G. Jonusauskas, *Russ. Chem. Bull.* **2009**, *58*, 1233–1240.

[115] M. Vonlanthen, N. S. Finney, *J. Org. Chem.* **2013**, *78*, 3980–3988.

[116] S. Herzig, S. Kritter, T. Lübbers, N. Marquardt, J.-U. Peters, S. Weber, *Synlett* **2005**, *5*, 3107–3108.

[117] D. H. Vance, A. W. Czarnik, *J. Am. Chem. Soc.* **1994**, *116*, 9397–9398.

[118] H.-I. Un, C.-B. Huang, C. Huang, T. Jia, X.-L. Zhao, C.-H. Wang, L. Xu, H.-B. Yang, *Org. Chem. Front.* **2014**, 1083–1090.

[119] C.-B. Huang, H.-R. Li, Y. Luo, L. Xu, *Dalton Trans.* **2014**, *43*, 8102–8108.

[120] L. Kang, Z. Y. Xing, X. Y. Ma, Y. T. Liu, Y. Zhang, *Spectrochim. Acta - Part A Mol. Biomol. Spectrosc.* **2016**, *167*, 59–65.

[121] S. Janakipriya, N. R. Chereddy, P. Korrapati, S. Thennarasu, A. B. Mandal, *Spectrochim. Acta. A. Mol. Biomol. Spectrosc.* **2016**, *153*, 465–70.

[122] F. Hu, B. Zheng, D. Wang, M. Liu, J. Du, D. Xiao, *Analyst* **2014**, *139*, 3607–3613.

[123] H.-I. Un, C.-B. Huang, J. Huang, C. Huang, T. Jia, L. Xu, *Chem. - An Asian J.* **2014**, *9*, 3397–3402.

[124] Y. F. Li, C. Y. Li, F. Xu, Y. Zhou, Q. C. Xiao, *Sensors Actuators, B Chem.* **2011**, *155*, 253–257.

[125] H.-I. Un, S. Wu, C.-B. Huang, Z. Xu, L. Xu, *Chem. Commun. (Camb).* **2015**, *2*, 2–5.

[126] Z. Xu, Y. Y. Ren, X. Fan, S. Cheng, Q. Xu, L. Xu, *Tetrahedron* **2015**, *71*, 5055–5058.

[127] Y. Fu, J. Zhang, H. Wang, J.-L. Chen, P. Zhao, G.-R. Chen, X.-P. He, *Dye. Pigment.* **2016**, *133*, 372–379.

[128] X.-F. Zhang, T. Zhang, S.-L. Shen, J.-Y. Miao, B.-X. Zhao, W. Guo, T. Tang, X. C. Weng, X. Zhou, T. Morii, et al., *J. Mater. Chem. B* **2015**, *3*, 3260–3266.

[129] M. H. Lee, N. Park, C. Yi, J. H. Han, J. H. Hong, K. P. Kim, D. H. Kang, J. L. Sessler, C. Kang, J. S. Kim, *J. Am. Chem. Soc.* **2014**, *136*, 14136–14142.

[130] P. Anzenbacher, in *Top. Heterocycl. Chem.*, **2010**, pp. 205–235.

[131] I. Basaran, M. Emami Khansari, A. Pramanik, B. M. Wong, M. A. Hossain, *Tetrahedron Lett.* **2015**, *56*, 115–118.

[132] I. Marques, A. R. Colaço, P. J. Costa, N. Busschaert, P. A. Gale, V. Félix, *Soft Matter* **2014**, *10*, 3608–3621.

[133] M. Emami Khansari, C. R. Johnson, I. Basaran, A. Nafis, J. Wang, J. Leszczynski, M. A. Hossain, *RSC Adv.* **2015**, *5*, 17606–17614.

[134] J. Gan, H. Tian, Z. Wang, K. Chen, J. Hill, P. . Lane, M. . Rahn, A. . Fox, D. D. . Bradley, *J. Organomet. Chem.* **2002**, *645*, 168–175.

[135] L. H. Perruchoud, A. Hadzovic, X. A. Zhang, *Chem. - A Eur. J.* **2015**, *21*, 8711–8715.

[136] R. R. Mittapalli, S. S. R. Namashivaya, A. S. Oshchepkov, E. Kuczynska, E. A. Kataev, *Chem. Commun.* **2017**, *53*, 4822–4825.

[137] Z. Fei, D. R. Zhu, X. Yang, L. Meng, Q. Lu, W. H. Ang, R. Scopelliti, C. G. Hartinger, P. J. Dyson, *Chem. - A Eur. J.* **2010**, *16*, 6473–6481.

[138] F. Zapata, A. Caballero, P. Molina, I. Alkorta, J. Elguero, *J. Org. Chem.* **2014**, *79*, 6959–6969.

[139] A. El Alaoui, F. Schmidt, M. Amessou, M. Sarr, D. Decaudin, J.-C. Florent, L. Johannes, *Angew. Chemie Int. Ed.* **2007**, *46*, 6469–6472.

[140] E. Schutte, T. J. R. Weakley, D. R. Tyler, *J. Am. Chem. Soc.* **2003**, *125*, 10319–10326.

[141] A. Hamdach, E. M. El Hadrami, M. L. Testa, S. Gil, E. Zaballos-García, J. Sepúlveda-Arques, P. Arroyo, L. R. Domingo, *Tetrahedron* **2004**, *60*, 12067–12073.

[142] C. Agami, F. Couty, L. Hamon, O. Venier, *Tetrahedron Lett.* **1993**, *34*, 4509–4512.

[143] K. A. Wilson, J. L. Kellie, S. D. Wetmore, *Nucleic Acids Res.* **2014**, *42*, 6726–6741.

[144] U. Heinemann, W. Saenger, *Nature* **1982**, *299*, 27–31.

[145] H. Matter, M. Nazaré, S. Güssregen, D. W. Will, H. Schreuder, A. Bauer, M. Urmann, K. Ritter, M. Wagner, V. Wehner, *Angew. Chemie Int. Ed.* **2009**, *48*, 2911–2916.

[146] A. K. Todd, A. Adams, J. H. Thorpe, W. A. Denny, L. P. G. Wakelin, C. J. Cardin, *J. Med. Chem.* **1999**, *42*, 536–540.

[147] L. M. Salonen, M. Ellermann, F. Diederich, *Angew. Chemie Int. Ed.* **2011**, *50*, 4808–4842.

[148] S. Grimme, *Angew. Chemie Int. Ed.* **2008**, *47*, 3430–3434.

[149] C. R. Martinez, B. L. Iverson, *Chem. Sci.* **2012**, *3*, 2191–2201.

[150] C. A. Hunter, J. K. M. Sanders, *J. Am. Chem. Soc.* **1990**, *112*, 5525–5534.

[151] A. L. Ringer, M. O. Sinnokrot, R. P. Lively, C. D. Sherrill, *Chem. - A Eur. J.* **2006**, *12*, 3821–3828.

[152] S. E. Wheeler, K. N. Houk, *J. Am. Chem. Soc.* **2008**, *130*, 10854–10855.

[153] S. E. Wheeler, *Acc. Chem. Res.* **2013**, *46*, 1029–1038.

[154] R. M. Parrish, C. D. Sherrill, *J. Am. Chem. Soc.* **2014**, *136*, 17386–17389.

[155] H. Sun, A. Horatscheck, V. Martos, M. Bartetzko, U. Uhrig, D. Lentz, P. Schmieder, M. Nazaré, *Angew. Chemie Int. Ed.* **2017**, *56*, 6454–6458.

[156] P. Li, J. M. Maier, E. C. Vik, C. J. Yehl, B. E. Dial, A. E. Rickher, M. D. Smith, P. J. Pellechia, K. D. Shimizu, *Angew. Chemie Int. Ed.* **2017**, *56*, 7209–7212.

[157] L.-J. Riwar, N. Trapp, B. Kuhn, F. Diederich, *Angew. Chemie Int. Ed.* **2017**, *56*, 11252–11257.

[158] P. Cysewski, *Phys. Chem. Chem. Phys.* **2008**, *10*, 2636–2645.

[159] J. Antony, S. Grimme, *Phys. Chem. Chem. Phys.* **2008**, *10*, 2722–2729.

[160] Y. Kubota, Y. Motosa, Y. Shigemune, Y. Fujisaki, *Photochem. Photobiol.* **1979**, *29*, 1099–1106.

[161] K. Mutai, B. A. Gruber, N. J. Leonard, *J. Am. Chem. Soc.* **1975**, *97*, 4095–4104.

[162] C. A. M. Seidel, A. Schulz, M. H. M. Sauer, *J. Phys. Chem.* **1996**, *100*, 5541–5553.

[163] Y. Zhou, Z. Xu, J. Yoon, *Chem. Soc. Rev.* **2011**, *40*, 2222–2235.

[164] S. Aoki, E. Kimura, *Chem. Rev.* **2004**, *104*, 769–788.

[165] M. Dhaenens, J. Lehn, J. Vigneron, *J. Chem. Soc. Perkin Trans. 2* **1993**, 1379–1381.

[166] M.-P. Teulade-fichou, J.-P. Vigneron, J.-M. Lehn, *Supramol. Chem.* **1995**, *5*, 139–147.

[167] O. Baudoin, F. Gonnet, M.-P. Teulade-Fichou, J.-P. Vigneron, J.-C. Tabet, J.-M. Lehn, *Chem. - A Eur. J.* **1999**, *5*, 2762–2771.

[168] J. Y. Kwon, N. J. Singh, H. N. Kim, S. K. Kim, K. S. Kim, J. Yoon, *J. Am. Chem. Soc.* **2004**, *126*, 8892–8893.

[169] P. P. Neelakandan, M. Hariharan, D. Ramaiah, *J. Am. Chem. Soc.* **2006**, *128*, 11334–

11335.

[170] A. K. Nair, P. P. Neelakandan, D. Ramaiah, *Chem. Commun.* **2009**, *7345*, 6352–6354.

[171] H. Abe, Y. Mawatari, H. Teraoka, K. Fujimoto, M. Inouye, *J. Org. Chem.* **2004**, *69*, 495–504.

[172] S. Wang, Y.-T. Chang, *J. Am. Chem. Soc.* **2006**, *128*, 10380–10381.

[173] H. Wang, W. Chan, *Org. Biomol. Chem.* **2008**, *6*, 162–168.

[174] N. Ahmed, B. Shirinfar, I. S. Youn, A. Bist, V. Suresh, K. S. Kim, *Chem. Commun.* **2012**, *48*, 2662–2664.

[175] Z. Xu, N. J. Singh, J. Lim, J. Pan, N. K. Ha, S. Park, K. S. Kim, J. Yoon, *J. Am. Chem. Soc.* **2009**, *131*, 15528–15533.

[176] J. F. Constant, J. Fahy, J. Lhomme, J. E. Anderson, *Tetrahedron Lett.* **1987**, *28*, 1777–1780.

[177] B. Askew, P. Ballester, C. Buhr, K. S. Jeong, S. Jones, K. Parris, K. Williams, J. Rebek, *J. Am. Chem. Soc.* **1989**, *111*, 1082–1090.

[178] V. M. Rotello, E. A. Viani, G. Deslongchamps, B. A. Murray, J. Rebek, *J. Am. Chem. Soc.* **1993**, *115*, 797–798.

[179] Y. Kato, M. M. Conn, J. J. Rebek, *J. Am. Chem. Soc.* **1994**, *116*, 3279–3284.

[180] A. Haghighat Jahromi, M. Honda, S. C. Zimmerman, M. Spies, *Nucleic Acids Res.* **2013**, *41*, 6687–6697.

[181] T. Sawada, M. Fujita, *J. Am. Chem. Soc.* **2010**, *132*, 7194–7201.

[182] G. Zong, L. Xian, G. Lu, *Tetrahedron Lett.* **2007**, *48*, 3891–3894.

[183] H. T. Ngo, X. Liu, K. A. Jolliffe, *Chem. Soc. Rev.* **2012**, *41*, 4928–4965.

[184] T. Sakamoto, A. Ojida, I. Hamachi, *Chem. Commun.* **2009**, 141–152.

[185] D. Wang, X. Zhang, C. He, C. Duan, *Org. Biomol. Chem.* **2010**, *8*, 2923–2925.

[186] A. Ojida, S. Park, Y. Mito-oka, I. Hamachi, *Tetrahedron Lett.* **2002**, *43*, 6193–6195.

[187] A. S. Rao, D. Kim, H. Nam, H. Jo, K. H. Kim, C. Ban, K. H. Ahn, *Chem. Commun. (Camb).* **2012**, *48*, 3206–3208.

[188] L. Götzke, K. Gloe, K. A. Jolliffe, L. F. Lindoy, A. Heine, T. Doert, A. Jäger, K. Gloe, *Polyhedron* **2011**, *30*, 708–714.

[189] S. A. de Silva, A. Zavaleta, D. E. Baron, O. Allam, E. V. Isidor, N. Kashimura, J. M. Percarpio, *Tetrahedron Lett.* **1997**, *38*, 2237–2240.

[190] S. M. Baldeau, C. H. Slinn, B. Krebs, A. Rompel, *Inorganica Chim. Acta* **2004**, *357*,

3295–3303.

[191] J. H. Kim, J. Y. Noh, I. H. Hwang, J. Kang, J. Kim, C. Kim, *Tetrahedron Lett.* **2013**, *54*, 2415–2418.

[192] E. Kataev, R. Arnold, T. Rüffer, H. Lang, *Inorg. Chem.* **2012**, *51*, 7948–7950.

[193] A. P. de Silva, H. Q. N. Gunaratne, P. L. M. Lynch, *J. Chem. Soc., Perkin Trans. 2* **1995**, 685–690.

[194] N. K. Modukuru, K. J. Snow, B. S. Perrin, J. Thota, C. V. Kumar, *J. Phys. Chem. B* **2005**, *109*, 11810–11818.

[195] M. R. Duff, V. K. Mudhivarthi, C. V. Kumar, *J. Phys. Chem. B* **2009**, *113*, 1710–1721.

[196] M. Inclán, M. T. Albelda, J. C. Frías, S. Blasco, B. Verdejo, C. Serena, C. Salat-Canela, M. L. Díaz, A. García-España, E. García-España, *J. Am. Chem. Soc.* **2012**, *134*, 9644–9656.

[197] M. Inclán, M. T. Albelda, E. Carbonell, S. Blasco, A. Bauzá, A. Frontera, E. García-España, *Chem. - A Eur. J.* **2014**, *20*, 3730–3741.

[198] E. M. Bianchi, S. A. A. Sajadi, B. Song, H. Sigel, *Inorganica Chim. Acta* **2000**, *300–302*, 487–498.

[199] B. E. Fischer, H. Sigel, *J. Am. Chem. Soc.* **1980**, *102*, 2998–3008.

[200] H. Sigel, B. E. Fischer, E. Farkas, *Inorg. Chem.* **1983**, *22*, 925–934.

[201] A. Sigel, B. P. Operschall, H. Sigel, *JBIC J. Biol. Inorg. Chem.* **2014**, *19*, 691–703.

[202] L. Goerigk, H. Kruse, S. Grimme, *ChemPhysChem* **2011**, *12*, 3421–3433.

[203] R. Moreno-Corral, K. O. Lara, *Supramol. Chem.* **2008**, *20*, 427–435.

[204] H. N. Kim, J. H. Moon, S. K. Kim, J. Y. Kwon, Y. J. Jang, J. Y. Lee, J. Yoon, *J. Org. Chem.* **2011**, *76*, 3805–3811.

[205] R. F. Ribeiro, A. V Marenich, C. J. Cramer, D. G. Truhlar, *Phys. Chem. Chem. Phys.* **2011**, *13*, 10908–10922.

[206] M. S. Cubberley, B. L. Iverson, *J. Am. Chem. Soc.* **2001**, *123*, 7560–7563.

[207] M. Sirish, H.-J. Schneider, *J. Am. Chem. Soc.* **2000**, *122*, 11274–11274.

[208] M. V Rekharsky, A. Nakamura, G. A. Hembury, Y. Inoue, *Bull. Chem. Soc. Jpn.* **2001**, *74*, 449–457.

[209] S. A. A. Sajadi, B. Song, H. Sigel, *Inorganica Chim. Acta* **1998**, *283*, 193–201.

[210] L. Fabbrizzi, M. Licchelli, F. Mancin, M. Pizzeghello, G. Rabaioli, A. Taglietti, P. Tecilla, U. Tonellato, *Chem. - A Eur. J.* **2002**, *8*, 94–101.

[211] H. Ihmels, D. Otto, in *Supermolecular Dye Chem.*, Springer-Verlag, Berlin/Heidelberg, **2005**, pp. 161–204.

[212] E. Pazos, J. Mosquera, M. E. Vázquez, J. L. Mascareñas, *ChemBioChem* **2011**, *12*, 1958–1973.

[213] S. N. Georgiades, N. H. Abd Karim, K. Suntharalingam, R. Vilar, *Angew. Chemie Int. Ed.* **2010**, *49*, 4020–4034.

[214] P. Dervan, *Bioorg. Med. Chem.* **2001**, *9*, 2215–2235.

[215] B. M. Zeglis, V. C. Pierre, J. K. Barton, *Chem. Commun.* **2007**, *7345*, 4565.

[216] E. Zahavy, M. A. Fox, *J. Phys. Chem. B* **1999**, *103*, 9321–9327.

[217] O. Treutler, R. Ahlrichs, *J. Chem. Phys.* **1995**, *102*, 346–354.

[218] K. Eichkorn, O. Treutler, H. Öhm, M. Häser, R. Ahlrichs, *Chem. Phys. Lett.* **1995**, *242*, 652–660.

[219] K. Eichkorn, F. Weigend, O. Treutler, R. Ahlrichs, *Theor. Chem. Accounts Theory, Comput. Model. (Theoretica Chim. Acta)* **1997**, *97*, 119–124.

[220] R. Ahlrichs, M. Bär, M. Häser, H. Horn, C. Kölmel, *Chem. Phys. Lett.* **1989**, *162*, 165–169.

[221] J. C. Slater, *Phys. Rev.* **1951**, *81*, 385–390.

[222] S. H. Vosko, L. Wilk, M. Nusair, *Can. J. Phys.* **1980**, *58*, 1200–1211.

[223] J. P. Perdew, *Phys. Rev. B* **1986**, *33*, 8822–8824.

[224] A. D. Becke, *Phys. Rev. A* **1988**, *38*, 3098–3100.

[225] A. Schäfer, H. Horn, R. Ahlrichs, *J. Chem. Phys.* **1992**, *97*, 2571–2577.

[226] F. Weigend, R. Ahlrichs, *Phys. Chem. Chem. Phys.* **2005**, *7*, 3297–3305.

[227] S. Grimme, J. Antony, S. Ehrlich, H. Krieg, *J. Chem. Phys.* **2010**, *132*, 154104.

[228] S. Grimme, S. Ehrlich, L. Goerigk, *J. Comput. Chem.* **2011**, *32*, 1456–1465.

[229] A. Klamt, G. Schüürmann, *J. Chem. Soc., Perkin Trans. 2* **1993**, 799–805.

[230] P. Deglmann, F. Furche, R. Ahlrichs, *Chem. Phys. Lett.* **2002**, *362*, 511–518.

[231] Y. Zhao, D. G. Truhlar, *J. Phys. Chem. A* **2005**, *109*, 5656–5667.

[232] F. Weigend, M. Häser, H. Patzelt, R. Ahlrichs, *Chem. Phys. Lett.* **1998**, *294*, 143–152.

Selbstständigkeitserklärung

Ich erkläre, dass ich die vorliegende Arbeit selbstständig und nur unter Verwendung der angegebenen Literatur und Hilfsmittel angefertigt habe.

Chemnitz, der 13. Oktober 2017 _____

Tatiana Shumilova

Acknowledgement

I wish to express my sincere gratitude to those people without whom it would not be possible to complete the work. First of all, I am thankful to my supervisor, Jun.-Prof. Dr. Evgeny Kataev for giving me a chance to work on different interesting projects and for introducing me to the exciting world of supramolecular chemistry. His helpful advice and moral support during my first time of staying far away from home cannot be overestimated.

I would like to thank Dr. T. Rüffer for carrying out X-ray experiments, and Dr. M. Hagedorn for his great help with 2D NMR experiments. I am also grateful to our colleagues from the theoretical chemistry group, who performed DFT calculations for the last part of this work: B. Fiedler, Dr. T. Anacker, and Dr. J. Friedrich.

I thank all former and present members of the supramolecular chemistry group. In particular, I am very grateful to Sharon for laying a synthetic groundwork for our first sulfate receptor, and for being the first friend to me in my new life. I thank Aleksandr A. for his contribution to the same sulfate project and for many other great things he has been helping me with. I am also thankful to Aleksandr O. for creating an unbelievably nice and warm atmosphere in the laboratory during his short but very productive visits.

Last but not least I thank my parents and my friends from home for their love and patience. I would not been able to finish this work without their immense help and support.

Curriculum Vitae

Tatiana Shumilova

Contact information

Address: Vettersstraße 72, Zi. 701, Chemnitz, 09126, Germany

Phone: +4915759110538

E-mail: tatiana.shumilova@chemie.tu-chemnitz.de

Personal Information

Date of birth: 05. February 1993

Place of birth: Novosibirsk, Russia

Citizenship: Russian

Education

since October2014 PhD candidate

laboratory of Supramolecular Chemistry, Institute of Chemistry, Department of Natural Science, Chemnitz University of Technology, Chemnitz, Germany

September 2009–June 2014 Diploma in Chemistry

Department of Natural Sciences, Novosibirsk State University, Novosibirsk, Russia

Thesis: "Synthesis of new monoterpene derivatives based on α-substituted oximes and epichlorohydrin"

September 2007–June 2009 Upper secondary education

Specialized Educational Scientific Center at Novosibirsk State University, Novosibirsk, Russia

Scientific experience

since October 2014 Scientific employee

laboratory of Supramolecular Chemistry, Institute of Chemistry, Department of Natural Science, Chemnitz University of Technology, Chemnitz, Germany

February 2011–September 2014 Student assistant

Terpenoids Laboratory of N.N. Vorozhtsov Novosibirsk Institute of Organic Chemistry SB RAS, Novosibirsk, Russia

Languages

- Russian – native
- English – fluent
- German – fluent
- Italian – beginner

List of publications, oral presentations and posters

Publications

1. T. A. Shumilova, T. Rüffer, H. Lang, E. A. Kataev, *Chem. - A. Eur. J.* **accepted for publication**. Straightforward design of fluorescent receptors for sulfate: study of non-covalent interactions contributing to host-guest formation.
2. R. R. Mittapalli, S. S. R. Namashivaya, A. S. Oshchepkov, T. A. Shumilova, T. Rüffer, H. Lang, E. A. Kataev, *Chem. Commun.* **2017**, *53*, 11345-11348. Selective recognition of oxalate in water: effect of pH on binding strength and sensing mechanisms.
3. S. Weheabby, M. A. Abdulmalic, E. A. Kataev, T. A. Shumilova, T. Rüffer, *Z. Naturforsch., B: Chem. Sci.* **2017**, *72(7)b*, 461–474. Synthesis and structure of large 24-mer and 36-mer oxamate-based macrocycles.
4. A. M. Agafontsev, T. A. Shumilova, P. A. Panchenko, S. Janz, O. A. Fedorova, E. A. Kataev, *Chem. - A. Eur. J.* **2016**, *22*, 15069–15074. Utilizing a pH-sensitive dye in selective fluorescent recognition of sulfate.
5. E. A. Kataev, T. A. Shumilova, B. Fiedler, T. Anacker, J. Friedrich, *J. Org. Chem.* **2016**, *81*, 6505–6514. Understanding stacking interactions between an aromatic ring and nucleobases in aqueous solution: experimental and theoretical study.
6. E. A. Kataev, N. Backmann, T. A. Shumilova, T. Rüffer, H. Lang, *Supramol. Chem.* **2016**, *28*, 53–61. Calix[4]pyrroles bearing quinolinium moiety for halide sensing in aqueous solution.
7. E. A. Kataev, T. A. Shumilova, *Molecules* **2016**, *20*, 3354–3370. Investigation of structural mimetics of natural phosphate ion binding motifs.
8. T. A. Shumilova, A. M. Agafontsev, A. V. Tkachev, *Russ. Chem. Bull. Int. Ed.* **2015**, *64*, 99–106. Synthesis of glycidyl ethers derived from terpene α-amino oximes and β-substituted alcohols on their basis.

Oral contributions

1. New fluorescent probes for sulfate in water. *Doktorandenseminar TU Chemnitz*, **07th July 2016**, Chemnitz, Germany.
2. New peptide-based synthetic receptors for phosphate. *13th Chemistry Conference for Young Scientists (ChemCYS 2016)*, **16–18 March 2016**, Blankenberge, Belgium.

Poster contributions

1. Detection of sulfate with the help of new naphthalimide-based receptors. *SupraChem 2017*, **12–14 February 2017**, Aachen, Germany.
2. New naphthalimide-based selective receptors for sulfate. *25. Lecture Conference on Photochemistry*, **26–28 September 2016**, Jena, Germany.
3. Investigation of structural mimetics of natural phosphate ion binding motifs. *SupraChem 2015*, **22–24 February 2015**, Berlin, Germany.
4. Synthesis of glycidyl ethers of monoterpenes' α-substituted oximes and their epoxides' ring opening derivatives. *12th Chemistry Conference for Young Scientists (ChemCYS 2014)*, **27–28 February 2014**, Blankenberge, Belgium.